An Evaluation of Heat Exchangers Using System Information and PEC

J. V. Pira, C. W. Bullard, and A. M. Jacobi

ACRC TR-175 August 2000

For additional information:

Air Conditioning and Refrigeration Center
University of Illinois
Mechanical & Industrial Engineering Dept.
1206 West Green Street
Urbana, IL 61801

(217) 333-3115

Prepared as part of ACRC Project 95
An Evaluation of Heat Exchangers
Using System Information and PEC
A. M. Jacobi and C. W. Bullard, Principal Investigator

The Air Conditioning and Refrigeration Center was founded in 1988 with a grant from the estate of Richard W. Kritzer, the founder of Peerless of America Inc. A State of Illinois Technology Challenge Grant helped build the laboratory facilities. The ACRC receives continuing support from the Richard W. Kritzer Endowment and the National Science Foundation. The following organizations have also become sponsors of the Center.

Amana Refrigeration, Inc.
Arçelik A. S.
Brazeway, Inc.
Carrier Corporation
Copeland Corporation
DaimlerChrysler Corporation
Delphi Harrison Thermal Systems
Frigidaire Company
General Electric Company
General Motors Corporation
Hill PHOENIX
Honeywell, Inc.
Hussmann Corporation
Hydro Aluminum Adrian, Inc.
Indiana Tube Corporation
Invensys Climate Controls
Lennox International, Inc.
Modine Manufacturing Co.
Parker Hannifin Corporation
Peerless of America, Inc.
The Trane Company
Thermo King Corporation
Valeo, Inc.
Visteon Automotive Systems
Whirlpool Corporation
Wolverine Tube, Inc.
York International, Inc.

For additional information:

Air Conditioning & Refrigeration Center
Mechanical & Industrial Engineering Dept.
University of Illinois
1206 West Green Street
Urbana, IL 61801

217 333 3115

Abstract

This report describes analyses aimed at integrating component optimization and system design by developing heat-exchanger *performance evaluation criteria* (PEC) that account for the system-level performance impacts of heat exchanger design. It builds on earlier studies that used relatively simple PEC to capture some of the component-level tradeoffs, but which usually ignore the system impact of component design. This report evaluates four PEC—j/f, heat transfer/pumping power (Θ), heat transfer/(pumping + compressor power) (Ω), and system COP. It is shown that j/f and Θ are better used as comparison criteria for existing heat exchangers of equal heat duty rather than as design criteria. The other two PEC, Ω and COP, include the system effect of compressor efficiency and therefore can be used more effectively in heat exchanger and system design. Through a combination of PEC and system optimization techniques, a method is developed to evaluate and design heat exchangers for maximum system performance.

Table of Contents

List of Tables

Page

List of Figures

Page

Nomenclature

a	constant used in COP curve fitting
A_{fin}	fin area [m^2]
A_{fr}	frontal area [m^2]
A_{min}	minimum free flow area (coincident with the maximum velocity) [m^2]
A_{tube}	tube area [m^2]
b	constant used in COP curve fitting
c_p	specific heat [J/kg-K]
c_{pm}	specific heat of moist air [J/kg-K]
COP	coefficient of performance
D_c	tube collar diameter [m]
D_h	hydraulic diameter [m]
f	friction factor
F_s	fin spacing (center to center) [m]
F_t	fin thickness [m]
G	mass velocity based on minimum free flow area [kg/m^2-s]
H	heat exchanger height [m]
h_c	heat transfer coefficient [W/m^2-K]
h_D	mass transfer proportionality constant
h_{fg}	heat of vaporization – heat of fusion
j	Colburn j factor
k	thermal conductivity [W/m-K]
L	heat exchanger depth in airflow direction [m]
L_h	louver height [m]
L_p	louver pitch [m]
$\dot{m}$	air mass flow rate [kg/s]
N	number of tube rows in airflow direction
ND	nondimensional
N_{tu}	number of transfer (thermal) units
Nu	Nusselt number

Δp	static pressure drop across heat exchanger [Pa]
P_l	longitudinal tube spacing [m]
P_t	transverse tube spacing [m]
PEC	performance evaluation criteria
Pr	Prandtl number
$q,\ \dot{Q}$	heat transfer rate [W]
r	radius [m]
Re	Reynolds number
RH	relative humidity
S_h	slit height [m]
S_n	number of slits between tubes
S_w	slit width transverse to air flow direction [m]
$T_{a,i}$	inlet air temperature [K]
T_c	condensing temperature [K]
T_e	evaporating temperature [K]
ΔT	T_c- $T_{a,i}$ [K]
UA	overall area-heat-transfer-coefficient product [W/K]
V_{fr}	frontal velocity [m/s]
V_{max}	maximum air velocity [m/s]
W	heat exchanger width [m]
W_h	wave height [m]
$\dot{W}_{pump}$	airside pumping power requirement [W]
$\dot{W}_{comp}$	compressor power requirement [W]

Greek symbols:

ε	heat exchanger effectiveness
ϕ	term used in fin efficiency calculation
η_f	fin efficiency
η_{fm}	fan and motor efficiency
η_0	surface efficiency

μ	dynamic viscosity [N-s/m^2]
Θ	PEC — heat transfer/pumping power
Π	dimensionless group
ρ	density [kg/m^3]
ω	specific humidity [kg H_2O/kg air]
Ω	PEC — heat transfer/(pumping + compressor power)

Subscripts:

a, air	air
ave	average
comp	compressor
cond	condenser
c	collar
Dc	based on tube collar diameter
dp	dewpoint
evap	evaporator
f	fin
i	inner
min	minimum
max	maximum
o	outer, ambient
wb	wet bulb

Superscripts:

*	nondimensional form of variable
-	lower limit
+	upper limit

Chapter 1 – Introduction

1.1 Introduction

The design or selection of an optimal heat exchanger for a specific refrigeration or air conditioning system can be a difficult and time-consuming process. Since the design space is large and complex, simplified performance evaluation criteria (PEC[1]) are sometimes used to find near optimal solutions with much less time and effort. PEC such as London's area-goodness factor (*j/f*), or Cowell's relative volume or pumping power, capture tradeoffs among many of the heat exchanger-specific variables. However, designs that appear to benefit component performance may not be beneficial for the system. Through this project we seek to develop and use PEC to compare heat-exchanger tradeoffs (e.g. vortex generators vs. louvered vs. wavy fins) in a manner that can be cleanly interfaced with other components and system performance.

1.2 Literature Review

For the evaluation of conventional and enhanced heat exchanger surfaces, numerous energy-based PEC are available, such as those presented by Bergles *et al.* (1974), Webb (1981), and Cowell (1990). Energy-based PEC rely on the first law and the transport rate equations. The rate equations for a heat exchanger often rely on correlations for nondimensionalized heat transfer (*j*) and pressure drop (*f*) expressed as functions of the Reynolds number and exchanger geometry. The simplest of these PEC is the so-called "Area-Goodness Factor", *j/f* (Kays and London 1984). Other energy-based PEC have been developed for heat exchangers with various constraints on duty, surface area, geometry, volume, air flow rate, pressure drop, or pumping power. Although choosing the appropriate constraints can be difficult, the implementation of energy-based PEC is straightforward; these criteria take the form of simple ratios that include the rate constants (*j* and *f*) and geometric parameters for the heat exchanger.

[1] PEC will be used as singular for "performance evaluation criterion" and as plural for "performance evaluation criteria" throughout the thesis.

Bergles *et al.* (1974) presented nine performance criteria to be used for the selection of enhanced fin configurations. These criteria were in the form of simple ratios of heat exchanger parameters, such as q_a/q_o, comparing augmented surfaces to a standard non-augmented case, and with different constraints for each PEC. The criteria were generated for use in shell-and-tube heat exchangers with single-phase flow. Four of the criteria were directed towards the use of promoters for improvement of existing heat exchangers; another four evaluated advantages of using promoters in the design of a new heat exchanger; and finally the last PEC was presented for economic evaluation of enhanced tubes. The economic criterion included tubing and shell costs, electrical costs, and interest rates, and allowed for comparisons to be made of operating costs and fixed costs of a heat exchanger.

Webb (1981) extended the work of Bergles to establish a much broader range of performance evaluation criteria for single phase flow in tubes. Three possible performance objectives were listed and applied to eleven cases of interest. The three objectives were:

1) Reduced heat transfer surface material (mass) for equal pumping power and heat duty
2) Increased UA for equal pumping power and fixed total length of exchanger tubing, with a higher UA being exploited in two possible ways:
   - to obtain increased heat duty for fixed entering fluid temperatures
   - to secure reduced LMTD for fixed heat duty
3) Reduced pumping power for equal heat duty and equal total length of exchanger tubing

These objectives were applied to cases with different constraints on the heat exchanger parameters, falling into three main categories of 1) fixed geometry criteria, 2) fixed flow area criteria, and 3) variable geometry cases. The PEC were formulated in a fashion similar to Bergles, using ratios of heat exchanger parameters of augmented tubes to parameters of a similar plain-tube design.

Kays and London (1984) proposed a method for heat exchanger evaluation in which a plot of *j/f* vs. Reynolds number could identify surface types which require smaller flow frontal areas (corresponding to a higher *j/f* value). The ratio *j/f* represents core-surface characteristics for a given fluid. Since a usual design problem provides a specification of both pressure drop and heat transfer performance, Kays and London derived a relationship between the two which suggested that *j/f*, a surface flow area "goodness factor", could be used to determine the proper surface type for heat exchangers with a design requirement of small frontal areas.

Cowell (1990) developed a method to compare heat transfer surfaces with various constraints on scale, frontal area, heat exchanger volume, pumping power, and combinations of those constraints. In his analysis, Cowell presented equations describing the performance of heat exchangers, then rearranged terms to derive equations for pumping power, frontal area, volume, etc. in terms of Reynolds number, N_{tu}, and other parameters. The parameters in these equations could then be separated into 2 groups—one group associated with a required heat transfer duty, and the other associated with a particular solution. The groups associated with particular solutions were called "relative volume", "relative pumping power", etc. When these terms were plotted against one another for multiple surface types in which *j* and *f* data were available as functions of the Reynolds number, the "relative" amount of volume one surface type required for a given pumping power could be compared to the other surface, as well as many other parameter comparisons.

Unfortunately, all energy-based PEC share a common limitation: most energy-based criteria tend to place equal weight on mechanical work and heat transfer interactions. Furthermore, simple energy-based PEC do not provide guidance as to the tradeoffs between first cost and operating cost. A second family of PEC attempts to overcome these limitations through entropy considerations. Such approaches cast all energy interactions into their available-work equivalent, thereby placing an appropriate weighting on heat transfer enhancement and pressure drop penalty. A number of entropy-based heat exchanger evaluations have been presented in the literature. A good

review of these methods was recently provided by Bejan (1996) (see also Bejan 1978, Sekulic 1990, Tagliafico and Tanda 1996). Relatively simple entropy-based PEC can be formed, for example, by considering the ratio of exergy (flow availability) appearing in the exchanger product stream to the total exergy supplied to the heat exchanger (see Wepfer *et al.* 1979). Sometimes rate-equation constraints on exchanger operation are included in this approach (Bejan 1996). The formulation and interpretation of entropy-based PEC can be subjective and are more complex than simple energy-based PEC.

Perhaps the most general heat exchanger optimization is one with a minimum life-cycle cost as its basis, subject to capacity, geometric, and other constraints. Some engineers propose to use an entropy analysis within a rigorous thermoeconomic treatment of the system. Such an approach properly accounts for the value of material, heat, work, and capital (London 1982 and Zubair *et al.* 1987), casting all costs and benefits into a single currency. Unfortunately, this approach is very complex, expensive to implement, and requires information difficult to obtain or with a high uncertainty early in the design process. Accurate cost data are rarely available in the public domain. The best that can be done without such cost data—retaining as much generality as possible—is to formulate evaluation criteria that provide a clear and direct linkage to cost. Witte (1988) presents a simplified thermoeconomic evaluation of heat exchangers, but his method neglects fan power—a major shortcoming in component evaluation.

Engineers have spent decades using heat exchanger PEC to help design exchangers, and the concept holds value as an engineering tool. The best applications of PEC are probably in choosing the best design and operating conditions for a particular *type* of heat exchanger. PEC may also be useful in making quick judgments *between* types of heat exchangers, e.g., between louvered fins and plain fins. However, all heat exchangers are part of a thermal system, and system performance and component performance are coupled. For example, the heat exchanger performance has a direct effect on condensing and evaporating temperatures which affect compressor performance and system COP. Some interactions are slightly more subtle; for example, heat exchanger design affects the refrigerant-side pressure drop, which affects compressor

work directly and also indirectly through its effect on temperature distribution. Some interactions even less direct, with complex issues like frost management, fouling, air-side condensate and noise playing roles in system and component design. Unfortunately, few air-side heat exchanger PEC consider system-level interactions.

DeJong *et al.* (1997) proposed a PEC defined as heat transfer/(supplied exergy + compressor penalty). This method incorporated conservation and rate equations as well as the second law to cast all energy interactions in their available-work equivalent. The compressor penalty was calculated from a curve fit to manufacturer's data. With a PEC defined in this way, it was shown that preferred operating conditions existed for particular heat exchanger configurations, and a preferred heat exchanger configuration existed for specified operating conditions.

COP can be considered a system level PEC that combines all parameters of interest in a system into one value that represents the efficiency of the system as a whole. Klein (1992) showed that Carnot COP is not a realistic design goal for real refrigeration cycles of finite cooling capacity. Because of irreversibilities associated with the heat transfer process at both the condenser and evaporator, Klein proposed a form of COP which included evaporator and condenser effectiveness, capacitance rates, and cooling capacity. The proposed form of COP was equal to Carnot COP at zero temperature differences between the refrigerant phase-change temperature and its corresponding sink temperature, and decreased below Carnot COP for real cycles. Klein further showed, using an analytical technique, that for internally reversible refrigeration cycles COP is maximized when the product of the heat transfer effectiveness and external fluid capacitance is the same for both heat exchangers.

1.3 Objective

The primary objective of this project was to develop a methodology for the optimization of heat exchangers in air conditioning and refrigeration systems. Developing this methodology was done first by analysis of various component level PEC to determine ideal heat exchanger geometries and air flow rates, then by combining them

into a system optimization model. The processes developed were applied to various heat exchanger surface types, including plain, wavy, slit, and louvered fin-on-tube condensers and evaporators.

Chapter 2 – Performance Evaluation Criteria

The performance evaluation criteria used in the optimization model are all nondimensional. The use of dimensionless variables provides flexibility and generality in comparing benefits or drawbacks of different heat exchanger designs. Furthermore, it allows an easier comparison to prior work, since most existing PEC are nondimensional. In this chapter, specific motivations for using this method are covered, as well as descriptions of each of the PEC studied.

2.1 Motivation for nondimensional model

Defining a nondimensional (ND) parameter space can prove beneficial in the use of PEC for heat exchanger design. In particular, it simplifies analysis in the following ways:

1) Reduces number of variables required for analysis

Creating a ND model for evaluating heat exchangers requires listing all parameters that can influence the PEC being used. Applying a Buckingham Π analysis on these parameters determines the ND variables that are relevant in evaluating the heat exchangers. These ND variables are simply various combinations of the dimensional variables. Some of the terms derived from this type of analysis are, for example, the Reynolds and Prandtl numbers, which are known to affect the heat transfer properties. By converting to a ND parameter space, the number of variables needed to describe a component or system is reduced by the number of dimensions in the analysis.

2) Provides for fluid generality in optimal solutions

Optimal solutions determined from this type of analysis can be applied to any fluid flowing over the heat exchanger. This project deals mainly with air flowing the heat exchanger; however, the optima could easily be applied to other fluids, provided the j and f correlations underlying this model are valid for those fluids.

3) Allows seamless integration of Colburn j and friction factor correlations

Empirical correlations for j and f factors of various heat exchanger designs are abundant in the open literature. Because the j and f factors are nondimensional, all parameter combinations in the correlations are also nondimensional. The use of a nondimensional parameter space enables these correlations to be written in terms of the same variables used to represent each PEC analyzed, allowing easy integration and comparison of included parameters.

2.2 Overview of PEC

A PEC is used as a figure of merit in seeking ways to improve performance of a component or system. It is a function of independent variables characterizing that system and its surroundings. It can be used to compare existing heat exchanger designs, or alternatively, to optimize a design given range limits on the independent variables. In this analysis, a generalized method for the optimization of crossflow finned-tube condensers using various PEC has been developed. This method allows PEC comparison in a way which may help designers gain a better understanding of their application to specific heat exchangers. Four PEC have been used to determine optimal configurations of heat exchangers, and they have been applied to four surface types: plain fins, wavy fins, slit fins, and louvered fins. These PEC include three component-level PEC, for use in optimizing a single heat exchanger, and one system-level PEC, for use in optimizing a condenser and evaporator combination. The evaluation of each PEC is described in detail below, followed by an explanation of the optimization method.

2.2.1 Colburn *j* factor / friction factor

The Colburn j factor and friction factor are commonly used to describe the thermal-hydraulic performance of heat exchangers. These parameters are usually determined experimentally, due to the complexity of heat exchangers. Regressions are performed on heat transfer and pressure drop data obtained from testing heat exchangers under controlled conditions, and curve fits are presented to describe heat exchanger performance as a function of various design variables.

Also known as the "Area-Goodness Factor" (Kays and London, 1984), *j/f* is the simplest of the energy-based PEC. An increase in heat transfer performance due to interrupted surfaces is generally accompanied by an increased frictional forces in the air flow. The *j/f* ratio evaluates the relative differences between these effects and is sometimes used as a comparison tool to optimize the design of the heat exchanger. Larger values of *j/f* denote better heat exchanger "performance". The Colburn *j* factor can be described as a function of the following 11 variables (for plain fin heat exchangers):

$$j = j\left(L, F_s, F_t, P_l, P_t, D_c, V_{fr}, \mu, \rho, c_p, k_a\right) \tag{2.1}$$

These variables represent the physical geometry of the heat exchanger and the properties of the fluid passing over it.

At this point the Buckingham Π theorem can be applied to cast this functional relationship in a nondimensional space. Four repeating parameters need to be chosen — one for each of the general dimensions of mass, length, time, and temperature. Initial analyses done in this project used the variables μ, ρ, c_p, and D_c as repeating parameters, enabling parameters having a length dimension to be normalized by the tube collar diameter. Other PEC in this analysis are dependent on an additional parameter, T_o, due to the use of compressor map curve fits which are dependent on absolute temperatures. Through the analysis of these PEC it has been shown that using T_o as a repeating parameter rather than D_c allows improved nondimensional analysis, because the value of D_c affects the optima and is better represented by a separate nondimensional variable. Using T_o as a repeating parameter allows isolation of a nondimensional tube collar diameter rather than having the tube collar diameter interspersed through many nondimensional variables. This method normalizes length scales by a combination of airflow properties, and is also advantageous to normalizing by a physical length scale such as tube collar diameter because of range limits that are imposed on optimization runs. Further details of the effects of limits are explained in Appendix A. For consistency in evaluating the PEC, similar repeating parameters for all cases were

chosen. The repeating parameters used were then μ, ρ, c_p, and T_o. Combinations of these terms are used to nondimensionalize the remaining terms. By using these repeating parameters, each nondimensional variable derived from the analysis can be converted to dimensional form simply by specifying the fluid type (air in this case) and an ambient temperature. With these repeating parameters, all variables become normalized by combinations of fluid properties. Applying the Buckingham Π theorem to this system results in the following expression for j as a function of 8 independent variables[1]:

$$j = j\left(L^*, F_s^*, F_t^*, P_l^*, P_t^*, D_c^*, V_{fr}^*, k_a^*\right) \tag{2.2}$$

The formulae for each of these nondimensional variables is listed in Table 2.1, and a detailed description of the steps involved in obtaining each nondimensional variable is given in Appendix A.

The friction factor can be similarly reduced to the following functional relationship:

$$f = f\left(L^*, F_s^*, F_t^*, P_l^*, P_t^*, D_c^*, V_{fr}^*\right) \tag{2.3}$$

in which the thermal conductivity of the air does not appear. Combining the j and f factor into a ratio, the following functional dependence results for the PEC j/f in terms of 8 nondimensional variables:

$$\frac{j}{f} = \frac{j}{f}\left(L^*, F_s^*, F_t^*, P_l^*, P_t^*, D_c^*, V_{fr}^*, k_a^*\right) \tag{2.4}$$

In order to optimize a heat exchanger using this PEC, experimentally determined equations for the j and f factor are written in terms of these variables. The correlations

[1] Note that if T_o were not introduced, Eq. 2.2 would have 7 independent variables (11-4=7, cf. Eq. 2.1); however, introducing T_o causes an additional nondimensional variable to appear (see Appendix A for discussion).

may or may not use all these ND variables. The derived ND variables are not unique; in fact, the choice of different repeating parameters changes the form of each variable. Many of the variables used in the literature for this type of regression analysis are combinations of these ND variables. Of particular importance is the Reynolds number, which can be written as an area ratio multiplied by V_{fr}^* and D_c^*:

$$\mathrm{Re}_{D_c} = \left(\frac{A_{fr}}{A_{\min}} \right) V_{fr}^* D_c^* \tag{2.5}$$

where

$$\frac{A_{fr}}{A_{\min}} = \frac{1}{1 - \frac{F_t^*}{F_s^*} - \frac{D_c^*}{P_t^*} + \frac{F_t^*}{F_s^*}\frac{D_c^*}{P_t^*}} \tag{2.6}$$

See Appendix B for the derivation of Equation 2.6 and other area ratios. The Reynolds number in Equation 2.5 is based on the tube collar diameter as the length scale and maximum velocity through the minimum free flow area as the velocity scale. Published correlations that use Reynolds numbers based on other scales (e.g. hydraulic diameter for the length scale) can be expressed as other combinations of the ND variables. The area ratio in Equation 2.6 is also a function of the derived ND variables; no new variables are introduced. As long as the total number of independent variables that define the objective function remains constant, the combination of terms is valid.

2.2.2 Heat transfer / pumping power

Taking a step beyond *j/f*, consider a PEC that takes into account the actual heat transfer rate and pumping power required for the heat exchanger. By adding a fan component, more information is included in the optimization process than with *j/f*. This new PEC, Θ, is defined as heat transfer/pumping power. Θ attempts to capture the tradeoff between the heat transfer enhancement and the increase in power often needed to provide airflow through the heat exchanger. This PEC is similar to *j/f* but is a function of more variables. Θ has the following functional dependence:

$$\Theta = \Theta\left(q, \dot{W}_p\right) \tag{2.7}$$

Pumping power is approximated to be $\dot{V}\Delta p / \eta_{fm}$, where η_{fm}, the fan and motor efficiency, is a newly introduced term to the ND parameter space. Converting the volumetric flow term to its component variables, A_{fr} and V_{fr}, the relationship becomes

$$\Theta = \Theta\left(q, A_{fr}, V_{fr}, \Delta p, \eta_{fm}\right) \tag{2.8}$$

The functional dependence of Θ can be expressed in a different manner with specific goals in mind. Such goals may include determination of the values of Δp and q/A_{fr} that result from maximization of the PEC. Or various constraints may be implemented during an optimization process, such as fixing the heat duty per unit frontal area. Writing Θ as a function of the desired independent variables eases its interpretation. Such a formulation requires application of the momentum and heat rate equations. Using the definition of the friction factor, as given by Kays and London (1986):

$$\begin{aligned} \Delta p &= \frac{G_a^2}{2\rho}\frac{A_T}{A_{\min}} f \\ &= \frac{1}{2}\rho V_{fr}^2 \left(\frac{A_{fr}}{A_{\min}}\right)^2 \left(\frac{A_T}{A_{\min}}\right) f \end{aligned} \tag{2.9}$$

Flow acceleration terms were neglected to obtain this equation, and fluid density is assumed constant at its inlet value to simplify the form of the equation. The ε-N_{tu} formulation was used for the heat transfer rate equation:

$$\begin{aligned} q &= \varepsilon \dot{m} c_p \Delta T_{\max} \\ &= \varepsilon \rho V_{fr} A_{fr} c_p \Delta T_{\max} \end{aligned} \tag{2.10}$$

The term ΔT_{max} denotes the temperature difference between the incoming air and the condensing or evaporating temperature of the internal fluid (refrigerant). At this point, latent heat transfer is not included in the definition of Θ. This initial analysis is therefore valid for only condensers and dry evaporators. Latent heat transfer, used for wet evaporator analysis, is represented by the addition of another term to Equation 2.10, and is discussed in Chapter 4. Within Equation 2.10, the heat exchanger effectiveness for a condenser or evaporator is taken as

$$\varepsilon = 1 - \exp(-\eta_0 N_{tu}) \tag{2.11}$$

where

$$N_{tu} = \frac{UA}{(\dot{m}c_p)_{air}} \tag{2.12}$$

In Equation 2.11, the heat capacity ratio of the internal fluid is assumed to be infinite, designating a phase change on the refrigerant side of the heat exchanger. This analysis assumes that for the refrigerant side, the entire heat exchanger is operating in the two-phase region, with no subcooled or superheated regions.

In order to simplify the analysis and preserve generality, the airside thermal resistance is considered to be dominant over the refrigerant-side resistance, tube-wall resistance, and fouling factors; therefore, the base (tube surface) temperature is equal to the refrigerant temperature. With the assumption of dominant airside resistance, the overall heat transfer coefficient can be approximated as equal to the airside heat transfer coefficient, and the effectiveness can be represented by

$$\begin{aligned} \varepsilon &= 1 - \exp\left(-\eta_0 \frac{UA_T}{\dot{m}c_p}\right) \\ &= 1 - \exp\left(-\eta_0 \frac{hA_T}{\dot{m}c_p}\right) \\ &= 1 - \exp\left(-\eta_0 j \,\mathrm{Pr}^{-2/3} \frac{A_T}{A_{\min}}\right) \end{aligned} \tag{2.13}$$

in which the j factor is defined as follows:

$$j = \frac{h}{\rho V_{\max} c_p} \mathrm{Pr}^{2/3} \tag{2.14}$$

Surface efficiency is derived in Appendix B using the sector method in conjunction with an analytical fin efficiency equation developed for circular fins, expressed in terms of Bessel functions (Kern and Kraus 1972). The equations are cast into functions of only the nondimensional parameters used in this analysis.

With substitution of parameters in Equation 2.8 from Equations 2.9 and 2.10, the functional dependence for Θ becomes

$$\Theta = \Theta\left(L, F_s, F_t, P_l, P_t, D_c, V_{fr}, \mu, \rho, c_p, k_a, \Delta T, \eta_{fm}\right) \tag{2.15}$$

with ε and the area ratios not listed because they are functions of the other listed parameters (see Appendix B). The term A_{fr} drops out of the functional form because it appears both in the numerator and denominator of Θ, thus canceling out. Nondimensionalizing as before with the repeating parameters μ, ρ, c_p, and T_o, we obtain Θ as a function of the same 8 variables as j/f, plus 3 more: k_f^*, ΔT^*, and η_{fm}.

$$\Theta = \Theta\left(L^*, F_s^*, F_t^*, P_l^*, P_t^*, D_c^*, V_{fr}^*, k_a^*, k_f^*, \Delta T^*, \eta_{fm}\right) \tag{2.16}$$

Again, V_{fr}^* may be substituted by Re_{Dc} while maintaining independence of the terms. The actual functional relation for Θ in this nondimensional parameter space is then

$$\Theta = \frac{2\eta_{fm}\varepsilon\Delta T^*}{f}\left(\frac{D_c^*}{\mathrm{Re}_{D_c}}\right)^2\left(\frac{A_{\min}}{A_T}\right) \tag{2.17}$$

If a log-mean temperature difference approach were employed for heat transfer evaluation rather than ε-N_{tu}, Θ would simply be *j/f* multiplied by an additional term. However, in this case the *j* factor is embedded in the heat exchanger effectiveness (ε) term.

2.2.3 Heat transfer / (pumping power + compressor power)

The third PEC studied, Ω, is defined to be heat transfer/(pumping + compressor power). This PEC adds a level of complexity to the analysis by including the compressor in the system, which already includes the heat exchanger and fan component. The air side performance of the heat exchanger becomes linked to penalties associated with refrigerant-side power requirements. In this way, changes to heat exchanger design can be studied to determine their effects on both pumping power and compressor penalty.

Compressor manufacturers provide tables which describe compressor performance under different operating conditions. From these compressor maps, we can obtain compressor power required for a given condensing and evaporating temperature. However, using compressor power directly from the table would include the scale of the particular compressor in the analysis. In order to avoid the optimal solution being dependent on a particular scale of compressor, COP information can be used. The system COP, which is also listed on compressor maps, tends to be nearly independent of scale within certain types of applications (e.g. residential a/c). COP is tabulated as a function of the condensing and evaporating temperatures. The form of COP used on a compressor map is

$$COP_{comp} = \frac{q_{evap}}{\dot{W}_c} = \frac{q_{cond} + q_{comp}}{\dot{W}_c} - 1 \tag{2.18}$$

If we neglect heat rejection from the compressor, Ω can be written in reasonably simple form as follows:

$$\Omega_{evap} = \frac{q_{evap}}{\dot{W}_c + \dot{W}_p} = \left[\frac{1}{\Theta} + \frac{\dot{W}_c}{q_{evap}}\right]^{-1} = \left[\frac{1}{\Theta} + \frac{1}{COP_{comp}}\right]^{-1} \tag{2.19}$$

$$\Omega_{cond} = \frac{q_{cond}}{\dot{W}_c + \dot{W}_p} = \left[\frac{1}{\Theta} + \frac{\dot{W}_c}{q_{cond}}\right]^{-1} = \left[\frac{1}{\Theta} + \frac{1}{1 + COP_{comp}}\right]^{-1} \tag{2.20}$$

Note that the previous discussion of Θ applies to both condensers and dry evaporators. When q_{comp} is large, compressor manufacturers also supply data on q_{comp} as a function of T_{evap} and T_{cond}, so it need not be neglected. However, more complexity would be added to the equation. Using Equations 2.19 and 2.20 enables a maximization of Ω to be valid for all compressors having similar COP characteristics, rather than being valid for only one compressor. For condensers, a linear approximation of the COP curve can be made for various condensing temperatures in the range of interest, and for a given evaporating temperature:

$$COP_{comp} = a - b\Delta T \tag{2.21}$$

Although Equation 2.21 is written in terms of ΔT, the compressor map is actually dependent on absolute condensing temperatures. Therefore, in addition to ΔT, the PEC Ω depends on either the condensing temperature or the ambient temperature; in particular, two of T_o, T_{cond}, and ΔT are needed in order to define the third. The ambient temperature T_o was chosen because condensing temperatures are desired as a result of the analysis rather than an input. The functional dependence of Ω in the dimensional parameter space is then

$$\Omega = \Omega\left(L, F_s, F_t, P_l, P_t, D_c, V_{fr}, \mu, \rho, c_p, k_a, \Delta T, \eta_{fm}, T_o, a, b\right) \tag{2.22}$$

The additional parameters are T_o, a, and b when compared to the functional form of Θ in Equation 2.15. In the compressor COP equation (Equation 2.21), the "b" term is

the only new term that requires nondimensionalization. The term "a" is already nondimensional, but a^* will be used to identify it to keep the nomenclature consistent with the other derived parameters. The variable a^* represents the best possible COP for an ideal (e.g. zero ΔT) condenser. The upper limit of possible values for a^* is therefore limited by the Carnot COP between the outdoor and indoor temperatures. The value of a^* for a real system is Carnot COP minus the COP penalty for inefficiencies in the evaporator. The value of a^* is independent of the condenser design. The variable b^* represents the slope of the COP penalty for increasing condensing temperatures. By using data from an actual compressor to obtain the a^* and b^* terms, compressor efficiency information becomes embedded into the parameters, with b^* defined as

$$b^* = bT_o \tag{2.23}$$

With this information the following form for Ω results:

$$\Omega_{cond} = \left[\frac{1}{\Theta} + \frac{1}{1+\left(a^* - b^*\Delta T^*\right)}\right]^{-1} \tag{2.24}$$

In full form:

$$\Omega_{cond} = \left[\frac{f}{2\eta_{fm}\varepsilon\Delta T^*}\left(\frac{\mathrm{Re}_{D_c}}{D_c^*}\right)^2\left(\frac{A_T}{A_{\min}}\right) + \frac{1}{1+\left(a^* - b^*\Delta T^*\right)}\right]^{-1} \tag{2.25}$$

Ω is a function of the following variables:

$$\Omega = \Omega\left(L^*, F_s^*, F_t^*, P_l^*, P_t^*, D_c^*, \mathrm{Re}_{D_c}, k_a^*, k_f^*, \Delta T^*, \eta_{fm}, a^*, b^*\right) \tag{2.26}$$

A large value of a^* and a small value of b^* are preferred by this PEC. A large value of a^* is achievable with an efficient evaporator (up to the Carnot COP limit), while

a small value of b^* denotes a compressor in which the power requirement does not increase greatly with increasing condensing temperature (which translates into smaller COP penalties as the isentropic limit is approached). This PEC attempts to balance out features of the previous two PEC by including more system information; in this case the information comes from the refrigerant side and the evaporator.

2.2.4 System COP

The fourth PEC studied was system COP, which is defined as

$$COP_{system} = \frac{q_{evap} - \dot{W}_{p,evap}}{\dot{W}_{p,evap} + \dot{W}_{p,cond} + \dot{W}_c} \tag{2.27}$$

System-level PEC such as COP include variables for both the condenser and evaporator, in addition to pumping power and compressor power variables. Therefore, the functional dependence of system COP in the nondimensional parameter space is shown as follows, for plain fin heat exchangers under dry conditions:

$$COP_{system,dry} = COP\left(\begin{Bmatrix} L^*, F_s^*, F_t^*, P_l^*, P_t^*, D_c^*, V_{fr}^*, k_a^*, k_f^*, \Delta T^*, \eta_{fm} \end{Bmatrix}_{evap}, \begin{Bmatrix} L^*, F_s^*, F_t^*, P_l^*, P_t^*, D_c^*, V_{fr}^*, k_a^*, k_f^*, \Delta T^*, \eta_{fm} \end{Bmatrix}_{cond}\right) \tag{2.28}$$

where

$$\Delta T_{evap}^* = \frac{\Delta T_{evap}}{T_{indoor}} \tag{2.29}$$

$$\Delta T_{cond}^* = \frac{\Delta T_{cond}}{T_{outdoor}} \tag{2.30}$$

$$\Delta T_{evap} = T_{indoor} - T_{evap} \tag{2.31}$$

$$\Delta T_{cond} = T_{cond} - T_{outdoor} \tag{2.32}$$

For this functional form the nondimensional variables for calculating compressor work are omitted. It is assumed that an accurate curve fit, as a function of both condensing and evaporating temperatures, can be made for a given compressor (similarly to Ω

optimization but as a function of two variables). The variables in this curve fit can then be viewed as constants during optimizations. This PEC is written in the nondimensional parameter space under dry conditions as

$$COP_{system,dry} = \frac{\left[\varepsilon \Delta T^*\right]_{evap} + \left[\frac{\mathrm{Re}_{D_c}^2 f}{2\eta_{fm}\left(D_c^*\right)^2}\left(\frac{A_T}{A_{\min}}\right)\right]_{evap}}{\left[\frac{\mathrm{Re}_{D_c}^2 f}{2\eta_{fm}\left(D_c^*\right)^2}\left(\frac{A_T}{A_{\min}}\right)\right]_{evap} + \left[\frac{\mathrm{Re}_{D_c}^2 f}{2\eta_{fm}\left(D_c^*\right)^2}\left(\frac{A_T}{A_{\min}}\right)\right]_{cond} + \left[\frac{\varepsilon \Delta T^*}{COP_{comp}}\right]_{evap}} \tag{2.33}$$

Table 2.1 ND variables for j factor

Dimensional variable	Nondimensional variable
D_c	$D_c^* = \frac{D_c \rho \sqrt{c_p T_o}}{\mu}$
L	$L^* = \frac{L \rho \sqrt{c_p T_o}}{\mu}$
F_s	$F_s^* = \frac{F_s \rho \sqrt{c_p T_o}}{\mu}$
F_t	$F_t^* = \frac{F_t \rho \sqrt{c_p T_o}}{\mu}$
P_l	$P_l^* = \frac{P_l \rho \sqrt{c_p T_o}}{\mu}$
P_t	$P_t^* = \frac{P_t \rho \sqrt{c_p T_o}}{\mu}$
V_{fr}	$V_{fr}^* = \frac{V_{fr}}{\sqrt{c_p T_o}}$
k_a	$k_a^* = \frac{k_a}{\mu c_p}$

Chapter 3 – Unconstrained Optimization Results and Discussion

In this chapter the four PEC defined in Chapter 2 are used to find optimal heat exchanger geometries and operating conditions. A completely "unconstrained" optimization of a heat exchanger can be viewed as a maximization of a PEC with respect to all the variables it is dependent upon, with no imposed design goals such as limited face area or required heat transfer rate. In this analysis, the search domain is limited by setting ranges on the independent variables, because many of them exhibit monotonic behavior which would lead to zero or infinite values when a PEC is maximized. Setting the appropriate ranges also ensures that results are not extrapolated beyond the ranges of the j and f correlations and the compressor maps used in the model. Also, certain variables in this section are fixed, either because of assumed fluid and material properties, or because of a known relationship to the PEC. The variables k_a^* and k_f^* were fixed, assuming air as the external fluid and aluminum as the heat exchanger material. Also fixed are the fan-and-motor efficiency, which always improves PEC value as it increases, and the compressor variables a^* and b^*, in order to optimize for a characteristic compressor application (residential a/c). The fixed variables are not limitations on heat transfer rates or face areas; thus, these optimizations are still referred to as "unconstrained". Chapter 4 continues PEC analysis with added constraints on heat transfer per unit frontal area (q/A_{fr}), number of tube rows, and latent heat transfer.

3.1 Unconstrained component-level optimization on plain-finned heat exchangers

The optimization method was applied to four surface types: plain, wavy, slit, and louvered fins, all assumed to be on crossflow finned heat exchangers with circular tubes. This section covers plain fin heat exchangers in order to gain an understanding of PEC behavior and interpretation of results before the other surface types are introduced. The j factor correlation used for plain fins was that of Wang and Chang (1998). This correlation was created from their test data plus those of Gray and Webb (1986). The f factor correlation was taken from Wang *et al.* (1996).

3.1.1 Unconstrained *j/f* optimization

The equation for *j/f* for plain fin-on-tube heat exchangers using the correlations listed above is

$$\frac{j}{f} = 0.341\left[2.24\left(\mathrm{Re}_{D_c}\right)^{-0.092}\left(\frac{1}{4}\frac{L^*}{P_l^*}\right)^{-0.031}\right]^{0.607\left(4-\frac{L^*}{P_l^*}\right)} \cdot\left(\frac{L^*}{D_c^*}\right)^{0.0935}\left(\frac{F_s^*}{D_c^*}\right)^{-0.166}\left(\frac{F_t^*}{D_c^*}\right)^{0.104}\left(\frac{P_l^*}{D_c^*}\right)^{-0.872}\left(\frac{P_t^*}{D_c^*}\right)^{-0.502}\left(\mathrm{Re}_{D_c}\right)^{0.090} \tag{3.1}$$

Note that this equation does not contain the independent variable k_a^*, which was listed in the functional form of *j/f* in Equation 2.4. This variable, which is equal to the inverse of the Prandtl number, does not appear because the correlations were developed from experiments conducted with air as the external fluid passing through the heat exchanger. The variable k_a, from which k_a^* is based, may also be an extraneous variable in the functional form shown in Equation 2.1; it may not affect the *j* factor. Such variables can be proven to be extraneous through experimental methods.

Equation 3.1 can be put into equation solver software capable of multidimensional searches such as Engineering Equation Solver, or EES (Klein and Alvarado, 1999). This program allows maximization of an objective function given its dependent variables. Ranges of the nondimensional variables are set to perform each optimization. The ranges are based on limits of the dimensional variables plus the ambient air properties. With Equation 3.1 implemented into the software, the PEC *j/f* can be maximized with respect to the nondimensional variables, revealing optimal values for each one within the ranges of the correlations used. The optimal solution is valid for all fluids, provided that correlations for *j* and *f* were developed for a broad range of fluids.

The parameter ranges for the plain fin correlations of Equation 3.1 are shown in Table 3.1. In this table both the dimensional and nondimensional limits are shown.

Table 3.1 Ranges of dimensional and nondimensional parameters

Minimum (ND)	Minimum (mm)	Parameter	Maximum (mm)	Maximum (ND)
2.53e5	7.52	D_c	13.3	4.48e5
5.92e5	17.6	L	164	5.53e6
3.60e4	1.07	F_s	3.00	1.01e5
4.95e3	0.147	F_t	0.360	1.21e4
4.27e5	12.7	P_l	27.4	9.22e5
6.86e5	20.4	P_t	31.7	1.01e6
300		Re_{Dc}		6000

The 7 degree of freedom *j/f* optimization is performed using Equation 3.1, within the ranges shown in Table 3.1. The Reynolds number was selected as a search variable instead of nondimensional frontal velocity, despite the fact that Re_{Dc} depends on the other 6 variables. The face velocity is determined from the Reynolds number and geometry obtained. Optimizations were performed with respect to the Reynolds number because not all authors of the correlations reported face velocities, but they all reported Reynolds numbers. If a more detailed analysis is required, face velocities could be extracted from the original sources that list all heat exchanger geometries used. The minimum and maximum Reynolds numbers could be used for each coil to determine the minimum and maximum face velocity, and the full range of face velocities can be obtained. However, for simplicity, Reynolds number ranges were used since they were listed directly in all sources used. The combination of a range limit on Reynolds number and range limits on the geometrical parameters provides a realistic bound on the possible values of face velocity that can be obtained in this analysis.

For this unconstrained case, values obtained for the optimal *j/f* geometry and Reynolds number are shown in Table 3.2. Since this analysis is concerned primarily with the use of air flowing over the heat exchanger, results of optimizations are displayed in terms of dimensional quantities.

Table 3.2 Optimal parameter values for *j/f*

j/f	0.85
D_c [mm]	13.3^{+}
L [mm]	17.6^{-}
F_s [mm]	1.07^{-}
F_t [mm]	0.36^{+}
P_l [mm]	12.7^{-}
P_t [mm]	20.4^{-}
Re_{Dc}	300^{-}

The superscripts for the parameter values in Table 3.2 denote whether the variable was pushed towards its lower bound or upper bound. All parameters were pushed to a bound to maximize this PEC. The suggested heat exchanger geometry is a thin design in the airflow direction, with dense, thick fins, and large diameter tubes spaced close together transverse to the airflow and in the airflow direction. The Reynolds number is pushed to its minimum allowed value.

In order to explore the effects of *j/f* maximization, the optimized variables need to be viewed as a subset of all possible variables that define heat exchanger performance. The number of variables in a PEC plays a large role in the manner in which it can be used for heat exchanger design. The variables determined from the *j/f* optimization specify an optimal geometry and air flow rate which is broadly applicable to all circular tube flat fin heat exchangers. It is independent of heat exchanger surface temperature or heat load. Further explanation of the *j/f* optimal point in relation to heat exchanger design, as well as the optimal points for Θ and Ω, will be covered in section 3.2.

3.1.2 Unconstrained Θ optimization

Using the same plain fin *j* and *f* factors as before, Θ differs from *j/f* in that it is also a function of the terms k_f^*, ΔT^*, and η_{fm}. A true "unconstrained" optimization of Θ would involve setting ranges for all 11 parameters in the functional relationship shown in Equation 2.19 before running the optimization. However, since we are interested in an optimization for air flowing over an aluminum heat exchanger, we can fix some of these values. Table 3.3 shows optimization results with fixed values of k_a^*, k_f^*, and η_{fm}. See

Appendix B for an explanation of the fan-and-motor efficiency used in the optimization. The ranges from Table 3.1 are still valid, with the addition of ΔT, for which the search interval is limited (in dimensional terms) from 0.1-30°C. This range covers realistic values of ΔT in air conditioning applications, with a rather high upper limit to consider the possibility of extreme conditions.

Table 3.3 Optimal parameter values for Θ

Θ	36000
D_c [mm]	13.3^+
L [mm]	17.6^-
F_s [mm]	3.00^+
F_t [mm]	0.36^+
P_l [mm]	12.7^-
P_t [mm]	30.3
Re_{Dc}	300^-
ΔT [°C]	30.0^+

All parameters are pushed to a bound except the transverse tube spacing P_t. Had a range on η_{fm} been set, it would have been pushed to its upper limit. Θ prefers thin heat exchangers with sparse, thick fins, and large-diameter tubes spaced close together in the longitudinal direction but fairly wide apart in the transverse direction. This layout differs from the *j/f* results in that *j/f* prefers a dense fin layout rather than sparse fins, and *j/f* preferred close transverse tube spacing. Θ was also maximized in relation to another parameter, ΔT^* (ΔT dimensionally), which was pushed to its maximum value. A large ΔT may be good for the ratio of heat transfer over pumping power, but carries with it penalties at the compressor. Therefore in the next subsection we analyze a PEC that captures this effect.

3.1.3 Unconstrained Ω optimization

Table 3.4 shows the results of an optimization of Ω. In this optimization fixed values were set for the following terms: k_a^*, k_f^*, η_{fm}, a^*, and b^*. The values of a^* and b^* were obtained from a curve fit of a compressor map of a Copeland ZP32K3E-PFV scroll compressor (see Appendix B). The linear curve fit obtained from this map is

$$COP = a - b\Delta T$$
$$= 6.508 - 0.17923\Delta T_c \tag{3.2}$$

for condensers. The values of a and b are then cast to the nondimensional variables a^* and b^*.

Table 3.4 Optimal parameter values for Ω

Ω	7.3
D_c [mm]	13.3^+
L [mm]	17.6^-
F_s [mm]	3.00^+
F_t [mm]	0.36^+
P_l [mm]	12.7^-
P_t [mm]	30.3
Re_{Dc}	300^-
ΔT [°C]	0.5

This ideal geometry and Reynolds number is exactly the same as for the Θ optimization. The only difference is in the ΔT term, which is optimal at a point within its defined range. The optimal ΔT is a result of increased compressor power required for increasing ΔT. This temperature difference is not pushed to its minimal value because of the competing effects of heat transfer/pumping power and heat transfer/compressor power in the definition of Ω (see Equation 2.20). A minimal ΔT would be beneficial for the 1/(1+COP) term, but negatively affects the 1/Θ term. Thus, the optimum ΔT can be viewed as a compromise that equalizes the rate of change of heat transfer/pumping power and heat transfer/compressor power. Since compressor power changes greatly with changes in condensing temperature, the optimal value for ΔT is near the low end of its range.

3.2 Design implications for component-level PEC

The next step in analyzing the optimal design point obtained from PEC maximization requires listing the appropriate equations governing heat exchanger

performance. The variables that have been predetermined from the optimal design point can then be viewed as a subset of all the variables describing heat exchanger performance. The remaining degrees of freedom may require setting values for frontal area, heat duty, etc. to complete a design specification.

We are primarily interested in the effects of the optimal PEC layout on dimensional heat transfer and pressure drop. These terms are calculated using the conservation of momentum and heat transfer rate equations, Equations 2.9 and 2.10. Since the PEC are functions of nondimensional variables, it is beneficial to also list these equations as functions of nondimensional variables, normalized by the same repeating parameters as used in the PEC analysis. In this way it can be seen directly which parameters are known or unknown after PEC optimization. The nondimensional heat exchanger equations are then expressed as follows:

$$\Delta p^* = \frac{1}{2}\left(V_{fr}^*\right)^2\left(\frac{A_{fr}}{A_{\min}}\right)^2\left(\frac{A_T}{A_{\min}}\right)f \tag{3.3}$$

$$\left(\frac{q}{A_{fr}}\right)^* = \varepsilon V_{fr}^* \Delta T^* \tag{3.4}$$

The nondimensional variable V_{fr}^* can be substituted with Re_{Dc} from Equation 2.5. The equations that result are

$$\Delta p^* = \frac{1}{2}\left(\frac{\mathrm{Re}_{D_c}}{D_c^*}\right)^2\left(\frac{A_T}{A_{\min}}\right)f \tag{3.5}$$

$$\left(\frac{q}{A_{fr}}\right)^* = \frac{\varepsilon\,\mathrm{Re}_{D_c}\,\Delta T^*}{D_c^*}\left(\frac{A_{\min}}{A_{fr}}\right) \tag{3.6}$$

with the following variables involved in each equation:

Momentum: $L^*, F_s^*, F_t^*, P_l^*, P_t^*, \mathrm{Re}_{D_c}, D_c^*, \Delta p^*$ (3.7)

Heat rate: $L^*, F_s^*, F_t^*, P_l^*, P_t^*, \mathrm{Re}_{D_c}, D_c^*, k_a^*, k_f^*, (q/A_{fr})^*, \Delta T^*$ (3.8)

See Appendix A for a listing of the formulae of all the newly introduced nondimensional variables (Δp^*, k_f^*, $(q/A_{fr})^*$, and ΔT^*). A maximum value of each of the PEC is obtained with optimal values for the nondimensional terms that comprise it. For the three component-level PEC studied, optimal values were obtained for the following terms (not including the fixed variables):

$$\left(\frac{j}{f}\right)_{optimal} = \frac{j}{f}\left(L^*, F_s^*, F_t^*, P_l^*, P_t^*, D_c^*, \mathrm{Re}_{D_c}\right) \tag{3.9}$$

$$\Theta_{optimal} = \Theta\left(L^*, F_s^*, F_t^*, P_l^*, P_t^*, D_c^*, \mathrm{Re}_{D_c}, \Delta T^*\right) \tag{3.10}$$

$$\Omega_{optimal} = \Omega\left(L^*, F_s^*, F_t^*, P_l^*, P_t^*, D_c^*, \mathrm{Re}_{D_c}, \Delta T^*\right) \tag{3.11}$$

The optimized variables can be compared to the parameter lists (3.7 and 3.8) for the pressure drop and heat transfer rate equations. The remaining degrees of freedom can then be seen. For *j/f*, we can see that the seven variables in the optimal design point have already defined Δp^* in the momentum equation. However, for the energy equation, three of k_a^*, k_f^*, $(q/A_{fr})^*$, or ΔT^* must be specified in order to determine the value of the fourth variable. In this analysis we will assume k_a^* and k_f^* are fixed to values representing air as the external fluid and aluminum as the heat exchanger material. Then only the nondimensional $(q/A_{fr})^*$ and ΔT^* terms remain. Their relationship is fixed by Equation 3.6.

The PEC *j/f* gives us an optimal geometry and Reynolds number. If a value for $(q/A_{fr})^*$ is then fixed after the optimization, possibly as a design goal, the result of

applying Equation 3.6 is a value for ΔT^*. The opposite is also true — fixing ΔT^* results in a value for $(q/A_{fr})^*$. Therefore, an ideal geometry determined by *j/f* maximization is valid for *paired* values of ΔT^* and $(q/A_{fr})^*$ as determined by the nondimensional heat transfer rate equation. While the nondimensional pressure drop is a result of the *j/f* maximization, completing the heat transfer analysis requires specification of either of the two terms as an input to determine the other. Therefore the optimization is independent of q/A_{fr} or condensing temperature. When dimensional conversions are included (specification of air at an ambient temperature), a possible result is a heat exchanger design that can only achieve required heat capacities by having a large ΔT.

In contrast, Θ and Ω include the term ΔT^* *within* the optimization process. The result is an optimal value for $(q/A_{fr})^*$. With specification of air as the external fluid, the unconstrained optimizations of Θ and Ω result in fixed q/A_{fr} values. These values are shown in Table 3.5. Table 3.5 also contains unconstrained optimizations for other surface types, which are discussed in section 3.3. The benefit of Θ and Ω over *j/f* is that optimizations can be run for a constrained q/A_{fr}, which changes the optimal design point. Such a constraint might be applied to reflect packaging or cost concerns. As seen in Equation 3.6, if a value for $(q/A_{fr})^*$ is fixed on the left-hand side of the equation, an optimization can still be done for the variables on the right-hand side of the equation, but the combination of these variables must also satisfy the equation. These types of optimizations are covered in Chapter 4.

As an example of using these unconstrained optimizations in a design method, consider the optimization of a condenser for a typical split system air conditioner. The condenser has an available face area of 1.4 m^2 and a required heat rejection of 14 kW, yielding a value for q/A_{fr} of 10 kW/m^2. The ambient temperature is assumed to be 35°C. If the heat exchanger is designed using the optimal *j/f* layout shown in Table 3.2, with an airflow corresponding to a Reynolds number of 300, the required condensing temperature of the refrigerant would be over 130°C! This result is unrealistic, and illustrates the fact that *j/f* optimization assumes any amount of frontal area is available to achieve a desired

heat rejection. The PEC *j/f* does not account for the *magnitudes* of either *j* or *f*, only their ratio.

Next consider the PEC Θ. In this case, optimization of Θ determines the optimal ΔT^*. With an "unconstrained" optimization of Θ, only one of either the heat transfer rate or the face area may be specified. Assume we still wish to reject 14 kW of heat. Using the optimal geometry shown in Table 3.3, the required area would then be 2.9 m^2, more than twice the area we had intended to use. This required area would be reduced if the upper limit on ΔT^* was set higher for the optimization, because a larger temperature difference would be available to achieve the design goal of 14 kW, although compressor power requirements would also increase, which this PEC does not account for.

With the third component-level PEC, Ω, the required face area becomes ridiculously large, at over 170 m^2. This large face area is due to the low condensing temperature of 35.5°C, less than one degree above ambient. The previous PEC, Θ, optimized the heat exchanger without regard for refrigerant side penalty, so the condensing temperature soared. Ω accounts for the refrigerant side penalty, so instead the required face area suffers because its only cost penalty in this PEC, increased pumping power, is small in comparison to increased compressor power requirements.

3.3 Unconstrained optimization for other fin types

Similar unconstrained optimizations were performed for wavy, slit, and louvered fin surface types. The results are summarized in Table 3.5, along with the plain-fin results for comparison. The surface types with more complex fins were optimized with respect to the same parameters as plain fins, plus other parameters used to describe the fins. Colburn *j* and *f* factor correlations describing the performance of wavy fins include the variable W_h^*, the nondimensional wave height. The correlations for both the *j* and *f* factor for wavy fins were obtained from Mirth and Ramadhyani (1994). Slit fins include S_h^*, the nondimensional slit height (distance offset from the fin surface), and S_w^*, the nondimensional slit width transverse to the airflow. The *j* and *f* correlations for slit fins were obtained from a new study by Wang and Du (2001). For louvers, the

nondimensional parameters L_h^* and L_p^* denote the louver height and pitch, respectively. The correlations used for louvered fins were taken from Wang *et al.* (1999). Louver angle, θ, is related to L_h^* and L_p^* through the following equation:

$$\tan\theta = \frac{L_h}{L_p} = \frac{L_h^*}{L_p^*} \tag{3.12}$$

It is important to note that when comparing PEC values for different surfaces, ranges of the correlations used in the optimization should be considered. For instance, the wavy fin optimization of Θ shows a very small value for Θ compared to the other surface types. This difference is due mainly to the underlying correlations having a minimum Reynolds number of 1100, compared to 300-350 for the other surface types, and a minimum number of tube rows of 4, while the other correlations had single-tube-row minimums. The combination of these two differences makes minimal pumping power for this optimization much higher than for the other surface types, which is penalized heavily by Θ. Full range listings for all the correlations used in this model are shown in Appendix C.

Table 3.5 shows the maximized values of the PEC, along with both quantitative and qualitative information on the direction in which variables were pushed to achieve the optimization. As with the earlier tables in this chapter, a (-) superscript denotes the variable was pushed to its lower limit, (+) denotes the upper limit, and lack of a superscript means the optimal value was found within the specified range. For correlations based on one value of a particular parameter (e.g. only one tested tube collar diameter), the combination (+-) is shown because this variable was not allowed to change. Since no fixed value of q/A_{fr} is set for these runs, any amount of frontal area is available to size the heat exchangers for a specified heat duty. Having no constraint on frontal area can be seen to yield an unrealistic result in some cases.

For the PEC *j/f*, maximum values were 0.85, 0.72, 4.59, and 3.72 for plain, wavy, slit, and louvered fins respectively. This result shows that *j/f* prefers slit fins as the best

enhancement strategy. However, the slit fin optimum resulted in a very small f factor. Although ranges were set on the limits of the variables used in the heat exchanger testing, the specific combination of parameters in this optimal point may be an untested design with effects on the f factor not accounted for in the development of the correlation. Nevertheless, with a different optimal geometry and Reynolds number, Θ and Ω also ranked slit fins as the best heat transfer enhancement method, followed by plain fins, louvered fins, and wavy fins.

Regarding the geometry of the enhanced fin surfaces, all PEC were agreed as to the direction of improvement of specific geometric features. For wavy fins, increasing the wave height aids in PEC maximization. For slit fins, increased slit width transverse to the airflow is seen as beneficial. The range of slit heights used in testing does not allow a adequate prediction of their effect on PEC value. Louvered heat exchangers are seen to benefit from decreased louver heights and increased louver pitch.

Table 3.5 includes information on the ideal q/A_{fr} that results from optimizations of Θ and Ω. This value is obtained with the assumption of air as the external fluid. As explained in section 3.1.2, Θ requires a large ΔT to maximize its value, which increases q/A_{fr}. However, q/A_{fr} is then limited by reduced airflow, sparse fin geometry, and shallow heat exchanger depth. The lowest number of tube rows for wavy fins is 4 for the correlations that were used, and the minimum Reynolds number is higher than the other surface types, resulting in a much higher q/A_{fr} than the other enhancements due to increased total heat transfer area in the airflow direction. While q/A_{fr} is high in comparison to the other surface types, the value of maximum Θ is much lower because of the extra pumping power required to push air through the heat exchanger. For Ω, large condensing temperatures are penalized but frontal area is not; therefore, the resulting q/A_{fr} values are low.

3.4 Unconstrained COP optimization

With the same fixed parameters as used in the component-level PEC analysis, the optimal point determined by the system-level PEC COP has a functional form similar to that of Θ and Ω, except for both an evaporator and condenser:

$$COP_{optimal} = COP\left(\begin{matrix}\left\{L^*, F_s^*, F_t^*, P_l^*, P_t^*, D_c^*, \mathrm{Re}_{D_c}, \Delta T^*\right\}_{evap}, \\ \left\{L^*, F_s^*, F_t^*, P_l^*, P_t^*, D_c^*, \mathrm{Re}_{D_c}, \Delta T^*\right\}_{cond}\end{matrix}\right) \tag{3.13}$$

Therefore, like Θ and Ω, unconstrained optimization yields a value for q/A_{fr}. Tables 3.6 and 3.7 summarize the results of unconstrained COP optimization. Fixed values of sensible heat transfer for the condenser and evaporator are listed in order to see the effect on required frontal area.

Note that the condenser and evaporator are optimized nearly identically. The evaporator ΔT is too small for latent heat transfer in this case. Also, note that the unconstrained optimizations of COP yield almost exactly the same results as unconstrained Ω optimization. The main difference is the ideal ΔT obtained, due to a more accurate quadratic-linear curve fit for the compressor COP term (as compared to the single-variable linear fits for the component-level optimizations). This curve fit is expressed as follows (see Appendix B):

$$\begin{aligned} COP_{comp} &= \left(-2113.22 + 8.5198T_e\right) \\ &+ \left(11.604 - 0.046894T_e\right)T_c \\ &+ \left(-0.016021 + 6.489\times10^{-5}T_e\right)T_c^2 \end{aligned} \tag{3.14}$$

3.5 PEC summary

In this chapter, the behaviors of four PEC were analyzed: *j/f*, Θ, Ω, and COP. Ideal geometries were obtained using each PEC without system design constraints. Currently available correlations for plain, wavy, slit, and louvered fin heat exchangers were used for the *j* and *f* factor in all four PEC. The ideal geometry for *j/f* was shown to

be independent of heat load or surface temperature of a heat exchanger. The result is that application of the maximum *j/f* criterion can result in a design which either a) requires an excessive frontal area, or b) requires excessive refrigerant side temperatures. The PEC *j/f* therefore would be better suited as a comparison tool for equal-duty heat exchangers rather than as a design tool. The definition of Θ included more parameters than *j/f* and thus could be optimized with respect to a temperature difference term, in addition to the terms used in *j/f* optimization. The optimum Θ criterion maximizes heat transfer per unit pumping power by requiring a large refrigerant side temperature. Ω improves upon Θ by accounting for the refrigerant side temperature through its effect on compressor work, and therefore results in an optimum design requiring a large frontal area. COP shows similar characteristics as Ω in requiring large face areas for an unconstrained optimization.

With these drawbacks it seems that unconstrained optimization of a PEC always results in an unusable geometry. The primary usefulness of a PEC, however, can be seen when optimizing heat exchangers using constraints. A constraint such as a fixed value for nondimensional q/A_{fr} may be employed for all the PEC analyzed except *j/f*, resulting in reduced optimal PEC value, but a heat exchanger which efficiently meets design requirements. Chapter 4 continues the evaluation of these PEC using various constraints, which highlight more of each PEC's features and usefulness in system design.

Table 3.5 Unconstrained optimization on plain, wavy, slit, and louvered fins

(a)

	Plain fins			*Wavy fins*		
j/f	0.85			0.72		
Θ		36000			1500	
Ω			7.3			6.7
D_c [mm]	13.3^+	13.3^+	13.3^+	16.7^+	16.7^+	16.7^+
L [mm]	18^-	18^-	18^-	110^-	110^-	110^-
F_s [mm]	1.1^-	3.0^+	3.0^+	1.5^-	3.1^+	3.1^+
F_t [mm]	0.36^+	0.36^+	0.36^+	0.15^{+-}	0.15^{+-}	0.15^{+-}
P_l [mm]	13^-	13^-	13^-	32^+	28^-	28^-
P_t [mm]	20^-	30	30	32^-	38^+	38^+
Re_{Dc}	300^-	300^-	300^-	1100^-	1100^-	1100^-
ΔT [°C]		30.0^+	0.5		30.0^+	2.4
W_h [mm]				3.2^+	3.2^+	3.2^+
S_h [mm]						
S_w [mm]						
L_h [mm]						
L_p [mm]						
q/A_{fr} [W/m^2]		4700	80		20000	1600

(b)

	Slit fins			*Louvered Fins*		
j/f	4.59			3.72		
Θ		120000			11000	
Ω			7.4			7.2
D_c [mm]	9.5	16^+	16^+	6.9^-	10.4^+	10.4^+
L [mm]	132^+	22^-	22^-	24	22	22
F_s [mm]	1.7	2.5^+	2.5^+	1.6	2.5^+	2.5^+
F_t [mm]	0.20^+	0.12^-	0.12^-	0.12^{+-}	0.12^{+-}	0.12^{+-}
P_l [mm]	33^+	33^+	33^+	22^+	22^+	22^+
P_t [mm]	25^-	25^-	25^-	18^-	19	19
Re_{Dc}	7000^+	350^-	350^-	1000	300^-	300^-
ΔT [°C]		30.0^+	0.3		30.0^+	0.9
W_h [mm]						
S_h [mm]	1.0^{+-}	1.0^{+-}	1.0^{+-}			
S_w [mm]	18^+	18^+	18^+			
L_h [mm]				0.8^-	0.8^-	0.8^-
L_p [mm]				3.8^+	3.8^+	3.8^+
q/A_{fr} [W/m^2]		2700	25		7200	210

Table 3.6 Unconstrained system optimization with plain and wavy fin heat exchangers

	Plain		*Wavy*	
	Evaporator	*Condenser*	*Evaporator*	*Condenser*
COP_{system}	9.78		6.34	
N	1.4	1.4	4.0	4.0
D_c [mm]	13.3^{+}	13.3^{+}	16.7^{+}	16.7^{+}
L [mm]	18^{-}	18^{-}	110^{-}	110^{-}
F_s [mm]	3.0^{+}	3.0^{+}	3.1^{+}	3.1^{+}
F_t [mm]	0.36^{+}	0.36^{+}	0.15^{+-}	0.15^{+-}
P_l [mm]	13^{-}	13^{-}	28^{-}	28^{-}
P_t [mm]	30	30	38^{+}	38^{+}
W_h [mm]			3.3^{+}	3.3^{+}
S_h [mm]				
S_w [mm]				
L_h [mm]				
L_p [mm]				
Re_{Dc}	300^{-}	300^{-}	1100^{-}	1100^{-}
q_s [W]	7680	14000	7680	14000
q_l [W]	0		0	
A_{fr} [m^2]	68	130	2.45	4.62
ΔT_{max} [°C]	0.7	0.7	4.8	4.6
Δp [Pa]	0.14	0.15	11	12
V_{fr} [m/s]	0.18	0.18	0.55	0.58
V_{dot} [m^3/s]	12.09	23.90	1.36	2.69
W_{fan} [W]	11	17	98	149
W_{comp} [W]	756		949	
Vol_{fin} [m^3]	0.1455	0.2747	0.0133	0.0250

Table 3.7 Unconstrained system optimization with slit and louvered fin heat exchangers

	Slit		*Louver*	
	Evaporator	*Condenser*	*Evaporator*	*Condenser*
COP_{system}	10.12		9.53	
N	0.7	0.7	0.9	0.9
D_c [mm]	16.0^{+}	16.0^{+}	10.4^{+}	10.4^{+}
L [mm]	22^{-}	22^{-}	14^{-}	14^{-}
F_s [mm]	2.5^{+}	2.5^{+}	2.5^{+}	2.5^{+}
F_t [mm]	0.12^{-}	0.12^{-}	0.12^{+-}	0.12^{+-}
P_l [mm]	33^{+}	33^{+}	15	15
P_t [mm]	25^{-}	25^{-}	24	24
W_h [mm]				
S_h [mm]	1.0^{+-}	1.0^{+-}		
S_w [mm]	18^{+}	18^{+}		
L_h [mm]			0.8^{-}	0.8^{-}
L_p [mm]			3.8^{+}	3.8^{+}
Re_{Dc}	350^{-}	350^{-}	300^{-}	300^{-}
q_s [W]	7680	14000	7680	14000
q_l [W]	0		0	
A_{fr} [m^2]	216	407	44	83
ΔT_{max} [°C]	0.4	0.4	1.0	0.9
Δp [Pa]	0.04	0.04	0.21	0.23
V_{fr} [m/s]	0.12	0.12	0.24	0.26
V_{dot} [m^3/s]	25.49	50.53	10.74	21.27
W_{fan} [W]	6	9	15	23
W_{comp} [W]	743		766	
Vol_{fin} [m^3]	0.2278	0.4299	0.0276	0.0522

Chapter 4 – Constrained Optimization Results and Discussion

The previous chapter dealt with optimizations yielding highest possible PEC values, without regard for their implications on a real system. These optimizations were done in order to gain a better understanding of how a maximization of each PEC will affect a heat exchanger in its most extreme case. This chapter deals with placing limitations on the combinations of variables that can result from an optimization, therefore yielding lower PEC values than an unconstrained case, but providing geometry and operating conditions of a heat exchanger that can satisfy system requirements.

Using the nondimensional forms of the heat exchanger performance equations along with the defined PEC equations, a constrained optimization method can be implemented to compare heat exchangers of different surface types, as well as improving designs of particular surface types. The following sections detail the constrained optimization model and some examples of its use. The order of sections in the chapter attempts to outline the use of the model starting from simple applications (i.e. improving an existing heat exchanger by altering fin spacing), and moving towards the more complex tasks of determining heat exchanger designs to maximize COP for an entire system.

4.1 PEC optimization on a single parameter

One of the benefits of using a PEC is the ability to improve upon an existing heat exchanger design. Such improvements can be done for any single parameter of the heat exchanger, such as fin spacing, tube spacing, Reynolds number, etc., as long as j and f factor correlations exist for that class of heat exchanger. The correlations must also include the parameter of interest as an independent variable. All other parameters are fixed to their baseline values, including the face area and heat transfer rate. Fixing these values constrains the optimization to a simple 1 degree-of-freedom case for quick design comparisons.

Figure 4.1 show trends for varying single parameters on a condenser while holding other parameters at their baseline value (see the condenser geometry in Table 4.7 for baseline values). The baseline condenser was a plain-fin 14kW design taken from a typical split system air conditioner. The parameters chosen for analysis were fin spacing and Reynolds number, due to changing trends when compared with different PEC. Baseline values are shown as single data points on each plot. Ideally they should fall precisely on each trend line; however, they sometimes do not because of the finite number of simulation runs performed to obtain each curve fit.

When comparing PEC trends for fin spacing on plots (a), (c), and (e) of Figure 4.1, *j/f* and Ω show that denser fins are beneficial to this design whereas Θ shows that a sparse fin arrangement is better. For *j/f*, this result means that the correlations suggest that *j* factors decrease at a faster rate than *f* factors as the fin spacing is increased. The results for Θ can be explained by its definition. Since Θ values heat transfer in relation to pumping power, a sparse fin arrangement allows decreased pumping power while the heat transfer can be maintained by a higher condensing temperature. The PEC Ω includes this penalty and thus reverses the trend back to that shown by *j/f*. Note that the baseline heat exchanger chosen for this example has a dense fin geometry in which the fin spacing is actually slightly under the range of the correlations used.

For the Reynolds number, both *j/f* and Θ indicate that a minimum value of Re_{Dc} maximizes PEC value. For *j/f*, higher *j* factor values for low face velocities in tested heat exchangers can explain this trend. Θ is concerned primarily with minimizing the pumping power and therefore relies on higher refrigerant side temperature for increasing heat transfer. Lower Reynolds numbers require less pumping power and is thus seen as beneficial. The plot of maximum Ω vs. Reynolds number differs from that of the other PEC in that it displays a local maximum. With Ω as a rating method, an ideal Reynolds number exists for this heat exchanger to operate most effectively. This value of Re_{Dc} balances out the pumping power requirement and the compressor penalty associated with increased required condensing temperatures as the airflow is decreased. The baseline value of Re_{Dc} is slightly below this ideal value.

4.2 Multidimensional optimization with constraints

As shown in Chapter 3, multidimensional optimizations can be performed using the PEC as rating criteria. These type of optimizations are independent of a baseline model, and can be used as a first step in heat exchanger design. In this section, constraints on q/A_{fr}, number of tube rows, and sensible heat ratio are imposed within the optimizations. Only the PEC Ω and COP are discussed with these constraints, as they have shown to provide more comprehensive heat exchanger evaluation than either *j/f* or Θ. As explained in Chapter 3, since *j/f* is not a function of ΔT or q/A_{fr}, the optimum point determined from its maximization is independent of constraints on these parameters. With Θ, since its definition is heat transfer/pumping power, fixing a value for q/A_{fr} simply leads to a minimal pumping power optimum with no regard for the value of the *j* factor; ΔT is pushed to its maximum to provide the necessary heat transfer, increasing compressor power requirements that are better accounted for in Ω and COP.

4.2.1 Condenser modeling

Modeling a condenser involves setting ranges on the nondimensional parameters for an external fluid at a set ambient temperature. Limits are set on nondimensional parameters rather than dimensional parameters so the solution may be valid for more than one fluid type. However, the results of the optimizations in this section are presented in dimensional terms using air at an ambient temperature of 35°C. q/A_{fr} is fixed in order to obtain a reasonable volume and cost of the heat exchanger. For *j/f* the optimal geometry applies to all values of q/A_{fr} because it is independent of ΔT^*. For Θ, a fixed q/A_{fr} simply leads to the minimization of pumping power per unit frontal area. It is with the application of constraints that the PEC Ω shows its greatest value in comparing heat exchanger designs. By setting values of required q/A_{fr}, more realistic geometries are obtained in the optimization process which reduce the maximum value of the PEC but at the same time enable useful comparisons to be made of different fin surface types. As explained in Chapter 3, this type of constraint, with the assumption of an external fluid for the normalizing parameters, fixes the left-hand side of the nondimensional heat rate equation:

$$\left(\frac{q}{A_{fr}}\right)^{*} = \frac{\varepsilon \,\mathrm{Re}_{D_c}\, \Delta T^{*}}{D_c^{*}}\left(\frac{A_{\min}}{A_{fr}}\right) \tag{3.6}$$

Therefore the geometry, Reynolds number, and temperature difference are limited to combinations that result in the required q/A_{fr}. Table 4.1 shows PEC optimizations performed with a constraint of $q/A_{fr}=10kW/m^2$. In this table it can be seen that the application of the constraint reduces the maximum value of the PEC compared to the unconstrained maximization in Table 3.5. Slit and louvered fins are shown to have very small pressure drops, resulting in low pumping power requirements. The small pressure drops are caused by the optimizations identifying geometries that result in low friction factors. With the low friction factor, volumetric flow across the heat exchanger can be fairly high without a large penalty in pumping power.

Figure 4.2 further compares optimal values of Ω for different constraints on q/A_{fr}. All fin surfaces show the same trend of decreased Ω as q/A_{fr} is increased. Therefore, this PEC considers limited frontal area (high heat transfer rates per unit frontal area) a hindrance to heat exchanger performance. This figure also reveals the amount of Ω penalty associated with higher q/A_{fr}. Slit fins are shown to have less of a penalty on Ω as q/A_{fr} is increased, due to its smaller slope when compared to the other surface types.

The heat exchanger geometries obtained in Table 4.1 are allowed to have any number of tube rows required to maximize the value of the PEC. In Tables 4.2-4.5 tube row constraints are applied in addition to the q/A_{fr} constraint, in order to view PEC value as a function of heat exchanger depth. The depth of the heat exchanger, which depends on the number of tube rows, is important in material cost considerations, as many condensers in use today have single tube rows. Approximate fin volume is included in Tables 4.2-4.5, in which the amount of aluminum that can be saved with thinner designs, with various effects on PEC value and optimal geometry, can be seen. Plain fins showed no change in the optimal point except for the required changes in depth of the heat

exchanger. Wavy fins required a smaller Reynolds number for increasing heat exchanger depth. For slit fins, the fin density decreased as well as Reynolds number for greater numbers of tube rows. The optimal louver fin geometry changed little with increasing heat exchanger depth.

The overall PEC value results for differing numbers of tube rows are summarized in Figure 4.3. An ideal number of tube rows within the range shown exists for louvered fins. Using a thinner design (i.e. single tube row) would require weighing the savings in material costs versus heat exchanger efficiency. Wavy fins actually show a decrease in Ω value for thicker designs; therefore, a thinner design saves material and improves performance. Slit fins are shown to have their best PEC value at 4 tube rows. However, with thinner slit-fin designs comes a penalty in efficiency. Reducing the thickness to 2 tube rows has a smaller effect on efficiency as compared to the drop from 2 to 1. Plain fins show a similar trend of decreased performance with less tube rows. Therefore, a cost analysis may be able to determine the optimal heat exchanger depth in these cases, as with the louvered fin case.

4.2.2 Evaporator modeling

Modeling an evaporator includes the transfer of latent heat as well as sensible heat. The addition of latent heat transfer does not affect the PEC *j/f* except through the use of wet correlations; however, it affects the three other PEC due to their use of a heat transfer term. Rather than only using the sensible heat transfer term q_s, a total evaporator heat transfer term is used:

$$q_{evap} = q_{s,evap} + q_{l,evap} \tag{4.1}$$

To implement latent heat transfer in the model, additional equations were added. The governing equation is as follows:

$$q_l = \eta_0 h_D A_T (w_{in} - w_{sat}) h_{fg} \tag{4.2}$$

Surface efficiency is described in Appendix B. The mass transfer proportionality constant h_D is expressed as

$$h_D = \frac{h_c}{c_{pm} Le^{2/3}} \tag{4.3}$$

where c_{pm} is the specific heat of moist air. Calculating the latent heat transfer requires determination of the heat transfer coefficient under wet surface conditions (using wet *j* and *f* correlations). Obtaining the heat transfer coefficient requires specification of external fluid type to extract the coefficient from the nondimensional variables used in the model. Therefore, the evaporator analysis is limited to the use of air as the external fluid, with a given relative humidity in order to calculate the specific humidity ratios. The inlet air humidity ratio ω_{in} is calculated from at the ambient air temperature and RH. The latent heat of vaporization h_{fg} is evaluated at the evaporating temperature. The saturated air humidity ratio is calculated at a surface temperature equal to the following:

$$T_{surf} = T_{amb} - \eta_0 \Delta T \tag{4.4}$$

This equation was obtained from the following relationship:

$$\begin{aligned} q_s &= \eta_0 hA\left(T_{air} - T_{evap}\right) \\ &= hA\left(T_{air} - T_{surf}\right) \end{aligned} \tag{4.5}$$

in which the tube wall thermal resistance is negligible. Therefore T_{surf} is the average wetted surface temperature, which is greater than the base (tube surface) temperature.

The ARI standard capacity rating point for unitary air conditioners is T_{indoor}=26.7°C (80°F) and T_{wb}=19.4°C (67°F). At this point, the following sensible-to-total heat transfer ratio exists for many air conditioners:

$$q_{rat} = \frac{q_s}{q_t} = \frac{q_s}{q_s + q_l} = 0.75 \tag{4.6}$$

Designing an evaporator to this rating point ensures that the evaporator provides adequate dehumidification of the incoming air. Therefore, Equation 4.6 was added to the model as a constraint. The addition of this equation reduces the combinations of independent parameters that can satisfy all the constraints, as did the q/A_{fr} constraint. Thus, the optimal PEC value is further reduced from the unconstrained case.

Wet *j* and *f* factor correlations were used for evaporator analysis. The wet plain-fin correlations used were from Wang *et al.* (1996). Wavy-fin optimizations still used Mirth and Ramadhyani (1994). Their *j* factor results for wet conditions had mixed results, with data points both over and under the dry *j* factor prediction. Because of these results, they did not present a separate correlation for the wet *j* factor. Therefore, the same *j* factor they obtained under dry conditions was used for wet conditions. Their friction factor results differed more from the dry case, however, and they added a wet friction factor multiplier to predict performance. For slit fins, Kim and Jacobi (2000) provided wet *j* and *f* factor correlations, although their testing was limited to heat exchangers of varying depth, fin spacing, and Reynolds number. For instance, all the tested heat exchangers had the same tube collar diameter and fin thickness, limiting the range of the optimization process when used in this model. Louvered-fin correlations under wet conditions were obtained from Wang *et al.* (2000).

Table 3.7 shows the results of evaporator optimization using the Ω criterion. Three constraints were imposed on the model to obtain these numbers:

- $q_s = 7680$ W
- $q_l = 2560$ W
- $A_{fr} = 0.32$ m^2

These constraints combine the q/A_{fr} and sensible heat ratio constraints. Slit fins are shown to have lower performance than the other surface types in Table 4.6. Note, however, that the available *j* and *f* correlations for slit fins are applicable to only a narrow range of geometries, when compared to the other correlations. In addition, condensate retention plays a major role in affecting the performance of wet evaporators with interrupted surfaces. Bridging of condensate between louvers and slits can negate the benefits of these enhancements by resulting in channel flow of the air through the heat exchanger rather than enhancement-directed flow. With regard to the amount of material used for each type of heat exchanger, the fin volume required for these designs decreases as one moves from the highest to lowest performance design.

4.2.3 System optimization

The previous analyses enabled optimization of a single heat exchanger, including such additional components as the fan and compressor. Performing separate optimizations for a condenser and evaporator may lead to differing power requirements for the compressor, which may result in inefficiencies once the new designs are implemented into a system. In order to use the optimization model for complete system design, the evaporator and condenser must be linked to the same compressor. A proper curve fit must be used to model the compressor power, one that takes into account both condensing and evaporating temperatures. Once this model is in place, the goal of finding maximum COP for a given system is possible once proper ranges are set for the design variables.

System COP was the fourth PEC studied, one that is used commonly as a measure of comparison for different air conditioning and refrigeration systems. Table 4.7 displays baseline data for a plain-fin split system air conditioner using all the previously defined equations and assumptions in this model. This table can be used for comparison with the optimization results. Tables 4.8 and 4.9 display the COP optimization results for the four surface types analyzed. Constraints on face areas, sensible and latent heat transfer were also implemented as described in the component optimization sections.

From observation of the maximum COP values in the tables, all optimizations were able to improve upon the baseline system. The optimal COP values did not vary greatly between the different surface types. Looking at the evaporator results, wavy-finned evaporators are shown to have the lowest pumping power requirement, similarly to the Ω optimization result. With the imposed evaporator constraints, Ω and COP prefer wavy fins over the other surface types in this analysis. Another important feature to note in the tables is the amount of fin volume required for the various designs. The louver results yield the minimum overall amount of fin material required and may be a more cost effective method of designing a split system air conditioner than the baseline design. The reduced fin volume can be attributed to decreased heat exchanger depths and wider fin spacing than the plain and slit fin optima.

When the evaporator results from system COP optimization are compared to component-level Ω evaporator optimization (with the q/A_{fr} constraints imposed), the results are nearly identical except for small differences for the wavy fin case. The implication is that a component-level PEC with the proper constraints may be able to yield the same results as a system-level PEC. When the Ω and COP optimizations are compared for condensers, more differences can be seen. All optima except wavy fins have larger Reynolds numbers for COP optimization than Ω optimization. However, slit fin geometrical results for the condenser are identical for the two cases. The plain fin optima are very different. With COP optimization, the ideal condenser has 3 tube rows, while the Ω optimization yielded over a 7 row heat exchanger. The differences in PEC value between these two designs may be small, however, because of relative insensitivity of PEC value to heat exchanger depth in this range. Again, a cost analysis would prove beneficial in determining an optimal heat exchanger depth in this case.

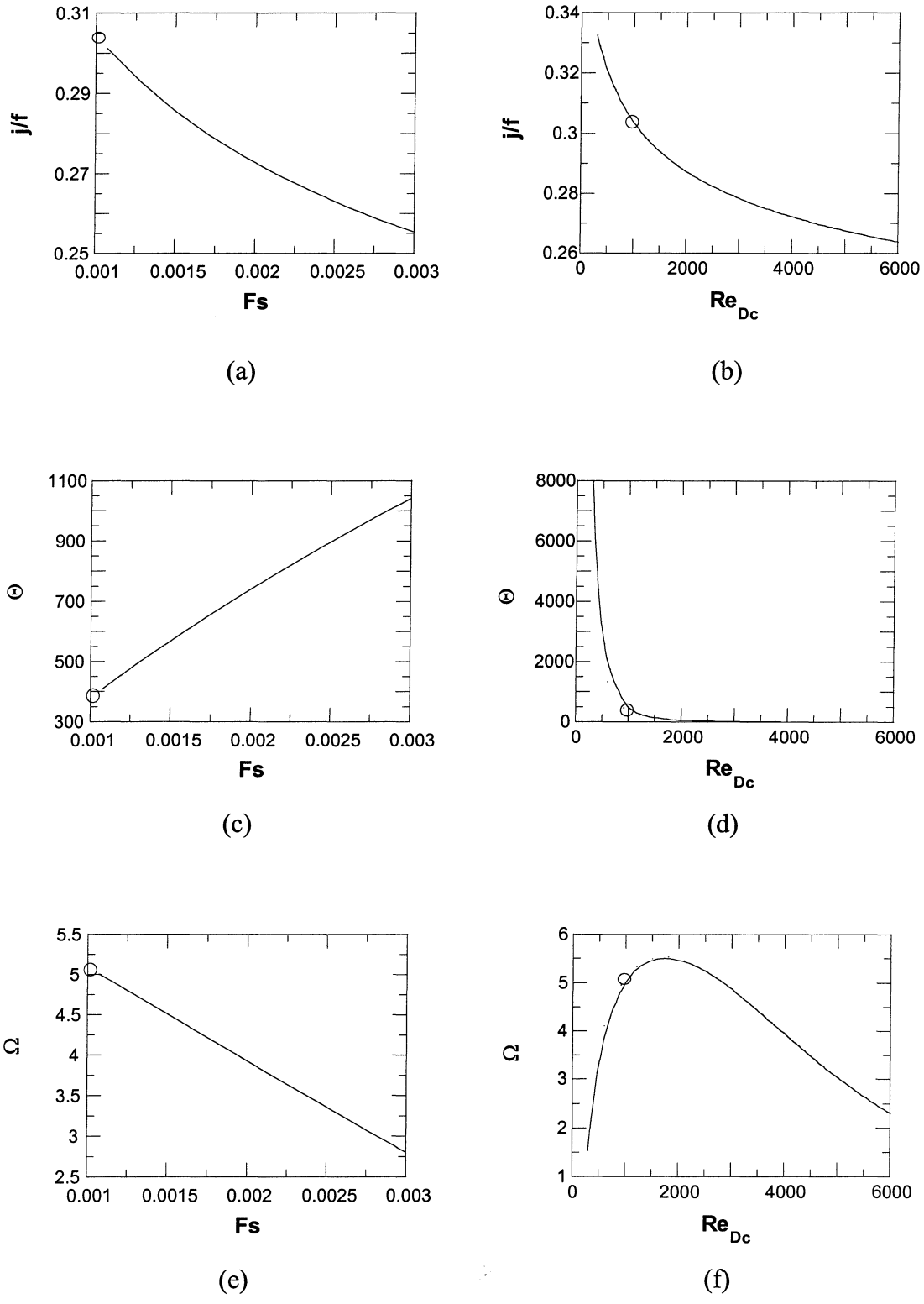

Figure 4.1 Max PEC values for varying fin spacing and Re_{Dc} on a plain fin-on-tube condenser (data point on each plot denotes baseline value)

Table 4.1 Condenser optimization with $q/A_{fr}=10kW/m^2$

	Plain	*Wavy*	*Slit*	*Louver*
Ω	5.9	5.8	6.5	6.1
N	7.5	4.0	4.0	2.5
D_c [mm]	13.3^{+}	13.5^{-}	8.0^{-}	6.9^{-}
L [mm]	95	110^{-}	132^{+}	56
F_s [mm]	3.0^{+}	2.5	1.7	2.5^{+}
F_t [mm]	0.23	0.15^{+-}	0.17	0.12^{+-}
P_l [mm]	13^{-}	28^{-}	33^{+}	22^{+}
P_t [mm]	32^{+}	38^{+}	25^{-}	25^{+}
W_h [mm]		3.2^{+}		
S_h [mm]			1.0^{+-}	
S_w [mm]			18^{+}	
L_h [mm]				0.8^{-}
L_p [mm]				3.8^{+}
Re_{Dc}	2190	1800	2150	980
q [W]	14000	14000	14000	14000
A_{fr} [m^2]	1.4	1.4	1.4	1.4
ΔT_{max} [°C]	6.9	7.2	4.2	6.2
Δp [Pa]	15.6	16.0	4.4	10.8
V_{fr} [m/s]	1.45	1.34	2.71	1.62
V_{dot} [m^3/s]	2.03	1.88	3.79	2.27
W_{pump} [W]	151	143	79	117
W_{comp} [W]	2230	2250	2070	2190
Vol_{fin} [m^3]	0.0101	0.0092	0.0191	0.0036

Table 4.2 Plain fin optimization with $q/A_{fr}=10kW/m^2$ for differing numbers of tube rows

N	1	2	3	4	5
Ω	5.17	5.48	5.67	5.77	5.83
D_c [mm]	13.3^+	13.3^+	13.3^+	13.3^+	13.3^+
L [mm]	18^-	33	38	51	64
F_s [mm]	3.0^+	3.0^+	3.0^+	3.0^+	3.0^+
F_t [mm]	0.36^+	0.36^+	0.36^+	0.35	0.30
P_l [mm]	13^-	17	13^-	13^-	13^-
P_t [mm]	32^+	32^+	32^+	32^+	32^+
Re_{Dc}	4440	3270	3110	2790	2540
q [W]	14000	14000	14000	14000	14000
A_{fr} [m^2]	1.4	1.4	1.4	1.4	1.4
ΔT_{max} [°C]	10.8	9.2	8.1	7.5	7.2
Δp [Pa]	10.3	12.3	11.9	13.0	13.6
V_{fr} [m/s]	2.81	2.07	1.97	1.78	1.64
V_{dot} [m^3/s]	3.93	2.90	2.76	2.49	2.30
W_{pump} [W]	193	170	156	154	149
W_{comp} [W]	2520	2390	2310	2270	2250
Vol_{fin} [m^3]	0.0030	0.0056	0.0064	0.0082	0.0089

Table 4.3 Wavy fin optimization with $q/A_{fr}=10kW/m^2$ for differing numbers of tube rows

N	4	5	6
Ω	5.84	5.80	5.76
D_c [mm]	13.5^-	13.5^-	13.5^-
L [mm]	110^-	138	165
F_s [mm]	2.5	2.9	3.1^+
F_t [mm]	0.15^{+-}	0.15^{+-}	0.15^{+-}
P_l [mm]	28^-	28^-	28^-
P_t [mm]	38^+	38^+	38^+
W_h [mm]	3.2^+	3.2^+	3.2^+
Re_{Dc}	1800	1710	1640
q [W]	14000	14000	14000
A_{fr} [m^2]	1.4	1.4	1.4
ΔT_{max} [°C]	7.2	7.5	7.6
Δp [Pa]	16.0	17.0	18.6
V_{fr} [m/s]	1.34	1.29	1.24
V_{dot} [m^3/s]	1.88	1.80	1.73
W_{pump} [W]	143	146	154
W_{comp} [W]	2250	2270	2280
Vol_{fin} [m^3]	0.0092	0.0099	0.0114

Table 4.4 Slit fin optimization with $q/A_{fr}=10kW/m^2$ for differing numbers of tube rows

N	1	2	3	4
Ω	6.24	6.44	6.48	6.50
D_c [mm]	8.6	8.0^-	8.0^-	8.0^-
L [mm]	33	66	99	132^+
F_s [mm]	1.2^-	1.2^-	1.5	1.7
F_t [mm]	0.20^+	0.18	0.18	0.17
P_l [mm]	33^+	33^+	33^+	33^+
P_t [mm]	25^-	25^-	25^-	25^-
S_h [mm]	1.0^{+-}	1.0^{+-}	1.0^{+-}	1.0^{+-}
S_w [mm]	8^-	9	15	18^+
Re_{Dc}	3120	2210	2210	2150
q [W]	14000	14000	14000	14000
A_{fr} [m^2]	1.4	1.4	1.4	1.4
ΔT_{max} [°C]	5.8	4.5	4.4	4.2
Δp [Pa]	3.5	4.6	4.3	4.4
V_{fr} [m/s]	3.30	2.65	2.74	2.71
V_{dot} [m^3/s]	4.62	3.71	3.84	3.79
W_{pump} [W]	77	81	79	79
W_{comp} [W]	2170	2090	2080	2070
Vol_{fin} [m^3]	0.0076	0.0134	0.0165	0.0191

Table 4.5 Louvered fin optimization with $q/A_{fr}=10kW/m^2$ for differing numbers of tube rows

N	1	2	3	4	5
Ω	5.97	6.06	6.06	6.01	5.95
D_c [mm]	7.0	6.9^-	6.9^-	6.9^-	6.9^-
L [mm]	22	44	66	88	110
F_s [mm]	1.2^-	2.1	2.5^+	2.5^+	2.5^+
F_t [mm]	0.12^{+-}	0.12^{+-}	0.12^{+-}	0.12^{+-}	0.12^{+-}
P_l [mm]	22^+	22^+	22^+	22^+	22^+
P_t [mm]	25^+	25^+	25^+	25^+	25^+
L_h [mm]	0.8^-	0.8^-	0.8^-	0.8^-	0.8^-
L_p [mm]	3.8^+	3.8^+	3.8^+	3.8^+	3.8^+
Re_{Dc}	1000	1000	940	880	840
q [W]	14000	14000	14000	14000	14000
A_{fr} [m^2]	1.4	1.4	1.4	1.4	1.4
ΔT_{max} [°C]	6.9	6.3	6.1	6.2	6.4
Δp [Pa]	10.9	10.2	12.0	14.4	16.6
V_{fr} [m/s]	1.56	1.64	1.56	1.46	1.39
V_{dot} [m^3/s]	2.19	2.30	2.18	2.04	1.94
W_{pump} [W]	113	112	125	140	153
W_{comp} [W]	2230	2200	2190	2190	2200
Vol_{fin} [m^3]	0.0029	0.0033	0.0043	0.0057	0.0071

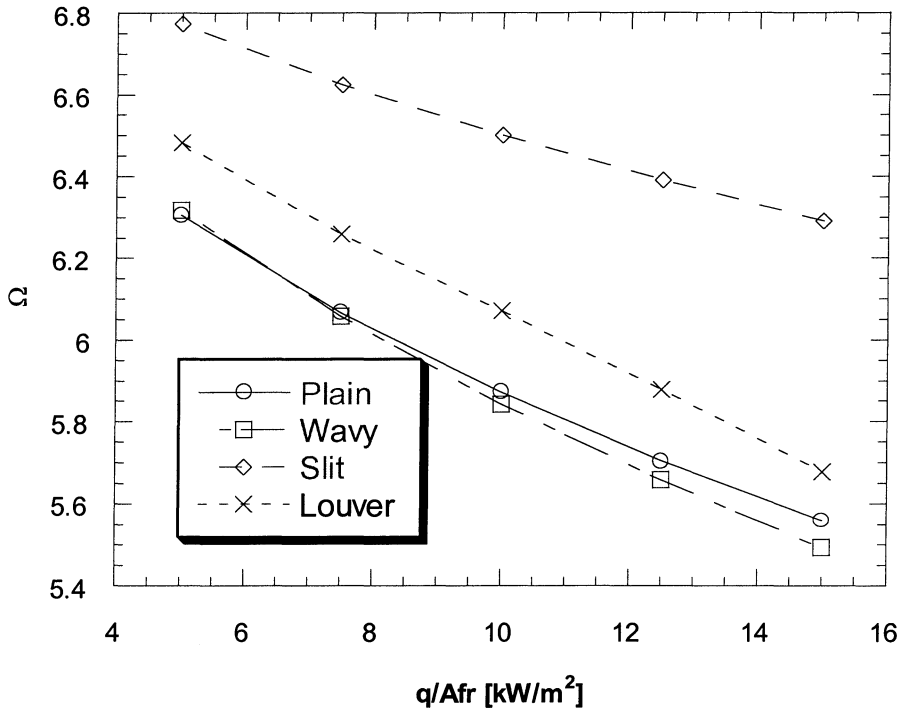

Figure 4.2 Max Ω values for varying constraints on q/A_{fr}

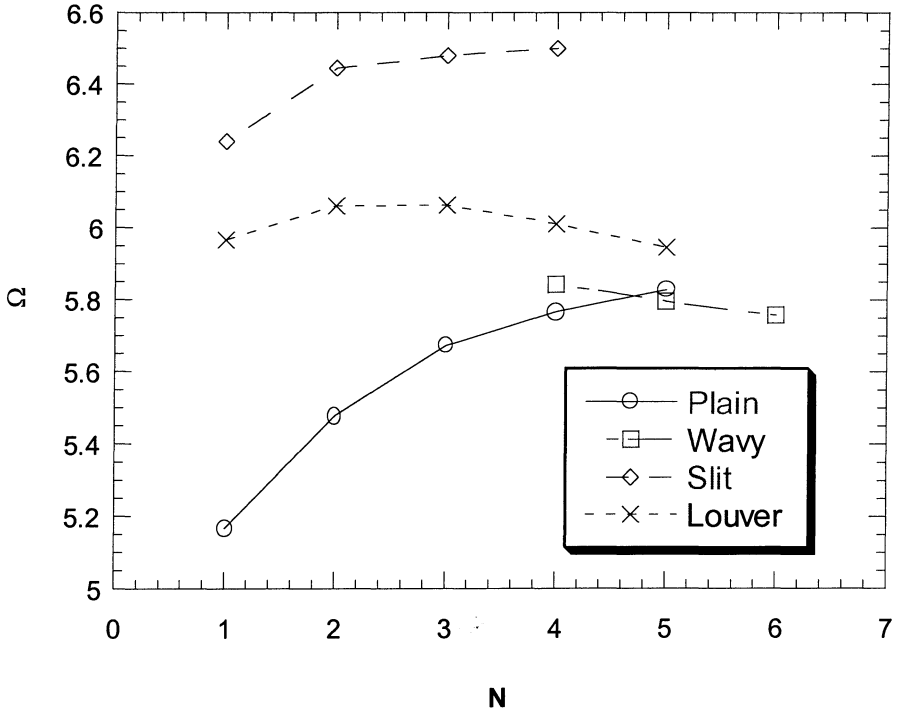

Figure 4.3 Max Ω values for varying number of tube rows, with fixed q/A_{fr}

Table 4.6 Wet evaporator optimization

	Plain	*Wavy*	*Slit*	*Louver*
Ω	4.0	4.1	3.7	4.0
N	3.0	4.1	3.0	2.3
D_c [mm]	10.3^{-}	13.6^{-}	7.5^{+-}	10.4^{+-}
L [mm]	66^{+}	114	38^{+}	44^{+}
F_s [mm]	1.8^{-}	2.2	1.7^{+}	1.2^{-}
F_t [mm]	0.13^{+-}	0.15^{+-}	0.08^{+-}	0.12^{+-}
P_l [mm]	22^{+-}	28^{-}	13^{+-}	19^{-}
P_t [mm]	26^{+-}	32^{-}	22^{+-}	26^{+-}
W_h [mm]		3.3^{+}		
S_h [mm]			0.76^{+-}	
S_w [mm]			9^{+-}	
L_h [mm]				1.1^{+-}
L_p [mm]				2.0^{-}
Re_{Dc}	2130	2350	1700	2020
q_s [W]	7680	7680	7680	7680
q_l [W]	2560	2560	2560	2560
A_{fr} [m^2]	0.32	0.32	0.32	0.32
ΔT_{max} [°C]	14.5	14.6	15.4	14.5
Δp [Pa]	51	47	76	72
V_{fr} [m/s]	1.84	1.49	2.30	1.67
V_{dot} [m^3/s]	0.59	0.48	0.74	0.54
W_{pump} [W]	198	148	374	257
W_{comp} [W]	2330	2340	2410	2330
Vol_{fin} [m^3]	0.0015	0.0025	0.0005	0.0013

Table 4.7 Baseline split system air conditioner

	Evaporator	*Condenser*
COP_{system}	4.08	
N	3.0	1.0
D_c [mm]	9.5	9.5
L [mm]	57	19
F_s [mm]	1.8	1.0
F_t [mm]	0.11	0.11
P_l [mm]	19	19
P_t [mm]	25	25
W_h [mm]		
S_h [mm]		
S_w [mm]		
L_h [mm]		
L_p [mm]		
Re_{Dc}	2050	970
q_s [W]	7680	14000
q_l [W]	2560	
A_{fr} [m^2]	0.32	1.4
ΔT_{max} [°C]	14.8	13.3
Δp [Pa]	30	6
V_{fr} [m/s]	2.02	0.94
V_{dot} [m^3/s]	0.65	1.32
W_{pump} [W]	131	36
W_{comp} [W]	2310	
Vol_{fin} [m^3]	0.0012	0.0028

Table 4.8 System optimization with plain and wavy fin heat exchangers

	Plain		*Wavy*	
	Evaporator	*Condenser*	*Evaporator*	*Condenser*
COP_{system}	4.63		4.44	
N	3.0	3.2	5.3	4.0
D_c [mm]	10.3^{-}	13.3^{+}	13.6	13.5^{-}
L [mm]	66^{+}	40	146	110^{-}
F_s [mm]	1.8^{-}	1.3	2.4	2.9
F_t [mm]	0.13^{+-}	0.15^{-}	0.15^{+-}	0.15^{+-}
P_l [mm]	22^{+-}	13^{-}	28^{-}	28^{-}
P_t [mm]	26^{+-}	32^{+}	38^{+}	38^{+}
W_h [mm]			3.3^{+}	3.2
S_h [mm]				
S_w [mm]				
L_h [mm]				
L_p [mm]				
Re_{Dc}	2130	2320	2040	1520
q_s [W]	7680	14000	7680	14000
q_l [W]	2560		2560	
A_{fr} [m^2]	0.32	1.4	0.32	1.4
ΔT_{max} [°C]	14.5	7.1	15.2	8.5
Δp [Pa]	51	15	41	25
V_{fr} [m/s]	1.84	1.48	1.46	1.14
V_{dot} [m^3/s]	0.59	2.07	0.47	1.60
W_{pump} [W]	198	152	129	192
W_{comp} [W]	1820		1960	
Vol_{fin} [m^3]	0.0015	0.0066	0.0029	0.0079

Table 4.9 System optimization with slit and louvered fin heat exchangers

	Slit		*Louver*	
	Evaporator	*Condenser*	*Evaporator*	*Condenser*
COP_{system}	4.60		4.69	
N	3.0	4.0	2.3	2.1
D_c [mm]	7.5^{+-}	8.0^{-}	10.4^{+-}	6.9^{-}
L [mm]	38^{+}	132^{+}	44^{+}	47
F_s [mm]	1.7^{+}	1.7	1.8	2.0
F_t [mm]	0.08^{+-}	0.17	0.12^{+-}	0.12^{+-}
P_l [mm]	13^{+-}	33^{+}	19^{-}	22^{+}
P_t [mm]	22^{+-}	25^{-}	26^{+-}	18^{-}
W_h [mm]				
S_h [mm]	0.8^{+-}	1.0^{+-}		
S_w [mm]	9^{+-}	18^{+}		
L_h [mm]			1.1^{+-}	0.8^{-}
L_p [mm]			2.2	3.8^{+}
Re_{Dc}	1700	2190	2030	1260
q_s [W]	7680	14000	7680	14000
q_l [W]	2560		2560	
A_{fr} [m^2]	0.32	1.4	0.32	1.4
ΔT_{max} [°C]	15.4	4.2	15.2	5.9
Δp [Pa]	76	5	61	11
V_{fr} [m/s]	2.30	2.76	1.74	1.73
V_{dot} [m^3/s]	0.74	3.87	0.56	2.42
W_{pump} [W]	374	84	225	127
W_{comp} [W]	1690		1780	
Vol_{fin} [m^3]	0.0005	0.0193	0.0009	0.0037

Chapter 5 – Conclusions and Recommendations

In this project, a model for the optimization of heat exchangers was developed. This model can be used to perform analyses of condensers and evaporators as separate components, or in combination with the inclusion of fan and compressor data. The model uses various performance evaluation criteria as objective functions and is capable of performing multidimensional searches to maximize the PEC values.

5.1 Conclusions

By performing unconstrained optimizations of the PEC j/f, Θ, Ω, and COP, various attributes of the criteria became clearer which enabled a better understanding of the type and layout of geometry and operating conditions each PEC valued. The PEC j/f favors thin designs that take advantage of developing thermal boundary layers, with short flow lengths to minimize frictional forces. However, an optimal j/f layout is independent of ΔT, and therefore may suggest designs with unreasonable condensing and evaporating temperatures.

The ratio of heat transfer to pumping power, termed Θ, was the second PEC studied. It favors reduced frictional dissipation through the heat exchanger, and thus pumping power—a close relation to *j/f* was demonstrated in this work. Unlike j/f, however, Θ depends on ΔT and is maximized for large ΔT. Therefore it too should be applied to compare heat exchangers having equal ΔT. Θ includes the fan component in addition to the heat exchanger, but neglects compressor power and may also suggest designs with unreasonable refrigerant-side temperatures.

Including compressor power in a PEC, as shown in Ω, effectively places a penalty function on large ΔT's. The unconstrained optimization showed that Ω yielded the same optimal geometry and Reynolds number as Θ but reached its maximum at a much lower ΔT. In fact, it tended to find an optimum ΔT near the minimum of its defined range by favoring geometries having a large frontal area. Therefore this PEC may be most useful

for comparing heat exchangers having equal frontal area. The real benefit of Ω can be derived from its application to heat exchangers of not only a limited frontal area but also a required heat transfer rate, placed in the form of a constraint on q/A_{fr}. Once q/A_{fr} is constrained, Θ does not consider effects of the j factor in its optimization, but Ω uses it in determination of condensing and evaporating temperatures and finds a compromise in design which balances out heat transfer requirements, pumping power requirements, and compressor power requirements. System level PEC such as COP cast important heat exchanger and system parameters into a single value, and prove beneficial in optimizing condensers and evaporators simultaneously. The implementation of accurate j and f data into a COP optimization model enable a system simulation to determine ideal geometry and airflow rates for a condenser and evaporator. System optimization differs from component optimization in that the power requirements at the compressor are linked to both elements at the same time.

The use of a PEC is beneficial when considering further aspects of heat exchanger design. The choice of surface enhancement to use on a particular air conditioning system can be made by a comparison of PEC values, and limited cost information could be included in such an analysis. For example, the cost of a heat exchanger is related to material use, so optimizations could be conducted for various numbers of tube rows to observe the effect on maximum PEC value and the optimal values of other geometric parameters. Of course other costs related to manufacturing and distribution might be important. Furthermore, noise or other quality metrics are not considered by a PEC. The use of a PEC does not ensure optimal system design, but it provides rational, limited guidance to the engineer.

5.2 Recommendations for future studies

There are several areas where additional research may help to refine the model developed in this study or expand it for better component and system optimization. The constant evaporating or condensing temperature assumption, describing a single-zone heat exchanger, can be replaced by multiple zone models with superheated and subcooled regions to increase accuracy. Partially wet evaporator equations can be implemented

rather than using the fully wet evaporator assumption. Additional compressor map data would assist in comparing designs using different compressor types with different isentropic efficiencies. Creating biquadratic or higher polynomial curve fits on compressor efficiency data may also improve accuracy. Also, surface efficiency calculations using the sector method for specific surface types rather than only plain fins may be applied to the model. Specialized equations for wet surface efficiency can also be implemented.

Whether such additional complexity would lead to different results is unknown at this time. Recall that the optimal heat exchanger designs obtained using the relatively simple PEC Ω did not differ greatly in certain cases from that obtained using the more comprehensive PEC COP. Finding similar PEC that are able to cast system effects into a simplified optimization method can greatly benefit designers in the evaluation of new heat exchanger designs. Having such a PEC yielding similar optimal points with the addition of complexity to the model can prove its usefulness in a general case.

The most beneficial improvement to such a model on system optimization, however, would be an increase in the accuracy of j and f correlations that the model is built upon. A large databank of heat exchangers on which correlations are based, with large variations in geometric parameters, increases the range on which the model can perform an optimization and at the same time improves the accuracy of its results. For PEC that push designs towards limits of existing correlations, with a large rate of change of the PEC with respect to a geometric parameter, this model also suggests that it may be beneficial to construct and test prototype heat exchangers with new designs that extend the range of such parameters for improved heat exchanger or system performance.

Appendix A – Buckingham Π Analysis

The analysis of flow over heat exchangers is very difficult to solve by analytical methods alone. The development of correlations to describe heat exchanger performance is therefore heavily dependent on experimental results. However, experimental work done in laboratories to test heat exchangers is both time-consuming and expensive. A goal of the work is to obtain the most information in the fewest amount of experiments. The use of dimensional analysis can assist in achieving this goal. Dimensionless parameters can be obtained and used to correlate data for presentation in the minimum number of plots (Fox and McDonald 1992).

A.1 Purpose of dimensional analysis

Because the heat transfer and pressure drop phenomena across a heat exchanger are very complex, many variables may be required to determine their values. Nondimensional variables can be derived from a method such as Buckingham Π which reduces the number of variables to allow a better presentation of data. For example, to determine the drag force on a sphere, the drag force F can be represented by

$$F = f_1(D, V, \rho, \mu)$$

where D is the diameter of the sphere, and V, ρ, and μ are the velocity, density, and viscosity of the air, respectively. A standard approach to experimentally determining the form of the function would be to build an experimental facility and run tests for 10 values of each of the independent variables, requiring 10^4 separate tests. Presenting all the data using all combinations of axes would also prove to be a daunting task. A much simpler method is to use dimensional analysis to reduce the form of the function to

$$\frac{F}{\rho V^2 D^2} = f_2\left(\frac{\rho V D}{\mu}\right)$$

The nature of the function can now be described with only 10 tests, providing a much more efficient method of obtaining and presenting experimental data.

The Buckingham Π theorem provides a link between a function expressed in terms of dimensional parameters and a related function expressed in terms of nondimensional parameters. Implementing the theorem reduces the amount of variables needed for determining a functional relationship and provides for a more efficient method of presenting the results.

A.2 Implementation of Buckingham Π theorem

The six main steps involved in applying the Buckingham Π theorem to obtain nondimensional variables was outlined in Fox and McDonald (1992):

1) List all the parameters involved
2) Select a set of primary dimensions
3) List the dimensions of all parameters in terms of the primary dimensions
4) Select from the list of parameters a number of repeating parameters equal to the number of primary dimensions, and including all the primary dimensions
5) Set up dimensional equations, combining the parameters selected in Step 4 with each of the other parameters in turn, to form dimensionless groups
6) Check to see that each group obtained is dimensionless

This method will first be used to derive the j factor as a function of nondimensional variables. In step 1 the parameters that affect the j factor are listed:

$$j = f\left(L, F_s, F_t, P_l, P_t, D_c, V_{fr}, \mu, \rho, c_p, k_a\right) \tag{A.1}$$

This includes geometric variables and fluid properties. For step 2, the primary dimensions of these variables are mass, length, time, and temperature (M, L, t, and T). The next step is listing the dimensions of all the parameters in Equation A.1 in terms of M, L, t, and T. These are listed as follows:

Table A.1 Parameter dimensions

Parameter	Dimension (SI)	Dimension (USCS)	Dimension (general)
D_c	m	ft	L
L	m	ft	L
F_s	m	ft	L
F_t	m	ft	L
P_l	m	ft	L
P_t	m	ft	L
V_{fr}	m/s	ft/hr	L/t
μ	$kg/m\text{-}s$	$lbm/ft\text{-}hr$	$M/L\text{-}t$
ρ	kg/m^3	lbm/ft^3	M/L^3
c_p	$m^2/s^2\text{-}K$	$lbm^2/hr^2\text{-}R$	$L^2/t^2\text{-}T$
k_a	$kg\text{-}m/s^3\text{-}K$	$lbm\text{-}ft/hr^3\text{-}R$	$M\text{-}L/t^3\text{-}T$
T_o	K	R	T

Four repeating parameters need to be chosen as the nondimensionalizing variables. These variables as a group must contain all the reference dimensions. In addition, the dimension of each of the repeating parameters must not be expressible as a product of powers of the dimensions of the other repeating parameters (i.e. 2 geometric parameters of dimension L cannot both be used as repeating parameters). The chosen variables were μ, ρ, c_p, and T_o. T_o is not listed in the functional form of the j factor, but as explained in Chapter 2, it exists in the functional forms of Ω and COP, and proved to be a useful choice of repeating parameter for these PEC. Ω and COP have different optima depending on the scale of the heat exchanger because of its effect on temperature and heat duty. In the interest of maintaining uniformity of the nondimensional parameter space between all the PEC, T_o was also chosen as a repeating parameter for the PEC j/f

and Θ. An additional benefit to using T_o as a repeating parameter for j/f and Θ is that results of optimizations are not extrapolated when compared to dimensional limits on the correlations. This is shown in section A.3. Section A.5 further outlines the effect of using T_o as a repeating parameter and a method of removing it from the analysis.

The next step in the nondimensionalization process is to set up equations representing each new ND variable as a combination of a dimensional variable and the repeating parameters raised to exponents. These equations are listed in Table A.2.

Table A.2 Equations for nondimensionalization

Nondimensional Π group Equation	
$V_{fr}^* = T_o^a \mu^b \rho^c c_p^d V_{fr} = (T)^a \left(\frac{M}{Lt}\right)^b \left(\frac{M}{L^3}\right)^c \left(\frac{L^2}{t^2 T}\right)^d \left(\frac{L}{t}\right) = M^0 L^0 t^0 T^0$	(A.2)
$k_a^* = T_o^a \mu^b \rho^c c_p^d k_a = (T)^a \left(\frac{M}{Lt}\right)^b \left(\frac{M}{L^3}\right)^c \left(\frac{L^2}{t^2 T}\right)^d \left(\frac{ML}{t^3 T}\right) = M^0 L^0 t^0 T^0$	(A.3)
$D_c^* = T_o^a \mu^b \rho^c c_p^d D_c = (T)^a \left(\frac{M}{Lt}\right)^b \left(\frac{M}{L^3}\right)^c \left(\frac{L^2}{t^2 T}\right)^d (L) = M^0 L^0 t^0 T^0$	(A.4)
$L^* = T_o^a \mu^b \rho^c c_p^d L = (T)^a \left(\frac{M}{Lt}\right)^b \left(\frac{M}{L^3}\right)^c \left(\frac{L^2}{t^2 T}\right)^d (L) = M^0 L^0 t^0 T^0$	(A.5)
. . .	. . .
$P_t^* = T_o^a \mu^b \rho^c c_p^d P_t = (T)^a \left(\frac{M}{Lt}\right)^b \left(\frac{M}{L^3}\right)^c \left(\frac{L^2}{t^2 T}\right)^d (L) = M^0 L^0 t^0 T^0$	(A.9)

Solving for the values of the exponents (a-d), the ND variables are derived in Table A.3.

Table A.3 Exponents of M, L, t, and T and final form of nondimensional variables

Equation	Exponents				Nondimensional Variable
	a	b	c	d	
A.2	-0.5	0	0	-0.5	$V_{fr}^* = \frac{V_{fr}}{\sqrt{c_p T_o}}$
A.3	0	-1	0	1	$k_a^* = \frac{k_a}{\mu c_p}$
A.4	0.5	-1	1	0.5	$D_c^* = \frac{D_c \rho \sqrt{c_p T_o}}{\mu}$
A.5	0.5	-1	1	0.5	$L^* = \frac{L \rho \sqrt{c_p T_o}}{\mu}$
. . .	. . .				. . .
A.9	0.5	-1	1	0.5	$P_t^* = \frac{P_t \rho \sqrt{c_p T_o}}{\mu}$

A simple check of dimensions verifies these variables to be nondimensional.

A similar method is used for the derivation of ND terms for the friction factor. The resulting ND variables are the same as those derived for j/f, with the exception of k_a^*. The thermal conductivity of the air does not affect the friction factor.

A.3 Implementation of ND variables with limits

When performing an optimization of an objective function based on these ND variables, ranges must be set on each of the variables. Since these ND variables are used in j and f factor correlations, care must be taken not to extrapolate beyond the ranges of heat exchanger parameters used to develop the correlations.

Figure A.1 Ranges and extrapolation

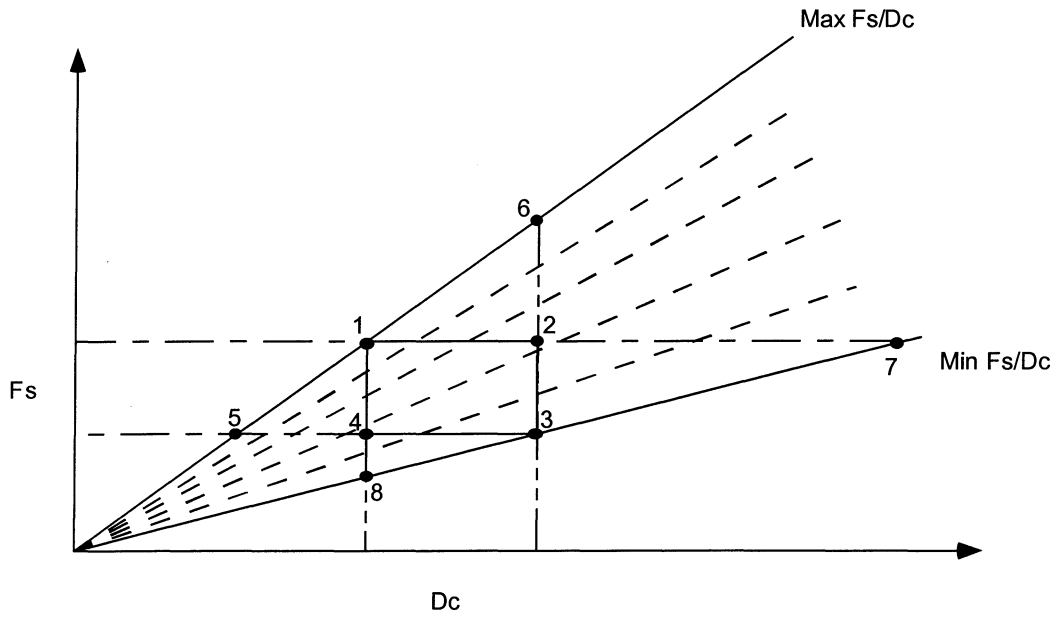

In Figure A.1 the limits of the physical parameters F_s (fin spacing) and D_c (tube collar diameter) are represented by the rectangle 1-2-3-4. This assumes the inclusion of an adequate number of test points within the rectangle for the development of correlations. The current method of nondimensionalization uses solely air properties as the nondimensionalizing variables. This allows ranges to be set for the ND parameters that correspond directly to the dimensional parameters, for a given fluid (air) and ambient temperature. An optimization run would then yield results that fall within the confines of 1-2-3-4. Had the nondimensionalization used a length scale such as D_c as a repeating parameter, the ND variable for F_s would be F_s/D_c. A maximum value for F_s/D_c could be defined as maximum F_s divided by minimum D_c. Similarly, a minimum value for F_s/D_c could be defined as minimum F_s divided by maximum D_c. However, any optimization run that pushes F_s/D_c to a range limit would extrapolate the correlation for all but one value of D_c. For example, if max F_s/D_c was determined to be optimal, all solutions for the full range of D_c would fall within the triangle 1-2-6 rather than the rectangle 1-2-3-4. With the current method of using a combination of air properties as a normalizing length scale, these extrapolations are eliminated, although the ND optimum that results is no longer independent of physical scale.

A.4 Additional ND terms

The derived parameters in Table A.3 are valid for the optimization of the PEC j/f. The PEC Θ and Ω include additional terms which require nondimensionalization. Also, since applying the results of an optimization to pressure drop and heat rate equations proves beneficial, the variables in these equations are also nondimensionalized. The new terms are listed below.

$$q/A_{fr},\ \Delta p,\ \Delta T,\ k_f,\ a,\ b \tag{A.2}$$

The units for these variables are listed in Table A.4.

Table A.4 Additional parameter dimensions

Parameter	Dimension (SI)	Dimension (USCS)	Dimension (general)
q/A_{fr}	kg/s^3	lbm/hr^3	M/t^3
Δp	$kg/m\text{-}s^2$	lbf/ft^2	$M/L\text{-}t^2$
ΔT_{max}	K	R	T
k_f	$kg\text{-}m/s^3\text{-}K$	$lbm\text{-}ft/hr^3\text{-}R$	$M\text{-}L/t^3\text{-}T$
a	-	-	-
b	$1/K$	$1/R$	$1/T$

The variables are normalized by the same repeating parameters as previously used, namely μ, ρ, c_p, and T_o. Equations are set up similar to those in Table A.2. Then the exponents are evaluated to obtain the final form of the ND variables, as shown in Table A.5.

Table A.5 ND form of additional parameters

Equation	Exponents				Nondimensional Variable
	a	b	c	d	
A.1	-1.5	0	-1	-1.5	$\left(\frac{q}{A_{fr}}\right)^* = \frac{q}{A_{fr}} \frac{1}{\rho(c_p T_o)^{3/2}}$
A.1	1	0	0	0	$\Delta T^* = \frac{\Delta T}{T_o}$
A.1	-1	0	-1	-1	$\Delta p^* = \frac{\Delta p}{\rho c_p T_o}$
A.1	0	-1	0	1	$k_f^* = \frac{k_f}{\mu c_p}$
A.1	0	0	0	0	$a^* = a$
A.1	1	0	0	0	$b^* = bT_o$

A.5 Effects of using T_o as a repeating parameter

The parameter T_o does not appear explicitly in the j/f and Θ PEC formulations; that is, those PEC do not depend directly on T_o—the dependence is indirect and properly reflected by dependence on fluid properties (μ, ρ, c_p, and k_a). Nevertheless, T_o has been used as a repeating parameter for all the nondimensionalization conducted in this study. This choice was mainly motivated by the explicit dependence of Ω and system COP on T_o, and its role as a natural temperature scale for those PEC. In order to formulate all PEC in a consistent nondimensional space, it is necessary to use the same repeating parameters in each Buckingham Π analysis. Thus, T_o was used for all four PEC in order to provide a consistent nondimensional space, making direct comparisons of optimization results easier in the nondimensional space.

Although the choice of repeating parameters is somewhat arbitrary—provided they are independent and span the dimensional space—the selection affects the resulting nondimensional space. It is important to note that optimization in any valid nondimensional space corresponds to identical optimal solutions in the dimensional

space; only the nondimensional representation is affected. Furthermore, adding an independent variable that does not bring a new physical dimension (T_o in this case) to a function (j/f and Θ in this case) with no explicit dependence on the variable does not vitiate the Buckingham Π analysis for those PEC. The additional parameter results in functional independence from one variable (or combination of variables) in the dimensionless space (see example below). Furthermore, it is possible to map between dimensionless spaces to prove the physical equivalence of two nondimensional results (and eliminate a physically irrelevant parameter). In the present situation that mapping can be accomplished with the following procedure:

1) Divide all nondimensional geometric variables by D_c^* (e.g.. L^*/D_c^*, F_s^*/D_c^*)
2) Multiply ΔT^* by $(D_c^*)^2$ (only for Θ)
3) Ignore D_c^* as an independent parameter

As an example, consider the unconstrained optimization of Θ. Ideal values are obtained for the following parameters (from Chapter 3):

$$\Theta_{optimal} = \Theta\left(L^*, F_s^*, F_t^*, P_l^*, P_t^*, D_c^*, \mathrm{Re}_{D_c}, \Delta T^*\right) \tag{3.10}$$

Writing out the full form of the nondimensional variables, Equation 3.10 can be expressed as follows:

$$\Theta_{optimal} = \Theta\left(\frac{L\rho\sqrt{c_pT_o}}{\mu}, \frac{F_s\rho\sqrt{c_pT_o}}{\mu}, \frac{F_t\rho\sqrt{c_pT_o}}{\mu}, \frac{P_l\rho\sqrt{c_pT_o}}{\mu}, \frac{P_t\rho\sqrt{c_pT_o}}{\mu}, \frac{D_c\rho\sqrt{c_pT_o}}{\mu}, \mathrm{Re}_{D_c}, \frac{\Delta T}{T_o}\right) \tag{A.3}$$

Applying the three steps outlined above, this functional relationship becomes

$$\Theta_{optimal} = \Theta\left(\frac{L^*}{D_c^*}, \frac{F_s^*}{D_c^*}, \frac{F_t^*}{D_c^*}, \frac{P_l^*}{D_c^*}, \frac{P_t^*}{D_c^*}, \mathrm{Re}_{D_c}, \Delta T^* \cdot \left(D_c^*\right)^2\right)$$
$$= \Theta\left(\frac{L}{D_c}, \frac{F_s}{D_c}, \frac{F_t}{D_c}, \frac{P_l}{D_c}, \frac{P_t}{D_c}, \mathrm{Re}_{D_c}, \frac{\Delta T D_c^2 \rho^2 c_p}{\mu^2}\right) \qquad \text{(A.4)}$$

with all occurences of T_o canceling out. These same nondimensional parameters would also result from a Buckingham Π analysis done initially with the repeating variables D_c, μ, ρ, and c_p. The optimal point obtained is now valid for any D_c within range of the correlations used; the value of D_c scales the value of the other geometric variables and the values of V_{fr} (in the Reynolds number) and ΔT. The same physical solution results.

The three steps outlined above recast the nondimensional variables to a format in which the tube collar diameter D_c is the normalizing length scale rather than a combination of air properties and T_o. The variable Re_{Dc} does not include T_o explicitly in its formula and thus does not require recasting. Dropping T_o requires the exclusion of the nondimensional parameter D_c^*, since D_c now becomes a repeating parameter. The nondimensional optimal point is then valid for any D_c (within range of the correlations), and the dimensional form of the variables are determined by specification of D_c. This is the major difference between performing an 8 degree-of-freedom optimization on the variables in Equation 3.10 (method 1) vs. a 7 degree-of-freedom optimization on the variable combinations in Equation A.4 (method 2). With T_o as a repeating parameter, D_c is "separated" from the other geometric variables in the optimization. When D_c is used as a repeating parameter, it becomes integrated within all the nondimensional variables. This changes the way in which the optimal solution can be visualized. Method 1 produces a fixed geometry per unit frontal area, while method 2 produces a geometry per unit frontal area that is scaled by specification of one geometric variable (i.e. D_c).

Appendix B – Model Calculations and Approximations

B.1 Area ratios

Several area ratios are presented in the heat exchanger performance and PEC equations. These can be expressed as functions of the variables in the nondimensional parameter space. The following equations define the minimum free flow area A_{min} and total heat transfer area A_T:

$$A_{\min} = \underbrace{HW}_{\text{frontal area}} - \underbrace{F_t H \frac{W}{F_s}}_{\text{fin frontal area}} - \underbrace{\frac{H}{P_t} D_c \left(W - F_t \frac{W}{F_s} \right)}_{\text{tube frontal area}} \tag{B.1}$$

$$A_T = \underbrace{\left(2\frac{W}{F_s} \right)}_{\text{\# fin surfaces}} \underbrace{\left(HL - \frac{H}{P_t}\frac{L}{P_l}\frac{\pi}{4} D_c^2 \right)}_{\text{area of fin surface}} + \underbrace{\left(\frac{H}{P_t}\frac{L}{P_l} \right)}_{\text{\# tube passes}} \underbrace{\left(W - F_t \frac{W}{F_s} \right) \pi D_c}_{\text{area of tube row}} \tag{B.2}$$

These equations use the height and width of the heat exchanger as separate variables, rather than using one A_{fr} term. However, it will be shown that these variables drop out of the equations when area ratios are considered rather than the area terms themselves. These area equations can be normalized by the square of the length scale, $\frac{\mu^2}{\rho^2 c_p T_o}$, in order to introduce the derived nondimensional variables:

$$\begin{aligned} A_{\min}^* &= \frac{A_{\min} \rho^2 c_p T_o}{\mu^2} = H^* W^* - H^* F_t^* \frac{W^*}{F_s^*} - \frac{H^*}{P_t^*} W^* D_c^* + \frac{H^*}{P_t^*}\frac{W^*}{F_s^*} F_t^* D_c^* \\ &= H^* W^* \left(1 - \frac{F_t^*}{F_s^*} - \frac{D_c^*}{P_t^*} + \frac{F_t^*}{F_s^*}\frac{D_c^*}{P_t^*} \right) \end{aligned} \tag{B.3}$$

$$A_T^* = \frac{A_T \rho^2 c_p T_o}{\mu^2} = 2\left(\frac{W^*}{F_s^*} H^* L^* - \frac{W^*}{F_s^*}\frac{H^*}{P_t^*}\frac{L^*}{P_l^*}\frac{\pi}{4}\left(D_c^*\right)^2\right) + \pi\left(\frac{H^*}{P_t^*}\frac{L^*}{P_l^*} W^* D_c^* - \frac{H^*}{P_t^*}\frac{L^*}{P_l^*}\frac{W^*}{F_s^*} F_t^* D_c^*\right)$$

$$= 2H^* W^* L^*\left(\frac{1}{F_s^*} - \frac{\pi}{4}\frac{\left(D_c^*\right)^2}{P_t^* P_l^* F_s^*} + \frac{\pi}{2}\frac{D_c^*}{P_t^* P_l^*} - \frac{\pi}{2}\frac{F_t^* D_c^*}{P_t^* P_l^* F_s^*}\right) \tag{B.4}$$

These area equations can then be divided by each other to determine the area ratios. The frontal area of the heat exchanger drops out, making these equations applicable to heat exchangers of any frontal area:

$$\frac{A_{fr}}{A_{\min}} = \frac{1}{1 - \frac{F_t^*}{F_s^*} - \frac{D_c^*}{P_t^*} + \frac{F_t^*}{F_s^*}\frac{D_c^*}{P_t^*}} \tag{B.5}$$

$$\frac{A_T}{A_{\min}} = \frac{2L^*\left(\frac{1}{F_s^*} - \frac{\pi}{4}\frac{\left(D_c^*\right)^2}{P_t^* P_l^* F_s^*} + \frac{\pi}{2}\frac{D_c^*}{P_t^* P_l^*} - \frac{\pi}{2}\frac{F_t^* D_c^*}{P_t^* P_l^* F_s^*}\right)}{1 - \frac{F_t^*}{F_s^*} - \frac{D_c^*}{P_t^*} + \frac{F_t^*}{F_s^*}\frac{D_c^*}{P_t^*}} \tag{B.6}$$

$$\frac{A_T}{A_{tube}} = \frac{\frac{2P_t^* P_l^*}{\pi F_s^* D_c^*} - \frac{D_c^*}{2F_s^*} + 1 - \frac{F_t^*}{F_s^*}}{1 - \frac{F_t^*}{F_s^*}} \tag{B.7}$$

$$\frac{A_{fin}}{A_T} = \frac{\frac{1}{F_s^*} - \frac{\pi}{4}\frac{\left(D_c^*\right)^2}{P_t^* P_l^* F_s^*}}{\frac{1}{F_s^*} - \frac{\pi}{4}\frac{\left(D_c^*\right)^2}{P_t^* P_l^* F_s^*} + \frac{\pi}{2}\frac{D_c^*}{P_t^* P_l^*} - \frac{\pi}{2}\frac{F_t^* D_c^*}{P_t^* P_l^* F_s^*}} \tag{B.8}$$

For the optimizations, these equations were used regardless of surface enhancement type. This may introduce a small amount of error in total heat transfer area calculations due to

enhancements (such as wavy fins) having more total fin area than that accounted for by these equations.

B.2 Reynolds number conversions

Correlations presented in the literature may be based on Reynolds numbers of differing length and velocity scales. Expressing these correlations in terms of the nondimensional parameters is simply a matter of multiplying by the appropriate area ratios and nondimensional terms together. A commonly used Reynolds number is one based on tube collar diameter and maximum velocity through minimum free flow area. The relationship is expressed as follows:

$$\mathrm{Re}_{D_c} = \left(\frac{A_{fr}}{A_{\min}} \right) V_{fr}^{*} D_c^{*} \tag{B.9}$$

For optimization runs, rather than setting a range of valid values for V_{fr}^{*}, a range for Re_{Dc} is defined. This effectively constrains V_{fr}^{*} to a certain range depending on the limits on the nondimensional heat exchanger geometry variables. Most correlations in the literature present valid ranges for the Reynolds number for their correlations rather than frontal velocities.

B.3 Surface efficiency

Specialized forms of surface efficiency equations were derived in order to be able to express them with nondimensional variables. Only the dimensional forms of the equations will be presented in this section. The surface efficiency is obtained from the fin efficiency with an area weighting factor (Incropera and DeWitt 1990):

$$\eta_0 = 1 - \frac{A_{fin}}{A_T} \left(1 - \eta_f \right) \tag{B.10}$$

The fin area over total heat transfer area is expressed as a function of nondimensional variables in Equation B.8. Fin efficiency is calculated using the sector method with conduction, described as follows.

The calculation of inner radius for the sector method depends on the fin-tube connection. ARI Standard 410 (1981) recommends the following equation for plate-type fins with collars touching the adjacent fin.

$$r_i = \frac{(D_o + 2F_t)}{2} = \frac{D_c}{2} \tag{B.11}$$

The sector method can be used to determine the fin efficiency of hexagonal fins of constant thickness attached to the round tubes. The hexagonal fin around each tube is divided into 8 different zone as shown in Figure B.1. Each individual zone is then divided into 4 sectors. The number of sectors can be increased for better approximation.

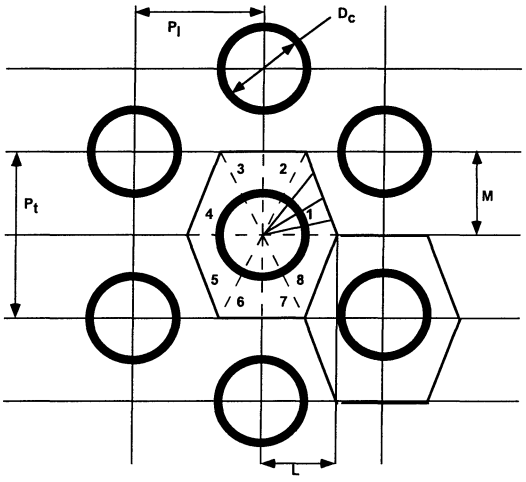

Figure B.1 Sector method with conduction (plain-fin)

The radius of each edge of sector is approximated and the radius ratio, R_n, and the surface area of each sector, S_n, are calculated as follows.

Sectors with constant M edge (for zone 2, 3, 6, and 7)

$$R_n = \frac{M}{r_i}\sqrt{\left(\frac{2n-1}{2N}\right)^2 + \left(\frac{L}{M}\right)^2} \tag{B.12}$$

$$S_n = \frac{r_i^2}{2}\left(R_n^2 - 1\right)\left[\tan^{-1}\left(\frac{nM}{NL}\right) - \tan^{-1}\left(\frac{(n-1)M}{NL}\right)\right] \tag{B.13}$$

where n = 1,2, 3... N is number of sectors in each zone.

Sectors with constant L edge (for zone 1, 4, 5, and 8)

$$R_n = \frac{M}{r_i}\sqrt{\left(\frac{2n-1}{2N}\right)^2\left(\frac{L}{M}\right)^2 + 1} \tag{B.14}$$

$$S_n = \frac{r_i^2}{2}\left(R_n^2 - 1\right)\left[\tan^{-1}\left(\frac{nL}{NM}\right) - \tan^{-1}\left(\frac{(n-1)L}{NM}\right)\right] \tag{B.15}$$

where n = 1,2, 3... N is number of sectors in each zone, and

$$M = \frac{P_t}{2}, \qquad L = \frac{P_l}{2} \tag{B.16), (B.17}$$

The calculated value, R_n, is used with the exact fin efficiency equation for circular fins, as developed by Kern and Kraus (1972). This fin efficiency equation is given in terms of modified Bessel functions:

$$\eta_n = \frac{2r_i}{m\left(r_o^2 - r_i^2\right)}\left[\frac{K_1(mr_i)I_1(mr_o) - K_1(mr_o)I_1(mr_i)}{K_1(mr_o)I_0(mr_i) + K_0(mr_i)I_1(mr_o)}\right] \tag{B.18}$$

where

$$m = \sqrt{\frac{2h}{k_f F_t}} \tag{B.19}$$

The total fin efficiency can be calculated by the sum of the multiplication of fin efficiencies for each sector in each zone and S_n divided by the sum of surface areas of all eight sectors in each zone.

$$\eta_f = \frac{\sum_{n=1}^{N} S_n \eta_n}{\sum_{n=1}^{N} S_n} \tag{B.20}$$

where n = 1, 2, 3, …, and N, N = number of sectors in each zone.

To implement these equations in the model, they were written in terms of the nondimensional variables used in the analysis. The only difference in intermediate calculations is that the surface areas S_n are normalized by air properties, but these air properties cancel out when Equation B.20 is used.

B.4 Pumping power

Pumping power required for flow over a heat exchanger can be expressed as follows:

$$\dot{W}_p = \frac{\dot{V}\Delta p}{\eta_{fm}} \tag{B.21}$$

The fan and motor efficiency was fixed at 0.21 for the condenser optimization runs and 0.15 for the evaporator runs. The condenser efficiency was determined from data obtained for two actual U-shaped condenser coil and fan setups (Beaver *et al.* 1999). In one case, the average pressure drop was 24 Pa at 2800 cfm with a power input of 207 W. In the other case, pressure drop data was taken at three points along the height of the

heat exchanger with air flow rates varying from 1900 to 2800 cfm. The acceleration of air from rest was included in the calculations; the first system required 16W and the second required 10W (at 2350 cfm, the midpoint of its airflow range). The fan and motor efficiency calculated in the two cases were 0.23 and 0.19, respectively. Therefore an average efficiency of 0.21 was chosen for the optimization model. Calculating fan and motor efficiency in this way adequately captures losses in the system resulting from ducting, since the pressure drop measurements included the turning losses.

For evaporators, the efficiency was calculated from a combination of test data and ARI standard 210/240-89. The ARI standard states that for units which do not have indoor air-circulating fans furnished as part of the model, total power input for both heating and cooling shall be increased by 365 W/1000 cfm of indoor air circulated. The evaporator test data used (Beaver *et al.* 1999) was obtained at 1440 cfm; this corresponds to a fan power of 526 W. When this power is input to Equation B.18 for the tested pressure drop reading of 78 Pa, and adding a minimal external resistance of 37.4 Pa as required by the ARI standard for system capacities of 8.5-12.4 kW, the resulting fan and motor efficiency is 0.15.

Pressure drops calculated in this model only account for core friction; entrance effects, flow acceleration, and exit effects are neglected (although flow acceleration was considered when obtaining the efficiency term). Therefore these pressure drops may be lower than those of real systems, and the corresponding reduction in required pumping power would then be multiplied through use of the fan and motor efficiency term.

B.5 Compressor efficiency

To introduce the compressor work term in the PEC Ω, COP information from a compressor map was used. A linearization of the effect on COP of changing condensing and evaporating temperatures was performed. The linearization process may introduce some error in the results of the optimizations. Equations were obtained for the condenser, evaporator, and system optimization models. The compressor map used was for a Copeland ZP32K3E-PFV scroll compressor.

B.5.1 Curve fit for condenser

An evaporating temperature of 10°C (50°F) was assumed, and the linearization was made through COP data points corresponding to condensing temperatures of 37.8, 43.3, and 48.9°C (100, 110, and 120°F respectively). The linearization was confined to these data points to increase accuracy for the range of outdoor temperatures where efficiency and capacity testing are done — 27-35°C (82-95°F). The resulting equation for COP in this range was

$$\begin{aligned} COP &= a - b\Delta T \\ &= 6.508 - 0.17923\Delta T_c \end{aligned} \tag{B.22}$$

with ΔT expressed in °C.

Since this linearization assumes a specific evaporation temperature, a^* represents the upper limit on COP of the system (e.g. zero ΔT for the condenser). The variable a^* also includes information on evaporator non-idealities. If zero ΔT is assumed for the evaporator, a^* represents Carnot COP. For finite ΔT for the evaporator, a^* is Carnot COP minus the COP penalty for a non-ideal evaporator. Although the COP term was first introduced in order to represent compressor work, this variable is independent of compressor operation.

The variable b^* represents the slope of COP penalty for a non-ideal condenser. This variable links the compressor work to this PEC by introducing a COP penalty for increasing ΔT, analogous to a compressor work penalty for increasing ΔT.

B.5.1 Curve fit for evaporator

Similarly, a curve fit was generated for varying evaporating temperatures, assuming a constant condensing temperature of 48.9°C (120°F). The result, for an ambient indoor temperature of 26.7°C (80°F), was

$$COP = 6.5906 - 0.15153\Delta T_e \tag{B.23}$$

B.5.1 Curve fit for system

To effectively model the compressor for system optimization, a function of two variables, condensing and evaporating temperatures, is required. A quadratic-linear curve fit of the compressor map was generated, resulting in the following equation:

$$\begin{aligned} COP = &\left(-2113.22 + 8.5198T_e\right) \\ &+ \left(11.604 - 0.046894T_e\right)T_c \\ &+ \left(-0.016021 + 6.489\times10^{-5}T_e\right)T_c^2 \end{aligned} \tag{B.24}$$

For this curve fit the temperatures need to be expressed in Kelvins. This method of using absolute temperatures rather than ΔT was chosen so the curve fit would still be valid if the ambient indoor and outdoor temperatures were changed. A quadratic-linear regression was chosen because of improved accuracy over regressions of other orders. The error (COP_{pred} - COP_{actual}) from using Equation B.24 is shown in Table B.1.

Table B.1 COP curve fit error

T_{cond} [°C]	T_{evap} [°C]			
	4	*7*	*10*	*13*
27	-0.06	-0.02	0.01	-0.07
32	0.04	0.07	0.07	0.02
38	0.00	0.07	0.05	0.03
43	-0.02	0.03	0.03	-0.02
49	-0.02	-0.02	-0.01	-0.04
54	-0.06	-0.03	-0.04	-0.05
60	-0.05	-0.03	-0.02	-0.05
66	0.00	0.03	0.03	0.00

Appendix C – Heat Transfer and Pressure Drop Correlations

Table C.1 Published j and f factor correlations used in optimization model

Surface type	Author	Correlation
Plain (dry)	*Wang & Chang* (1998)	$j_4 = 0.357\,\mathrm{Re}_{D_c}^{-0.328}\left(\frac{P_t}{P_l}\right)^{-0.502}\left(\frac{F_s}{D_c}\right)^{0.0312}\left(\frac{P_l}{D_c}\right)^{-1.28}$ $\frac{j_N}{j_4} = 0.991\left[2.24\,\mathrm{Re}_{D_c}^{-0.092}\left(\frac{N}{4}\right)^{-0.031}\right]^{0.607(4-N)}$
Plain (dry)	*Wang et al.* (1996)	$f = 1.039\,\mathrm{Re}_{D_c}^{-0.418}\left(\frac{F_t}{D_c}\right)^{-0.104} N^{-0.0935}\left(\frac{F_s}{D_c}\right)^{0.197}$
Plain (wet)	*Wang et al.* (1997)	$j_4 = 0.29773\,\mathrm{Re}_{D_c}^{-0.364}\,\varepsilon^{-0.168}$ $j_N = 0.4\,\mathrm{Re}_{D_c}^{-0.468+0.04076N}\,\varepsilon^{0.159}N^{-1.261}$ $f = 28.209\,\mathrm{Re}_{D_c}^{-0.5653}\,N^{-0.1026}\left(\frac{F_s}{D_c}\right)^{-1.3405}\varepsilon^{-1.3343}$ where $\varepsilon = \frac{A_T}{A_{tube}}$
Wavy (dry)	*Mirth & Ramadhyani* (1994)	$j = 0.0197\,\mathrm{Re}_{2F_s}^{-0.06}\left(\frac{P_t - D_c}{2F_s}\right)^{-0.3}\left(1+\frac{111900}{\left[\mathrm{Re}_{2F_s}\left(\frac{L}{2F_s}\right)\right]^{1.2}}\right)$ $f = \frac{0.331}{\mathrm{Re}_{W_h}^{0.368}}\left(\frac{2F_s}{W_h}\right)^{0.473}$
Wavy (wet)	*Mirth & Ramadhyani* (1994)	$f = \frac{2.71}{\mathrm{Re}_{a,wh}^{0.737}} + f(dry)$
Slit (dry)	*Wang and Du* (anticipated	$j = 5.98\,\mathrm{Re}_{D_c}^{j_1}\left(\frac{F_s}{D_c}\right)^{j_2} N^{j_3}\left(\frac{S_w}{S_h}\right)^{j_4}\left(\frac{P_t}{P_l}\right)^{0.804}$

	2001)	$j_1 = -0.647 + 0.198\frac{N}{\ln(\mathrm{Re}_{D_c})} - 0.458\frac{F_s}{D_c} + 2.52\frac{N}{\mathrm{Re}_{D_c}}$ $j_2 = 0.116 + 1.125\frac{N}{\ln(\mathrm{Re}_{D_c})} + 47.6\frac{N}{\mathrm{Re}_{D_c}}$ $j_3 = 0.49 + 175\frac{F_s/D_c}{\mathrm{Re}_{D_c}} - \frac{3.08}{\ln(\mathrm{Re}_{D_c})}$ $j_4 = -0.63 + 0.086S_n$ $f = 0.1851\,\mathrm{Re}_{D_c}^{f_1}\left(\frac{F_s}{D_c}\right)^{f_2}\left(\frac{S_w}{S_h}\right)^{f_3} N^{-0.046}$ $f_1 = -1.485 + 0.656\left(\frac{F_s}{D_c}\right) + 0.855\left(\frac{P_t}{P_l}\right)$ $f_2 = -1.04 - \frac{125}{\mathrm{Re}_{D_c}}$ $f_3 = -0.83 + 0.117S_n$
Slit (wet)	*Kim & Jacobi* (2000)	$j = 0.3647\,\mathrm{Re}_{D_c}^{-0.1457}\left(\frac{F_s}{D_c}\right)^{1.21}\left(\frac{P_l N}{D_c}\right)^{-0.3181}$ $f = 1.265\,\mathrm{Re}_{D_c}^{-0.2991}\left(\frac{F_s}{D_c}\right)^{-0.2918}\left(\frac{P_l N}{D_c}\right)^{-0.1985}$
Louver (dry)	*Wang et al.* (1999)	For $\mathrm{Re}_{Dc}<1000$ $j = 14.3117\,\mathrm{Re}_{D_c}^{J1}\left(\frac{F_p}{D_c}\right)^{J2}\left(\frac{L_h}{L_p}\right)^{J3}\left(\frac{F_p}{P_l}\right)^{J4}\left(\frac{P_l}{P_t}\right)^{-1.724}$ where $J1 = -0.991 - 0.1055\left(\frac{P_l}{P_t}\right)^{3.1}\ln\left(\frac{L_h}{L_p}\right)$ $J2 = -0.7344 + 2.1059\left(\frac{N^{0.55}}{\ln(\mathrm{Re}_{D_c}) - 3.2}\right)$

$$J3 = 0.08485\left(\frac{P_l}{P_t}\right)^{-4.4} N^{-0.68}$$

$$J4 = -0.1741\ln(N)$$

For $Re_{Dc} \geq 1000$

$$j = 1.1373\,\mathrm{Re}_{D_c}^{J5}\left(\frac{F_p}{P_l}\right)^{J6}\left(\frac{L_h}{L_p}\right)^{J7}\left(\frac{P_l}{P_t}\right)^{J8}(N)^{0.3545}$$

where

$$J5 = -0.6027 + 0.02593\left(\frac{P_l}{D_h}\right)^{0.52}(N)^{-0.5}\ln\left(\frac{L_h}{L_p}\right)$$

$$J6 = -0.4776 + 0.40774\left(\frac{N^{0.7}}{\ln(\mathrm{Re}_{D_c})-4.4}\right)$$

$$J7 = -0.58655\left(\frac{F_p}{D_h}\right)^{2.3}\left(\frac{P_l}{P_t}\right)^{-1.6} N^{-0.65}$$

$$J8 = 0.0814\left(\ln(\mathrm{Re}_{D_c})-3\right)$$

$$D_h = \frac{4A_{\min}}{L}$$

For N=1,

$$f = 0.00317\,\mathrm{Re}_{D_c}^{F1}\left(\frac{F_p}{P_l}\right)^{F2}\left(\frac{D_h}{D_c}\right)^{F3}\left(\frac{L_h}{L_p}\right)^{F4}\left(\ln\left(\frac{A_T}{A_{tube}}\right)\right)^{-6.0483}$$

where

$$F1 = 0.1691 + 4.4118\left(\frac{F_p}{P_l}\right)^{-0.3}\left(\frac{L_h}{L_p}\right)^{-2}\left(\ln\left(\frac{P_l}{P_t}\right)\right)\left(\frac{F_p}{P_t}\right)^{3}$$

$$F2 = -2.6642 - 14.3809\left(\frac{1}{\ln(\mathrm{Re}_{D_c})}\right)$$

		$F3 = -0.6816 \ln\left(\frac{F_p}{P_l}\right)$ $F4 = 6.4668\left(\frac{F_p}{P_t}\right)^{1.7} \ln\left(\frac{A_T}{A_{tube}}\right)$ For N>1, $f = 0.06393 \mathrm{Re}_{D_c}^{F5}\left(\frac{F_p}{D_c}\right)^{F6}\left(\frac{D_h}{D_c}\right)^{F7}\left(\frac{L_h}{L_p}\right)^{F8} N^{F9}\left(\ln\left(\mathrm{Re}_{D_c}\right)-4.0\right)^{-1.0}$ where $F5 = 0.1395 - 0.0101\left(\frac{F_p}{P_l}\right)^{0.58}\left(\frac{L_h}{L_p}\right)^{-2}\left(\ln\left(\frac{A_T}{A_{tube}}\right)\right)\left(\frac{P_l}{P_t}\right)^{1.9}$ $F6 = -6.4367\left(\frac{1}{\ln\left(\mathrm{Re}_{D_c}\right)}\right)$ $F7 = 0.07191 \ln\left(\mathrm{Re}_{D_c}\right)$ $F8 = -2.0585\left(\frac{F_p}{P_t}\right)^{1.67} \ln\left(\mathrm{Re}_{D_c}\right)$ $F9 = 0.1036\left(\ln\left(\frac{P_l}{P_t}\right)\right)$
Louver (wet)	*Wang et al.* (2000)	$j = 9.717 \mathrm{Re}_{D_c}^{j1}\left(\frac{F_s}{D_c}\right)^{j2}\left(\frac{P_l}{P_t}\right)^{j3} \ln\left(3 - \frac{L_p}{F_s}\right)^{0.07162} N^{-0.543}$ where $j1 = -0.023634 - 1.2475\left(\frac{F_s}{D_c}\right)^{0.65}\left(\frac{P_l}{P_t}\right)^{0.2} N^{-0.18}$ $j2 = 0.856 \exp(\tan\theta)$ $j3 = 0.25 \ln\left(\mathrm{Re}_{D_c}\right)$

		$f = 2.814\,\mathrm{Re}_{D_c}^{f1}\left(\frac{F_s}{D_c}\right)^{f2}\left(\frac{P_l}{D_c}\right)^{f3}\left(\frac{P_l}{P_t}+0.091\right)^{f4}\left(\frac{L_p}{F_s}\right)^{1.958} N^{0.04674}$ where $f1 = 1.223 - 2.857\left(\frac{F_s}{D_c}\right)^{0.71}\left(\frac{P_l}{P_t}\right)^{-0.05}$ $f2 = 0.8079\ln\left(\mathrm{Re}_{D_c}\right)$ $f3 = 0.8932\ln\left(\mathrm{Re}_{D_c}\right)$ $f4 = -0.999\ln\left(\frac{2\Gamma}{\mu_f}\right)$

Table C.2 Optimization ranges — Condenser

	Plain			*Wavy*			*Slit*			*Louver*	
	Min	*Max*		*Min*	*Max*		*Min*	*Max*		*Min*	*Max*
D_c [mm]	7.52	13.33		13.5	16.7		8	16		6.93	10.42
L [mm]	17.6	164.4		110	260		22	132		13.6	114.3
F_s [mm]	1.07	3		1.47	3.05		1.21	2.5		1.2	2.49
F_t [mm]	0.147	0.36		0.15	0.15		0.12	0.2		0.115	0.115
P_l [mm]	12.7	27.4		27.5	32.5		15	33		12.7	22
P_t [mm]	20.4	31.7		31.8	38.1		25	38		17.7	25.4
Re_{Dc}	300	6000		1100	7700		350	7000		300	6000
W_h [mm]				2.38	3.25						
S_h [mm]							0.99	1			
S_w [mm]							8	18			
L_h [mm]										0.79	1.4
L_p [mm]										1.7	3.75
D_c^*	2.530E+05	4.484E+05		4.541E+05	5.618E+05		2.691E+05	5.382E+05		2.331E+05	3.505E+05
L^*	5.921E+05	5.530E+06		3.700E+06	8.746E+06		7.401E+05	4.440E+06		4.575E+05	3.845E+06
F_s^*	3.599E+04	1.009E+05		4.945E+04	1.026E+05		4.070E+04	8.410E+04		4.037E+04	8.376E+04
F_t^*	4.945E+03	1.211E+04		5.046E+03	5.046E+03		4.037E+03	6.728E+03		3.869E+03	3.869E+03
P_l^*	4.272E+05	9.217E+05		9.251E+05	1.093E+06		5.046E+05	1.110E+06		4.272E+05	7.401E+05
P_t^*	6.863E+05	1.066E+06		1.070E+06	1.282E+06		8.410E+05	1.278E+06		5.954E+05	8.545E+05
Re_{Dc}	300	6000		1100	7700		350	7000		300	6000
W_h^*				8.006E+04	1.093E+05						
S_h^*							3.330E+04	3.364E+04			
S_w^*							2.691E+05	6.055E+05			
L_h^*										2.658E+04	4.710E+04
L_p^*										5.719E+04	1.262E+05
ΔT [°C]	0.1	30		0.1	30		0.1	30		0.1	30
ΔT^*	3.245E-04	9.736E-02		3.245E-04	9.736E-02		3.245E-04	9.736E-02		3.245E-04	9.736E-02

Table C.3 Optimization ranges — Dry evaporator

	Plain			*Wavy*			*Slit*			*Louver*	
	Min	*Max*		*Min*	*Max*		*Min*	*Max*		*Min*	*Max*
D_c [mm]	7.52	13.33		13.5	16.7		8	16		6.93	10.42
L [mm]	17.6	164.4		110	260		22	132		13.6	114.3
F_s [mm]	1.07	3		1.47	3.05		1.21	2.5		1.2	2.49
F_t [mm]	0.147	0.36		0.15	0.15		0.12	0.2		0.115	0.115
P_l [mm]	12.7	27.4		27.5	32.5		15	33		12.7	22
P_t [mm]	20.4	31.7		31.8	38.1		25	38		17.7	25.4
Re_{Dc}	300	6000		1100	7700		350	7000		300	6000
W_h [mm]				2.38	3.25						
S_h [mm]							0.99	1			
S_w [mm]							8	18			
L_h [mm]										0.79	1.4
L_p [mm]										1.7	3.75
D_c^*	2.619E+05	4.643E+05		4.702E+05	5.817E+05		2.786E+05	5.573E+05		2.414E+05	3.629E+05
L^*	6.130E+05	5.726E+06		3.831E+06	9.056E+06		7.663E+05	4.598E+06		4.737E+05	3.981E+06
F_s^*	3.727E+04	1.045E+05		5.120E+04	1.062E+05		4.214E+04	8.708E+04		4.180E+04	8.673E+04
F_t^*	5.120E+03	1.254E+04		5.225E+03	5.225E+03		4.180E+03	6.966E+03		4.005E+03	4.005E+03
P_l^*	4.423E+05	9.543E+05		9.578E+05	1.132E+06		5.225E+05	1.149E+06		4.423E+05	7.663E+05
P_t^*	7.105E+05	1.104E+06		1.108E+06	1.327E+06		8.708E+05	1.324E+06		6.165E+05	8.847E+05
Re_{Dc}	300	6000		1100	7700		350	7000		300	6000
W_h^*				8.290E+04	1.132E+05						
S_h^*							3.448E+04	3.483E+04			
S_w^*							2.786E+05	6.269E+05			
L_h^*										2.752E+04	4.876E+04
L_p^*										5.921E+04	1.306E+05
ΔT [°C]	0.1	30		0.1	30		0.1	30		0.1	30
ΔT^*	3.335E-04	1.001E-01		3.335E-04	1.001E-01		3.335E-04	1.001E-01		3.335E-04	1.001E-01

Table C.4 Optimization ranges — Wet evaporator

	Plain			*Wavy*			*Slit*			*Louver*	
	Min	*Max*		*Min*	*Max*		*Min*	*Max*		*Min*	*Max*
D_c [mm]	10.23	10.23		13.5	16.7		7.416	7.416		10.33	10.33
L [mm]	44	66		110	260		25.4	38.1		19.05	44
F_s [mm]	1.82	3.2		1.47	3.05		1.3	1.7		1.21	2.49
F_t [mm]	0.13	0.13		0.15	0.15		0.076	0.076		0.115	0.115
P_l [mm]	22	22		27.5	32.5		12.7	12.7		19.05	22
P_t [mm]	25.4	25.4		31.8	38.1		21.65	21.65		25.4	25.4
Re_{Dc}	300	5500		1100	7700		550	2000		400	3000
W_h [mm]				2.38	3.25						
S_h [mm]							0.76	0.76			
S_w [mm]							8.5	8.5			
L_h [mm]										1.07	1.07
L_p [mm]										2	2.35
D_c^*	3.563E+05	3.563E+05		4.702E+05	5.817E+05		2.583E+05	2.583E+05		3.598E+05	3.598E+05
L^*	1.533E+06	2.299E+06		3.831E+06	9.056E+06		8.847E+05	1.327E+06		6.635E+05	1.533E+06
F_s^*	6.339E+04	1.115E+05		5.120E+04	1.062E+05		4.528E+04	5.921E+04		4.214E+04	8.673E+04
F_t^*	4.528E+03	4.528E+03		5.225E+03	5.225E+03		2.647E+03	2.647E+03		4.005E+03	4.005E+03
P_l^*	7.663E+05	7.663E+05		9.578E+05	1.132E+06		4.423E+05	4.423E+05		6.635E+05	7.663E+05
P_t^*	8.847E+05	8.847E+05		1.108E+06	1.327E+06		7.541E+05	7.541E+05		8.847E+05	8.847E+05
Re_{Dc}	300	5500		1100	7700		550	2000		400	3000
W_h^*				8.290E+04	1.132E+05						
S_h^*							2.647E+04	2.647E+04			
S_w^*							2.961E+05	2.961E+05			
L_h^*										3.727E+04	3.727E+04
L_p^*										6.966E+04	8.185E+04
ΔT [°C]	0.1	30		0.1	30		0.1	30		0.1	30
ΔT^*	3.335E-04	1.001E-01		3.335E-04	1.001E-01		3.335E-04	1.001E-01		3.335E-04	1.001E-01

Appendix D – Optimization Code

The EES code for the optimization model is listed in this section. In the interest of space, only the plain fin code for system optimization is listed here; the code for other surface types is the same, although different code sections are commented out. For component optimization, separate EES files were used for condensers and evaporators, as well as for different surface types.

Table D.1 Plain fin system optimization code

```
"Nondimensional system optimization routine"

"System equations"
COP_system=(q_t_evap-W_pump_evap)/(W_pump_evap+W_pump_cond+W_comp_evap)
COP_comp=(-2113.22+8.5198*T_e_evap)+(11.604-0.046894*T_e_evap)*T_c_cond+(-
0.016021+6.489e-5*T_e_evap)*T_c_cond^2

"*********************************************************************************************************"
"*********************************************************************************************************"
"*********************************************************************************************************"
"*********************************************************************************************************"
"*********************************************************************************************************"
"*********************************************************************************************************"


"Evaporator"
"*********************************************************************************************************"
"Nondimensional pressure drop and heat rate equations"
DELTAp_star_evap=1/2*Vfr_star_evap^2*(Afr_Amin_evap)^2*(AT_Amin_evap)*f_evap
qA_star_evap=epsilon_evap*Vfr_star_evap*DELTAT_star_evap
epsilon_evap=1-exp(-eta_0_evap*j_evap*ka_star_evap^(2/3)*AT_Amin_evap)
q_l_evap=eta_0_evap*h_D_evap*A_T_evap*(w_air_in_evap-w_air_sat_evap)*h_fg_evap"[W]"

"Reynolds number conversions"
Re_Dc_evap=Afr_Amin_evap*Vfr_star_evap*Dc_star_evap
Re_Dh_evap=Afr_Amin_evap*Vfr_star_evap*Dh_star_evap
Re_2Fs_evap=Afr_Amin_evap*Vfr_star_evap*2*Fs_star_evap
"Re_Wh_evap=Afr_Amin_evap*Vfr_star_evap*Wh_star_evap"

Dh_star_evap=4*Amin_AT_evap*L_star_evap


"*********************************************************************************************************"
"j and f correlations"

j_evap=if(N_evap,4,j_plain_evap,j_plain_4_evap,j_plain_4_evap)
"j_evap=j_wavy_evap"
```

```
"j_evap=j_slit_evap"
"j_evap=if(Re_Dc_evap,1000,j_louv_1_evap,j_louv_2_evap,j_louv_2_evap)"

f_evap=f_plain_evap
"f_evap=f_wavy_evap"
"f_evap=f_slit_evap"
"f_evap=if(N_evap,1,f_louv_1_evap,f_louv_2_evap,f_louv_2_evap)"


"-----------------------------------------------------"
"Plain fins"
{
"Dry"
"Gray and Webb (1986)"
j_plain_gw_4_evap=0.14*Re_Dc_evap^(-0.328)*(Pt_star_evap/Pl_star_evap)^(-
0.502)*(Fs_star_evap/Dc_star_evap)^0.0312
j_plain_gw_evap=0.991*(2.24*Re_Dc_evap^(-0.092)*(L_star_evap/Pl_star_evap/4)^(-
0.031))^(0.607*(4-L_star_evap/Pl_star_evap))*j_plain_gw_4_evap

"Wang and Chang (1998)"
j_plain_4_evap=j_plain_gw_4_evap*2.55*(Pl_star_evap/Dc_star_evap)^(-1.28)
j_plain_evap=j_plain_gw_evap*2.55*(Pl_star_evap/Dc_star_evap)^(-1.28)

"Wang et al (1996)"
f_plain_evap=1.039*Re_Dc_evap^(-0.418)*(Ft_star_evap/Dc_star_evap)^(-
0.1040)*(L_star_evap/Pl_star_evap)^(-0.0935)*(Fs_star_evap/Dc_star_evap)^0.197
}
"Wet"
"Wang et al. (1997)"
j_plain_4_evap=0.29773*Re_Dc_evap^(-0.364)*AT_Atube_evap^(-0.168)
j_plain_evap=0.4*Re_Dc_evap^(-0.468+0.04076*N_evap)*AT_Atube_evap^0.159*N_evap^(-
1.261)

f_evap=28.209*Re_Dc_evap^(-0.5653)*N_evap^(-0.1026)*(Fs_star_evap/Dc_star_evap)^(-
1.3405)*AT_Atube_evap^(-1.3343)

{
"-----------------------------------------------------"
"Wavy fins"
"Mirth and Ramadhyani (1994)"
j_wavy_evap=0.0197*Re_2Fs_evap^(-0.06)*((Pt_star_evap-Dc_star_evap)/(2*Fs_star_evap))^(-
0.3)*(1+111900/(Re_2Fs_evap*L_star_evap/2/Fs_star_evap)^1.2)
f_wavy_evap=8.64/Re_Wh_evap^0.457*(2*Fs_star_evap/Wh_star_evap)^0.473*(L_star_evap/W
h_star_evap)^(-0.545)
}

"-----------------------------------------------------"
"Slit fins"
{
"Wang,Chang, and Tao (1999)"
j_slit_evap=1.6409*Re_Dc_evap^j_slit_1_evap*(Ss_star_evap/Sh_star_evap)^1.16*(Pt_star_eva
p/Pl_star_evap)^1.37*(Fs_star_evap/Dc_star_evap)^j_slit_2_evap*(L_star_evap/Pl_star_evap)^j
_slit_3_evap
```

```
j_slit_1_evap=-0.674+0.1316*(L_star_evap/Pl_star_evap)/ln(Re_Dc_evap)-
0.3769*Fs_star_evap/Dc_star_evap-1.8857*(L_star_evap/Pl_star_evap)/Re_Dc_evap
j_slit_2_evap=-
0.0178+0.996*(L_star_evap/Pl_star_evap)/ln(Re_Dc_evap)+26.7*(L_star_evap/Pl_star_evap)/Re
_Dc_evap
j_slit_3_evap=1.865+1244.03/Re_Dc_evap*(Fs_star_evap/Dc_star_evap)-14.37/ln(Re_Dc_evap)

f_slit_evap=0.3929*Re_Dc_evap^(-
3.585+0.8846*Fs_star_evap/Dc_star_evap+2.677*Pt_star_evap/Pl_star_evap)*(L_star_evap/Pl_
star_evap)^(-0.009*ln(Re_Dc_evap))*(Ss_star_evap/Sh_star_evap)^(-
2.48)*(Fs_star_evap/Dc_star_evap)^(-1.5706*157.06/Re_Dc_evap)
}
{
"Wang & Du (2001)"
j_slit_evap=5.98*Re_Dc_evap^j_slit_1_evap*(Fs_star_evap/Dc_star_evap)^j_slit_2_evap*(L_star
_evap/Pl_star_evap)^j_slit_3_evap*(Sw_star_evap/Sh_star_evap)^j_slit_4_evap*(Pt_star_evap/P
l_star_evap)^0.804
j_slit_1_evap=-0.647+0.198*(L_star_evap/Pl_star_evap)/ln(Re_Dc_evap)-
0.458*(Fs_star_evap/Dc_star_evap)+2.52*(L_star_evap/Pl_star_evap)/Re_Dc_evap
j_slit_2_evap=0.116+1.125*(L_star_evap/Pl_star_evap)/ln(Re_Dc_evap)+47.6*(L_star_evap/Pl_s
tar_evap)/Re_Dc_evap
j_slit_3_evap=0.49+175*Fs_star_evap/Dc_star_evap/Re_Dc_evap-3.08/ln(Re_Dc_evap)
j_slit_4_evap=(-0.63)+0.086*S_n

f_slit=0.1851*Re_Dc_evap^f_slit_1_evap*(Fs_star_evap/Dc_star_evap)^f_slit_2_evap*(Sw_star_
evap/Sh_star_evap)^f_slit_3_evap*(L_star_evap/Pl_star_evap)^(-0.046)
f_slit_1=(-1.485)+0.656*Fs_star_evap/Dc_star_evap+0.855*(Pt_star_evap/Pl_star_evap)
f_slit_2=(-1.04)-125/Re_Dc_evap
f_slit_3=(-0.83)+0.117*S_n
}
{
"------------------------------------------------------"
"Louvered fins"
"Re_Dc_evap<1000"
j_louv_1_evap=14.3117*Re_Dc_evap^j_1_evap*(Fs_star_evap/Dc_star_evap)^j_2_evap*(Lh_sta
r_evap/Lp_star_evap)^j_3_evap*(Fs_star_evap/Pl_star_evap)^j_4_evap*(Pl_star_evap/Pt_star_e
vap)^(-1.724)
j_1_evap=(-0.991)-0.1055*(Pl_star_evap/Pt_star_evap)^3.1*ln(Lh_star_evap/Lp_star_evap)
j_2_evap=(-0.7344)+2.1059*((L_star_evap/Pl_star_evap)^0.55/(ln(Re_Dc_evap)-3.2))
j_3_evap=0.08485*(Pl_star_evap/Pt_star_evap)^(-4.4)*(L_star_evap/Pl_star_evap)^(-0.68)
j_4_evap=(-0.1741)*ln(L_star_evap/Pl_star_evap)

"Re_Dc_evap>=1000"
j_louv_2_evap=1.1373*Re_Dc_evap^j_5_evap*(Fs_star_evap/Pl_star_evap)^j_6_evap*(Lh_star_
evap/Lp_star_evap)^j_7_evap*(Pl_star_evap/Pt_star_evap)^j_8_evap*(L_star_evap/Pl_star_eva
p)^0.3545
j_5_evap=(-0.6027)+0.02593*(Pl_star_evap/Dh_star_evap)^0.52*(L_star_evap/Pl_star_evap)^(-
0.5)*ln(Lh_star_evap/Lp_star_evap)
j_6_evap=(-0.4776)+0.40774*((L_star_evap/Pl_star_evap)^(0.7)/(ln(Re_Dc_evap)-4.4))
j_7_evap=(-0.58655)*(Fs_star_evap/Dh_star_evap)^2.3*(Pl_star_evap/Pt_star_evap)^(-
1.6)*(L_star_evap/Pl_star_evap)^(-0.65)
j_8_evap=0.0814*(ln(Re_Dc_evap)-3)

"N=1"
```

```
f_louv_1_evap=0.00317*Re_Dc_evap^f_1_evap*(Fs_star_evap/Pl_star_evap)^f_2_evap*(Dh_sta
r_evap/Dc_star_evap)^f_3_evap*(Lh_star_evap/Lp_star_evap)^f_4_evap*(ln(AT_Atube_evap))^(
-6.0483)
f_1_evap=0.1691+4.4118*(Fs_star_evap/Pl_star_evap)^(-0.3)*(Lh_star_evap/Lp_star_evap)^(-
2)*ln(Pl_star_evap/Pt_star_evap)*(Fs_star_evap/Pt_star_evap)^3
f_2_evap=(-2.6642)-14.3809*(1/ln(Re_Dc_evap))
f_3_evap=(-0.6816)*ln(Fs_star_evap/Pl_star_evap)
f_4_evap=6.4668*(Fs_star_evap/Pt_star_evap)^(1.7)*ln(AT_Atube_evap)

"N>1"
f_louv_2_evap=0.06393*Re_Dc_evap^f_5_evap*(Fs_star_evap/Dc_star_evap)^f_6_evap*(Dh_st
ar_evap/Dc_star_evap)^f_7_evap*(Lh_star_evap/Lp_star_evap)^f_8_evap*(L_star_evap/Pl_star_
evap)^f_9_evap*(ln(Re_Dc_evap)-4.0)^(-1.093)
f_5_evap=0.1395-0.0101*(Fs_star_evap/Pl_star_evap)^0.58*(Lh_star_evap/Lp_star_evap)^(-
2)*ln(AT_Atube_evap)*(Pl_star_evap/Pt_star_evap)^1.9
f_6_evap=(-6.4367)*(1/ln(Re_Dc_evap))
f_7_evap=0.07191*ln(Re_Dc_evap)
f_8_evap=(-2.0585)*(Fs_star_evap/Pt_star_evap)^1.67*ln(Re_Dc_evap)
f_9_evap=0.1036*ln(Pl_star_evap/Pt_star_evap)
}

"*************************************************************************************************"
"Area ratios"
Amin_AT_num_evap=(1-Ft_star_evap/Fs_star_evap-
Dc_star_evap/Pt_star_evap+Ft_star_evap/Fs_star_evap*Dc_star_evap/Pt_star_evap)
Amin_AT_den_evap=(2*L_star_evap*(1/Fs_star_evap-
pi/4*(Dc_star_evap)^2/Pt_star_evap/Pl_star_evap/Fs_star_evap+pi/2*Dc_star_evap/Pt_star_eva
p/Pl_star_evap-pi/2*Ft_star_evap*Dc_star_evap/Pt_star_evap/Pl_star_evap/Fs_star_evap))
Amin_AT_evap=Amin_AT_num_evap/Amin_AT_den_evap
AT_Amin_evap=1/Amin_AT_evap
Amin_Afr_evap=1-Ft_star_evap/Fs_star_evap-
Dc_star_evap/Pt_star_evap+Ft_star_evap/Fs_star_evap*Dc_star_evap/Pt_star_evap
sigma_evap=Amin_Afr_evap
Afr_Amin_evap=1/(1-Ft_star_evap/Fs_star_evap-
Dc_star_evap/Pt_star_evap+Ft_star_evap/Fs_star_evap*Dc_star_evap/Pt_star_evap)
Afin_AT_num_evap=(1/Fs_star_evap-
pi/4*Dc_star_evap^2/(Fs_star_evap*Pt_star_evap*Pl_star_evap))
Afin_AT_den_evap=(1/Fs_star_evap-
pi/4*Dc_star_evap^2/(Fs_star_evap*Pt_star_evap*Pl_star_evap)+pi/2*Dc_star_evap/(Pt_star_ev
ap*Pl_star_evap)-pi/2*Ft_star_evap*Dc_star_evap/(Fs_star_evap*Pt_star_evap*Pl_star_evap))
Afin_AT_evap=Afin_AT_num_evap/Afin_AT_den_evap
AT_Atube_evap=(2*Pt_star_evap*Pl_star_evap/(pi*Fs_star_evap*Dc_star_evap)-
Dc_star_evap/2/Fs_star_evap+1-Ft_star_evap/Fs_star_evap)/(1-Ft_star_evap/Fs_star_evap)

"Surface efficiency - Sector method using Bessel functions"
mD_c_evap=(2*j_evap*Afr_Amin_evap*Vfr_star_evap*Dc_star_evap^2/Ft_star_evap/ka_star_ev
ap^(1/3)*ka_star_evap/kf_star_evap)^0.5
mr_i_evap=mD_c_evap/2
N_sectors_evap=4

{Counter side}
Duplicate iter_evap=1, N_sectors_evap
{Octans 2 ,3,6 and 7}
```

```
    R_evap[iter_evap]=(Pt_star_evap/Dc_star_evap)*(((((2*iter_evap-
1)/(2*N_sectors_evap))^2)+(Pl_star_evap/Pt_star_evap)^2))^0.5
    S_evap[iter_evap]=(Dc_star_evap^2)/8*((R_evap[iter_evap]^2)-
1)*(arctan(iter_evap/N_sectors_evap*Pt_star_evap/Pl_star_evap)-arctan((iter_evap-
1)/N_sectors_evap*Pt_star_evap/Pl_star_evap))
    mr_o_evap[iter_evap]=mr_i_evap*R_evap[iter_evap]
    bessel_num_evap[iter_evap]=Bessel_K1(mr_i_evap)*Bessel_I1(mr_o_evap[iter_evap])-
Bessel_K1(mr_o_evap[iter_evap])*Bessel_I1(mr_i_evap)
    bessel_den_evap[iter_evap]=Bessel_K1(mr_o_evap[iter_evap])*Bessel_I0(mr_i_evap)+Bess
el_K0(mr_i_evap)*Bessel_I1(mr_o_evap[iter_evap])
    Eff_evap[iter_evap]=2/(mr_i_evap*(R_evap[iter_evap]^2-
1))*bessel_num_evap[iter_evap]/bessel_den_evap[iter_evap]
    Num_evap[iter_evap]=4*Eff_evap[iter_evap]*S_evap[iter_evap]
    Den_evap[iter_evap]=4*S_evap[iter_evap]
{Octans 1 , 4, 5 and 8}
    R_evap[2*N_sectors_evap+1-iter_evap]=(Pt_star_evap/Dc_star_evap)*(((((2*iter_evap-
1)/(2*N_sectors_evap))^2)*(Pl_star_evap/Pt_star_evap)^2)+1)^0.5
    S_evap[2*N_sectors_evap+1-iter_evap]=(Dc_star_evap^2)/8*((R_evap[2*iter_evap+1-
iter_evap]^2)-1)*(arctan(iter_evap/N_sectors_evap*Pl_star_evap/Pt_star_evap)-
arctan((iter_evap-1)/N_sectors_evap*Pl_star_evap/Pt_star_evap))
    mr_o_evap[2*N_sectors_evap+1-iter_evap]=mr_i_evap*R_evap[2*N_sectors_evap+1-
iter_evap]
    bessel_num_evap[2*N_sectors_evap+1-
iter_evap]=Bessel_K1(mr_i_evap)*Bessel_I1(mr_o_evap[2*N_sectors_evap+1-iter_evap])-
Bessel_K1(mr_o_evap[2*N_sectors_evap+1-iter_evap])*Bessel_I1(mr_i_evap)
    bessel_den_evap[2*N_sectors_evap+1-
iter_evap]=Bessel_K1(mr_o_evap[2*N_sectors_evap+1-
iter_evap])*Bessel_I0(mr_i_evap)+Bessel_K0(mr_i_evap)*Bessel_I1(mr_o_evap[2*N_sectors_ev
ap+1-iter_evap])
    Eff_evap[2*N_sectors_evap+1-iter_evap]=2/(mr_i_evap*(R_evap[2*N_sectors_evap+1-
iter_evap]^2-1))*bessel_num_evap[2*N_sectors_evap+1-
iter_evap]/bessel_den_evap[2*N_sectors_evap+1-iter_evap]
    Num_evap[2*N_sectors_evap+1-iter_evap]=4*Eff_evap[2*N_sectors_evap+1-
iter_evap]*S_evap[2*N_sectors_evap+1-iter_evap]
    Den_evap[2*N_sectors_evap+1-iter_evap]=4*S_evap[2*N_sectors_evap+1-iter_evap]
End

Num_evap=SUM(Num_evap[iter_evap],
iter_evap=1,N_sectors_evap)+SUM(Num_evap[2*N_sectors_evap+1-iter_evap], iter_evap=1,
N_sectors_evap)
Den_evap=SUM(Den_evap[iter_evap],
iter_evap=1,N_sectors_evap)+SUM(Den_evap[2*N_sectors_evap+1-iter_evap], iter_evap=1,
N_sectors_evap)

eta_f_evap=Num_evap/Den_evap
eta_0_evap=1-Afin_AT_evap*(1-eta_f_evap)


"************************************************************************************************"
"PECs"

"Area-Goodness Ratio"
PEC_j_over_f_evap=j_evap/f_evap
```

```
"Heat Transfer/Pumping Power"
PEC_THETA_old_evap=2*eta_fm_evap*epsilon_evap*DELTAT_star_evap/(Vfr_star_evap^2*f_e
vap)*Amin_Afr_evap^2*Amin_AT_evap
PEC_THETA_evap=q_t_evap/W_pump_evap

"Heat Transfer/(Pumping Power + Compressor Power)"
PEC_OMEGA_evap=(1/PEC_THETA_evap+1/(a_star_evap-
b_star_evap*DELTAT_star_evap))^(-1)

"*********************************************************************************************"
"Nondimensional geometric variables normalized by D_c"
"Plain fins"
L_Dc_evap=L_star_evap/Dc_star_evap
Fs_Dc_evap=Fs_star_evap/Dc_star_evap
Ft_Dc_evap=Ft_star_evap/Dc_star_evap
Pl_Dc_evap=Pl_star_evap/Dc_star_evap
Pt_Dc_evap=Pt_star_evap/Dc_star_evap
{
"Wavy fins"
Wh_Dc_evap=Wh_star_evap/Dc_star_evap

"Slit fins"
Sh_Dc_evap=Sh_star_evap/Dc_star_evap
Sw_Dc_evap=Sw_star_evap/Dc_star_evap

"Louvered fins"
Lh_Dc_evap=Lh_star_evap/Dc_star_evap
Lp_Dc_evap=Lp_star_evap/Dc_star_evap
}

"Inputs to model"
eta_fm_evap=0.15          "taken from system data"
D_AB_evap=0.26e-4         "[m2/s]"
S_n_evap=4                "slit fins - use to constrain number of slits"
rh_air_in_evap=0.5        "inlet relative humidity"
T_o_evap=299.82           "[K]"       "ambient temperature in Kelvins"
P_atm_evap=101            "[kPa]"     "ambient pressure"
k_fin_evap=222.05         "[W/m-K]"   "aluminum"
"D_c_evap=0.009525"       "[m]"       "different tube diameters affect optimization results"
a_cop_evap=6.5906         "[]"        "Copeland ZP32K3E-PFV compressor, Te=50F"
b_cop_evap=0.15153        "[1/K]"     "Copeland ZP32K3E-PFV compressor, Te=50F"
"q_over_A_evap=24000"     "[W/m2]"    "set to constrain heat flux"
A_fr_evap=0.32            "[m2]"      "set to constrain frontal area"
q_s_evap=7680             "[W]"       "set to constrain heat duty"
Dc_star_evap=3.563e5
Ft_star_evap=4528
Pl_star_evap=7.663e5
Pt_star_evap=8.847e5

"Air properties"
mu_air_evap=viscosity(AirH2O,T=T_o_evap,P=P_atm_evap,w=w_air_in_evap)  "[kg/m-s]"
rho_air_evap=density(AirH2O,T=T_o_evap,P=P_atm_evap,w=w_air_in_evap)   "[kg/m3]"
cp_air_evap=specheat(AirH2O,T=T_o_evap,P=P_atm_evap,R=rh_air_in_evap)*1000"[J/kg-K]"
k_air_evap=conductivity(AirH2O,T=T_o_evap,P=P_atm_evap,w=w_air_in_evap) "[W/m-K]"
```

```
Le_evap=k_air_evap/rho_air_evap/cp_air_evap/D_AB_evap
w_air_in_evap=humrat(AirH2O,t=T_o_evap,p=P_atm_evap,r=rh_air_in_evap)
    "[kg H2O/kg dry air]"
T_dp_evap=dewpoint(AirH2O,t=T_o_evap,P=P_atm_evap,w=w_air_in_evap)    "[K]"
"T_surf_evap=(T_e_evap+T_dp_evap)/2"    "[K]""average temperature at wetted surface"
T_surf_evap=T_o_evap-eta_0_evap*DELTAT_evap                    "[K]"
w_air_sat_evap=humrat(AirH2O,t=T_surf_evap,p=P_atm_evap,r=1)
    "[kg H2O/kg dry air]"  "humidity ratio of saturated air at wetted surface temp"
cp_moist_air_evap=specheat(AirH2O,t=T_o_evap,p=P_atm_evap,r=rh_air_in_evap)*1000
    "[J/kg-K]"
h_D_evap=h_c_evap/cp_moist_air_evap*Le_evap^(-2/3)                "[kg/m2-s]"
h_fg_evap=(enthalpy(water,t=T_e_evap,x=1)-enthalpy(water,t=T_e_evap,x=0))*1000
    "[J/kg]"

q_t_evap=if(q_l_evap,0,q_s_evap,q_s_evap,q_s_evap+q_l_evap)          "[W]"
q_rat_evap=q_s_evap/q_t_evap
q_rat_evap=0.75

"Dimensional-Nondimensional conversion equations"
ka_star_evap=k_air_evap/(mu_air_evap*cp_air_evap)                    "1.41"
kf_star_evap=k_fin_evap/(mu_air_evap*cp_air_evap)                    "11663"
D_c_evap=Dc_star_evap*mu_air_evap/(rho_air_evap*sqrt(cp_air_evap*T_o_evap))"[m]"
V_fr_evap=Vfr_star_evap*sqrt(cp_air_evap*T_o_evap)                   "[m/s]"
DELTAT_evap=DELTAT_star_evap*T_o_evap                                "[C]"
DELTAp_evap=DELTAp_star_evap*T_o_evap*rho_air_evap*cp_air_evap
    "[Pa] (equivalent to kg/m-s2)"
q_over_A_evap=qA_star_evap*rho_air_evap*(cp_air_evap*T_o_evap)^1.5    "[W/m2]"
q_over_A_evap=q_s_evap/A_fr_evap
a_star_evap=a_cop_evap          "best COP possible for a given condenser and Tc"
b_star_evap=b_cop_evap*T_o_evap  "slope of COP penalty for increasing DELTAT"
Pr_evap=1/ka_star_evap
Nu_Dc_evap=j_evap*Re_Dc_evap*Pr_evap^(1/3)
h_c_evap=Nu_Dc_evap*k_air_evap/D_c_evap                          "[W/m2-K]"
A_T_evap=AT_Amin_evap/Afr_Amin_evap*A_fr_evap                    "[m2]"


"Other terms of interest"
T_e_evap=T_o_evap-DELTAT_evap                                    "[K]"
V_dot_evap=V_fr_evap*A_fr_evap*convert(m3/s,cfm)                 "[cfm]"
W_pump_evap=V_fr_evap*A_fr_evap*DELTAp_evap/eta_fm_evap          "[W]"
"W_pump_evap=(V_dot_evap/1000)^3*365"                            "[W]"
"W_comp_evap=q_t_evap/COP_evap"                                  "[W]"
W_comp_evap=q_t_evap/COP_comp                                    "[W]"
COP_evap=a_star_evap-b_star_evap*DELTAT_star_evap                "based on curve
fit from compressor map"
N_evap=L_star_evap/Pl_star_evap          "can use to constrain number of tube rows"
Vol_fin_evap=L_evap*F_t_evap/F_s_evap*A_fr_evap                  "[m3]"


"Use this section for non-optimization runs (i.e. analyzing an existing design)"
i_evap=3

"H_evap=lookup(i_evap,1)*convert(ft,m)
W_evap=lookup(i_evap,2)*convert(ft,m)"
```

```
"L_evap=lookup(i_evap,3)*convert(ft,m)
F_s_evap=lookup(i_evap,4)*convert(ft,m)"
"F_t_evap=lookup(i_evap,5)*convert(ft,m)"
"P_l_evap=lookup(i_evap,6)*convert(ft,m)
P_t_evap=lookup(i_evap,7)*convert(ft,m)"
"V_dot_evap=lookup(i_evap,8)"
"q_s_evap=lookup(i_evap,10)*convert(Btu/hr,W)"

L_evap=L_star_evap*mu_air_evap/(rho_air_evap*sqrt(cp_air_evap*T_o_evap))  "[m]"
F_s_evap=Fs_star_evap*mu_air_evap/(rho_air_evap*sqrt(cp_air_evap*T_o_evap))"[m]"
F_t_evap=Ft_star_evap*mu_air_evap/(rho_air_evap*sqrt(cp_air_evap*T_o_evap))"[m]"
P_l_evap=Pl_star_evap*mu_air_evap/(rho_air_evap*sqrt(cp_air_evap*T_o_evap))"[m]"
P_t_evap=Pt_star_evap*mu_air_evap/(rho_air_evap*sqrt(cp_air_evap*T_o_evap))"[m]"

"A_fr_evap=H_evap*W_evap"                                                    "[m2]"


"*************************************************************************************************"
"*************************************************************************************************"
"*************************************************************************************************"
"*************************************************************************************************"
"*************************************************************************************************"
"*************************************************************************************************"
"*************************************************************************************************"
"*************************************************************************************************"


"Condenser"
"*************************************************************************************************"
"Nondimensional pressure drop and heat rate equations"
DELTAp_star_cond=1/2*Vfr_star_cond^2*(Afr_Amin_cond)^2*(AT_Amin_cond)*f_cond
qA_star_cond=epsilon_cond*Vfr_star_cond*DELTAT_star_cond
epsilon_cond=1-exp(-eta_0_cond*j_cond*ka_star_cond^(2/3)*AT_Amin_cond)

"Reynolds number conversions"
Re_Dc_cond=Afr_Amin_cond*Vfr_star_cond*Dc_star_cond
Re_Dh_cond=Afr_Amin_cond*Vfr_star_cond*Dh_star_cond
Re_2Fs_cond=Afr_Amin_cond*Vfr_star_cond*2*Fs_star_cond
"Re_Wh_cond=Afr_Amin_cond*Vfr_star_cond*Wh_star_cond"

Dh_star_cond=4*Amin_AT_cond*L_star_cond


"*************************************************************************************************"
"j and f correlations"

j_cond=if(N_cond,4,j_plain_cond,j_plain_4_cond,j_plain_4_cond)
"j_cond=j_wavy_cond"
"j_cond=j_slit_cond"
"j_cond=if(Re_Dc_cond,1000,j_louv_1_cond,j_louv_2_cond,j_louv_2_cond)"

f_cond=f_plain_cond
"f_cond=f_wavy_cond"
"f_cond=f_slit_cond"
```

```
"f_cond=if(N_cond,1,f_louv_1_cond,f_louv_2_cond,f_louv_2_cond)"


"-------------------------------------------------------"
"Plain fins"
"Gray and Webb (1986)"
j_plain_gw_4_cond=0.14*Re_Dc_cond^(-0.328)*(Pt_star_cond/Pl_star_cond)^(-
0.502)*(Fs_star_cond/Dc_star_cond)^0.0312
j_plain_gw_cond=0.991*(2.24*Re_Dc_cond^(-0.092)*(L_star_cond/Pl_star_cond/4)^(-
0.031))^(0.607*(4-L_star_cond/Pl_star_cond))*j_plain_gw_4_cond

"Wang and Chang (1998)"
j_plain_4_cond=j_plain_gw_4_cond*2.55*(Pl_star_cond/Dc_star_cond)^(-1.28)
j_plain_cond=j_plain_gw_cond*2.55*(Pl_star_cond/Dc_star_cond)^(-1.28)

"Wang et al (1996)"
f_plain_cond=1.039*Re_Dc_cond^(-0.418)*(Ft_star_cond/Dc_star_cond)^(-
0.1040)*(L_star_cond/Pl_star_cond)^(-0.0935)*(Fs_star_cond/Dc_star_cond)^0.197

{
"-------------------------------------------------------"
"Wavy fins"
"Mirth and Ramadhyani (1994)"
j_wavy_cond=0.0197*Re_2Fs_cond^(-0.06)*((Pt_star_cond-Dc_star_cond)/(2*Fs_star_cond))^(-
0.3)*(1+111900/(Re_2Fs_cond*L_star_cond/2/Fs_star_cond)^1.2)
f_wavy_cond=8.64/Re_Wh_cond^0.457*(2*Fs_star_cond/Wh_star_cond)^0.473*(L_star_cond/W
h_star_cond)^(-0.545)
}

"-------------------------------------------------------"
"Slit fins"
{
"Wang,Chang, and Tao (1999)"
j_slit_cond=1.6409*Re_Dc_cond^j_slit_1_cond*(Ss_star_cond/Sh_star_cond)^1.16*(Pt_star_con
d/Pl_star_cond)^1.37*(Fs_star_cond/Dc_star_cond)^j_slit_2_cond*(L_star_cond/Pl_star_cond)^j
_slit_3_cond
j_slit_1_cond=-0.674+0.1316*(L_star_cond/Pl_star_cond)/ln(Re_Dc_cond)-
0.3769*Fs_star_cond/Dc_star_cond-1.8857*(L_star_cond/Pl_star_cond)/Re_Dc_cond
j_slit_2_cond=-
0.0178+0.996*(L_star_cond/Pl_star_cond)/ln(Re_Dc_cond)+26.7*(L_star_cond/Pl_star_cond)/Re
_Dc_cond
j_slit_3_cond=1.865+1244.03/Re_Dc_cond*(Fs_star_cond/Dc_star_cond)-14.37/ln(Re_Dc_cond)

f_slit_cond=0.3929*Re_Dc_cond^(-
3.585+0.8846*Fs_star_cond/Dc_star_cond+2.677*Pt_star_cond/Pl_star_cond)*(L_star_cond/Pl_
star_cond)^(-0.009*ln(Re_Dc_cond))*(Ss_star_cond/Sh_star_cond)^(-
2.48)*(Fs_star_cond/Dc_star_cond)^(-1.5706*157.06/Re_Dc_cond)
}
{
"Wang & Du (2001)"
j_slit_cond=5.98*Re_Dc_cond^j_slit_1_cond*(Fs_star_cond/Dc_star_cond)^j_slit_2_cond*(L_star
_cond/Pl_star_cond)^j_slit_3_cond*(Sw_star_cond/Sh_star_cond)^j_slit_4_cond*(Pt_star_cond/P
l_star_cond)^0.804
```

```
j_slit_1_cond=-0.647+0.198*(L_star_cond/Pl_star_cond)/ln(Re_Dc_cond)-
0.458*(Fs_star_cond/Dc_star_cond)+2.52*(L_star_cond/Pl_star_cond)/Re_Dc_cond
j_slit_2_cond=0.116+1.125*(L_star_cond/Pl_star_cond)/ln(Re_Dc_cond)+47.6*(L_star_cond/Pl_s
tar_cond)/Re_Dc_cond
j_slit_3_cond=0.49+175*Fs_star_cond/Dc_star_cond/Re_Dc_cond-3.08/ln(Re_Dc_cond)
j_slit_4_cond=(-0.63)+0.086*S_n

f_slit=0.1851*Re_Dc_cond^f_slit_1_cond*(Fs_star_cond/Dc_star_cond)^f_slit_2_cond*(Sw_star_
cond/Sh_star_cond)^f_slit_3_cond*(L_star_cond/Pl_star_cond)^(-0.046)
f_slit_1=(-1.485)+0.656*Fs_star_cond/Dc_star_cond+0.855*(Pt_star_cond/Pl_star_cond)
f_slit_2=(-1.04)-125/Re_Dc_cond
f_slit_3=(-0.83)+0.117*S_n
}
{
"-------------------------------------------------------"
"Louvered fins"
"Re_Dc_cond<1000"
j_louv_1_cond=14.3117*Re_Dc_cond^j_1_cond*(Fs_star_cond/Dc_star_cond)^j_2_cond*(Lh_sta
r_cond/Lp_star_cond)^j_3_cond*(Fs_star_cond/Pl_star_cond)^j_4_cond*(Pl_star_cond/Pt_star_c
ond)^(-1.724)
j_1_cond=(-0.991)-0.1055*(Pl_star_cond/Pt_star_cond)^3.1*ln(Lh_star_cond/Lp_star_cond)
j_2_cond=(-0.7344)+2.1059*((L_star_cond/Pl_star_cond)^0.55/(ln(Re_Dc_cond)-3.2))
j_3_cond=0.08485*(Pl_star_cond/Pt_star_cond)^(-4.4)*(L_star_cond/Pl_star_cond)^(-0.68)
j_4_cond=(-0.1741)*ln(L_star_cond/Pl_star_cond)

"Re_Dc_cond>=1000"
j_louv_2_cond=1.1373*Re_Dc_cond^j_5_cond*(Fs_star_cond/Pl_star_cond)^j_6_cond*(Lh_star_
cond/Lp_star_cond)^j_7_cond*(Pl_star_cond/Pt_star_cond)^j_8_cond*(L_star_cond/Pl_star_con
d)^0.3545
j_5_cond=(-0.6027)+0.02593*(Pl_star_cond/Dh_star_cond)^0.52*(L_star_cond/Pl_star_cond)^(-
0.5)*ln(Lh_star_cond/Lp_star_cond)
j_6_cond=(-0.4776)+0.40774*((L_star_cond/Pl_star_cond)^(0.7)/(ln(Re_Dc_cond)-4.4))
j_7_cond=(-0.58655)*(Fs_star_cond/Dh_star_cond)^2.3*(Pl_star_cond/Pt_star_cond)^(-
1.6)*(L_star_cond/Pl_star_cond)^(-0.65)
j_8_cond=0.0814*(ln(Re_Dc_cond)-3)

"N=1"
f_louv_1_cond=0.00317*Re_Dc_cond^f_1_cond*(Fs_star_cond/Pl_star_cond)^f_2_cond*(Dh_sta
r_cond/Dc_star_cond)^f_3_cond*(Lh_star_cond/Lp_star_cond)^f_4_cond*(ln(AT_Atube_cond))^(
-6.0483)
f_1_cond=0.1691+4.4118*(Fs_star_cond/Pl_star_cond)^(-0.3)*(Lh_star_cond/Lp_star_cond)^(-
2)*ln(Pl_star_cond/Pt_star_cond)*(Fs_star_cond/Pt_star_cond)^3
f_2_cond=(-2.6642)-14.3809*(1/ln(Re_Dc_cond))
f_3_cond=(-0.6816)*ln(Fs_star_cond/Pl_star_cond)
f_4_cond=6.4668*(Fs_star_cond/Pt_star_cond)^(1.7)*ln(AT_Atube_cond)

"N>1"
f_louv_2_cond=0.06393*Re_Dc_cond^f_5_cond*(Fs_star_cond/Dc_star_cond)^f_6_cond*(Dh_st
ar_cond/Dc_star_cond)^f_7_cond*(Lh_star_cond/Lp_star_cond)^f_8_cond*(L_star_cond/Pl_star_
cond)^f_9_cond*(ln(Re_Dc_cond)-4.0)^(-1.093)
f_5_cond=0.1395-0.0101*(Fs_star_cond/Pl_star_cond)^0.58*(Lh_star_cond/Lp_star_cond)^(-
2)*ln(AT_Atube_cond)*(Pl_star_cond/Pt_star_cond)^1.9
f_6_cond=(-6.4367)*(1/ln(Re_Dc_cond))
f_7_cond=0.07191*ln(Re_Dc_cond)
```

```
f_8_cond=(-2.0585)*(Fs_star_cond/Pt_star_cond)^1.67*ln(Re_Dc_cond)
f_9_cond=0.1036*ln(Pl_star_cond/Pt_star_cond)
}

"***************************************************************************************************"
"Area ratios"
Amin_AT_num_cond=(1-Ft_star_cond/Fs_star_cond-
Dc_star_cond/Pt_star_cond+Ft_star_cond/Fs_star_cond*Dc_star_cond/Pt_star_cond)
Amin_AT_den_cond=(2*L_star_cond*(1/Fs_star_cond-
pi/4*(Dc_star_cond)^2/Pt_star_cond/Pl_star_cond/Fs_star_cond+pi/2*Dc_star_cond/Pt_star_con
d/Pl_star_cond-pi/2*Ft_star_cond*Dc_star_cond/Pt_star_cond/Pl_star_cond/Fs_star_cond))
Amin_AT_cond=Amin_AT_num_cond/Amin_AT_den_cond
AT_Amin_cond=1/Amin_AT_cond
Amin_Afr_cond=1-Ft_star_cond/Fs_star_cond-
Dc_star_cond/Pt_star_cond+Ft_star_cond/Fs_star_cond*Dc_star_cond/Pt_star_cond
sigma_cond=Amin_Afr_cond
Afr_Amin_cond=1/(1-Ft_star_cond/Fs_star_cond-
Dc_star_cond/Pt_star_cond+Ft_star_cond/Fs_star_cond*Dc_star_cond/Pt_star_cond)
Afin_AT_num_cond=(1/Fs_star_cond-
pi/4*Dc_star_cond^2/(Fs_star_cond*Pt_star_cond*Pl_star_cond))
Afin_AT_den_cond=(1/Fs_star_cond-
pi/4*Dc_star_cond^2/(Fs_star_cond*Pt_star_cond*Pl_star_cond)+pi/2*Dc_star_cond/(Pt_star_co
nd*Pl_star_cond)-pi/2*Ft_star_cond*Dc_star_cond/(Fs_star_cond*Pt_star_cond*Pl_star_cond))
Afin_AT_cond=Afin_AT_num_cond/Afin_AT_den_cond
AT_Atube_cond=(2*Pt_star_cond*Pl_star_cond/(pi*Fs_star_cond*Dc_star_cond)-
Dc_star_cond/2/Fs_star_cond+1-Ft_star_cond/Fs_star_cond)/(1-Ft_star_cond/Fs_star_cond)

"Surface efficiency - Sector method using Bessel functions"
mD_c_cond=(2*j_cond*Afr_Amin_cond*Vfr_star_cond*Dc_star_cond^2/Ft_star_cond/ka_star_co
nd^(1/3)*ka_star_cond/kf_star_cond)^0.5
mr_i_cond=mD_c_cond/2
N_sectors_cond=4

{Counter side}
Duplicate iter_cond=1, N_sectors_cond
{Octans 2 ,3,6 and 7}
    R_cond[iter_cond]=(Pt_star_cond/Dc_star_cond)*(((((2*iter_cond-
1)/(2*N_sectors_cond))^2)+(Pl_star_cond/Pt_star_cond)^2))^0.5
    S_cond[iter_cond]=(Dc_star_cond^2)/8*((R_cond[iter_cond]^2)-
1)*(arctan(iter_cond/N_sectors_cond*Pt_star_cond/Pl_star_cond)-arctan((iter_cond-
1)/N_sectors_cond*Pt_star_cond/Pl_star_cond))
    mr_o_cond[iter_cond]=mr_i_cond*R_cond[iter_cond]
    bessel_num_cond[iter_cond]=Bessel_K1(mr_i_cond)*Bessel_I1(mr_o_cond[iter_cond])-
Bessel_K1(mr_o_cond[iter_cond])*Bessel_I1(mr_i_cond)
    bessel_den_cond[iter_cond]=Bessel_K1(mr_o_cond[iter_cond])*Bessel_I0(mr_i_cond)+Bess
el_K0(mr_i_cond)*Bessel_I1(mr_o_cond[iter_cond])
    Eff_cond[iter_cond]=2/(mr_i_cond*(R_cond[iter_cond]^2-
1))*bessel_num_cond[iter_cond]/bessel_den_cond[iter_cond]
    Num_cond[iter_cond]=4*Eff_cond[iter_cond]*S_cond[iter_cond]
    Den_cond[iter_cond]=4*S_cond[iter_cond]
{Octans 1 , 4, 5 and 8}
    R_cond[2*N_sectors_cond+1-iter_cond]=(Pt_star_cond/Dc_star_cond)*(((((2*iter_cond-
1)/(2*N_sectors_cond))^2)*(Pl_star_cond/Pt_star_cond)^2)+1)^0.5
```

```
    S_cond[2*N_sectors_cond+1-iter_cond]=(Dc_star_cond^2)/8*((R_cond[2*iter_cond+1-
iter_cond]^2)-1)*(arctan(iter_cond/N_sectors_cond*Pl_star_cond/Pt_star_cond)-
arctan((iter_cond-1)/N_sectors_cond*Pl_star_cond/Pt_star_cond))
    mr_o_cond[2*N_sectors_cond+1-iter_cond]=mr_i_cond*R_cond[2*N_sectors_cond+1-
iter_cond]
    bessel_num_cond[2*N_sectors_cond+1-
iter_cond]=Bessel_K1(mr_i_cond)*Bessel_I1(mr_o_cond[2*N_sectors_cond+1-iter_cond])-
Bessel_K1(mr_o_cond[2*N_sectors_cond+1-iter_cond])*Bessel_I1(mr_i_cond)
    bessel_den_cond[2*N_sectors_cond+1-
iter_cond]=Bessel_K1(mr_o_cond[2*N_sectors_cond+1-
iter_cond])*Bessel_I0(mr_i_cond)+Bessel_K0(mr_i_cond)*Bessel_I1(mr_o_cond[2*N_sectors_co
nd+1-iter_cond])
    Eff_cond[2*N_sectors_cond+1-iter_cond]=2/(mr_i_cond*(R_cond[2*N_sectors_cond+1-
iter_cond]^2-1))*bessel_num_cond[2*N_sectors_cond+1-
iter_cond]/bessel_den_cond[2*N_sectors_cond+1-iter_cond]
    Num_cond[2*N_sectors_cond+1-iter_cond]=4*Eff_cond[2*N_sectors_cond+1-
iter_cond]*S_cond[2*N_sectors_cond+1-iter_cond]
    Den_cond[2*N_sectors_cond+1-iter_cond]=4*S_cond[2*N_sectors_cond+1-iter_cond]
End

Num_cond=SUM(Num_cond[iter_cond],
iter_cond=1,N_sectors_cond)+SUM(Num_cond[2*N_sectors_cond+1-iter_cond], iter_cond=1,
N_sectors_cond)
Den_cond=SUM(Den_cond[iter_cond],
iter_cond=1,N_sectors_cond)+SUM(Den_cond[2*N_sectors_cond+1-iter_cond], iter_cond=1,
N_sectors_cond)

eta_f_cond=Num_cond/Den_cond
eta_0_cond=1-Afin_AT_cond*(1-eta_f_cond)


"***************************************************************************************************"
"PECs"

"Area-Goodness Ratio"
PEC_j_over_f_cond=j_cond/f_cond

"Heat Transfer/Pumping Power"
PEC_THETA_cond=2*eta_fm_cond*epsilon_cond*DELTAT_star_cond/(Vfr_star_cond^2*f_cond)
*Amin_Afr_cond^2*Amin_AT_cond

"Heat Transfer/(Pumping Power + Compressor Power)"
PEC_OMEGA_cond=(1/PEC_THETA_cond+1/(a_star_cond-
b_star_cond*DELTAT_star_cond))^(-1)

"***************************************************************************************************"
"Nondimensional geometric variables normalized by D_c"
"Plain fins"
L_Dc_cond=L_star_cond/Dc_star_cond
Fs_Dc_cond=Fs_star_cond/Dc_star_cond
Ft_Dc_cond=Ft_star_cond/Dc_star_cond
Pl_Dc_cond=Pl_star_cond/Dc_star_cond
Pt_Dc_cond=Pt_star_cond/Dc_star_cond
{
```

```
"Wavy fins"
Wh_Dc_cond=Wh_star_cond/Dc_star_cond

"Slit fins"
Sh_Dc_cond=Sh_star_cond/Dc_star_cond
Sw_Dc_cond=Sw_star_cond/Dc_star_cond

"Louvered fins"
Lh_Dc_cond=Lh_star_cond/Dc_star_cond
Lp_Dc_cond=Lp_star_cond/Dc_star_cond
}

"Inputs to model"
eta_fm_cond=0.21                "taken from system data"
S_n_cond=4                      "slit fins - use to constrain number of slits"
T_o_cond=308.15                 "[K]"     "ambient temperature in Kelvins"
P_atm_cond=101                  "[kPa]"   "ambient pressure"
k_fin_cond=222.05               "[W/m-K]" "aluminum"
"D_c_cond=0.009525"   "[m]"     "different tube diameters affect optimization results"
a_cop_cond=6.5078     "[]"      "Copeland ZP32K3E-PFV compressor, Te=50F"
b_cop_cond=0.17923    "[1/K]"   "Copeland ZP32K3E-PFV compressor, Te=50F"
"q_over_A_cond=10000"           "[W/m2]" "set to constrain heat flux"
A_fr_cond=1.4                   "[m2]"   "set to constrain frontal area"
q_s_cond=14000                  "[W]"    "set to constrain heat duty"

"Air properties"
mu_air_cond=viscosity(air,t=T_o_cond)                                   "[kg/m-s]"
rho_air_cond=density(air,t=T_o_cond,p=P_atm_cond)                       "[kg/m3]"
cp_air_cond=specheat(air,t=T_o_cond)*1000                               "[J/kg-K]"
k_air_cond=conductivity(air,t=T_o_cond)                                 "[W/m-K]"

"Dimensional-Nondimensional conversion equations"
ka_star_cond=k_air_cond/(mu_air_cond*cp_air_cond)                       "1.41"
kf_star_cond=k_fin_cond/(mu_air_cond*cp_air_cond)                       "11663"
D_c_cond=Dc_star_cond*mu_air_cond/(rho_air_cond*sqrt(cp_air_cond*T_o_cond))"[m]"
V_fr_cond=Vfr_star_cond*sqrt(cp_air_cond*T_o_cond)                      "[m/s]"
DELTAT_cond=DELTAT_star_cond*T_o_cond                                   "[C]"
DELTAp_cond=DELTAp_star_cond*T_o_cond*rho_air_cond*cp_air_cond
    "[Pa] (equivalent to kg/m-s2)"
q_over_A_cond=qA_star_cond*rho_air_cond*(cp_air_cond*T_o_cond)^1.5       "[W/m2]"
q_over_A_cond=q_s_cond/A_fr_cond
a_star_cond=a_cop_cond          "best COP possible for a given condenser and Tc"
b_star_cond=b_cop_cond*T_o_cond "slope of COP penalty for increasing DELTAT"
Pr_cond=1/ka_star_cond
Nu_Dc_cond=j_cond*Re_Dc_cond*Pr_cond^(1/3)
h_c_cond=Nu_Dc_cond*k_air_cond/D_c_cond                                  "[W/m2-K]"
A_T_cond=AT_Amin_cond/Afr_Amin_cond*A_fr_cond                           "[m2]"


"Other terms of interest"
T_c_cond=T_o_cond+DELTAT_cond                                           "[K]"
V_dot_cond=V_fr_cond*A_fr_cond*convert(m3/s,cfm)                        "[cfm]"
W_pump_cond=V_fr_cond*A_fr_cond*DELTAp_cond/eta_fm_cond                 "[W]"
"W_comp_cond=q_s_cond/(COP_cond+1)"                                     "[W]"
```

```
W_comp_cond=q_s_cond/(COP_comp+1)                                    "[W]"
COP_cond=a_star_cond-b_star_cond*DELTAT_star_cond                    "based on curve fit from
compressor map"
N_cond=L_star_cond/Pl_star_cond          "can use to constrain number of tube rows"
Vol_fin_cond=L_cond*F_t_cond/F_s_cond*A_fr_cond                      "[m3]"


"Use this section for non-optimization runs (i.e. analyzing an existing design)"
i_cond=2

"H_cond=lookup(i_cond,1)*convert(ft,m)
W_cond=lookup(i_cond,2)*convert(ft,m)"
"L_cond=lookup(i_cond,3)*convert(ft,m)
F_s_cond=lookup(i_cond,4)*convert(ft,m)"
"F_t_cond=lookup(i_cond,5)*convert(ft,m)"
"P_l_cond=lookup(i_cond,6)*convert(ft,m)
P_t_cond=lookup(i_cond,7)*convert(ft,m)
V_dot_cond=lookup(i_cond,8)"
"q_s_cond=lookup(i_cond,10)*convert(Btu/hr,W)"

L_cond=L_star_cond*mu_air_cond/(rho_air_cond*sqrt(cp_air_cond*T_o_cond))  "[m]"
F_s_cond=Fs_star_cond*mu_air_cond/(rho_air_cond*sqrt(cp_air_cond*T_o_cond))"[m]"
F_t_cond=Ft_star_cond*mu_air_cond/(rho_air_cond*sqrt(cp_air_cond*T_o_cond))"[m]"
P_l_cond=Pl_star_cond*mu_air_cond/(rho_air_cond*sqrt(cp_air_cond*T_o_cond))"[m]"
P_t_cond=Pt_star_cond*mu_air_cond/(rho_air_cond*sqrt(cp_air_cond*T_o_cond))"[m]"

"A_fr_cond=H_cond*W_cond"                                                "[m2]"
```

References

[1] ARI, 1989, *Standard for Unitary Air-Conditioning and Air-Source Heat Pump Equipment*, ARI-210/240.

[2] ARI, 1981, *Standard for Forced-Circulation Air-Cooling and Air-Heating Coils*, ARI-410.

[3] Beaver, A. C., Yin, J. M., Bullard, C. W., and Hrnjak, P. S., 1999, "An Experimental Investigation of Transcritical Carbon Dioxide Systems for Residential Air Conditioning," Masters thesis, University of Illinois at Urbana-Champaign, IL.

[4] Bejan, A., 1996, *Entropy Generation Minimization*, New York: CRC Press.

[5] Bejan, A., 1978, "General Criterion for Rating Heat-Exchanger Performance," *International Journal of Heat and Mass Transfer*, 21: 655-658.

[6] Bergles, A.E., Blumenkrantz, A.R., and Taborek, J., 1974, "Performance Evaluation Criteria for Enhanced Heat Transfer Surfaces," *Proceedings of the Fifth International Heat Transfer Conference,* Tokyo, 239-243.

[7] Bridges, B. D., and Bullard, C. W., 1995, "Simulation of Room Air Conditioner Performance," MS thesis, University of Illinois at Urbana-Champaign, IL.

[8] Cowell, T.A., 1990, "A General Method for the Comparison of Compact Heat Transfer Surfaces," *Journal of Heat Transfer,* 112: 288-294.

[9] DeJong, N. C., Gentry, M. C., and Jacobi, A. M., 1997, "An Entropy-Based, Air-Side Heat Exchanger Performance Evaluation Method: Application to a Condenser," *HVAC&R Research.* 3(3): 185-195.

[10] Elmahdy, A. H., and Biggs, R. C., 1979, "Finned Tube Heat Exchanger: Correlation of Dry Surface Heat Transfer Data," *ASHRAE Transactions*, 85(2): 262-273.

[11] Fox, R. W., and McDonald, A. T., 1992, *Introduction to Fluid Mechanics*, 4th Edition, John Wiley & Sons, Inc., New York, 287-294.

[12] Gray, D. L., and Webb, R. L., 1986, "Heat Transfer and Friction Correlations for Plate Finned-Tube Heat Exchangers Having Plain Fins," *Proceedings of the 8th International Heat Transfer Conference*, 6: 2745-2750.

[13] Incropera, F. P. and DeWitt, D. P., 1990, *Fundamentals of Heat and Mass Transfer,* 3rd ed., New York: John Wiley & Sons.

[14] Kayansayan, N., 1993, "Heat Transfer Characterization of Flat Plain Fins and Round Tube Heat Exchangers," *Experimental Thermal and Fluid Science*, 6: 263-272.

[15] Kays, W. M., and London, A. L., 1984, *Compact Heat Exchangers*, 3rd ed., New York: McGraw-Hill Book Company.

[16] Kern, D. Q., and Kraus, D. A., 1972, *Extended Surface Heat Transfer*, New York: McGraw-Hill Book Company.

[17] Kim, G. J., and Jacobi, A. M., 2000, "Condensate Accumulation Effects on the Air-side Thermal Performance of Slit-fin Surfaces," Masters thesis, University of Illinois at Urbana-Champaign, IL.

[18] Klein, S. A., 1992, "Design Considerations for Refrigeration Cycles," *International Journal of Refrigeration*, 15(3): 181-185.

[19] Klein, S. A., Alvarado, F. L., 1999, *Engineering Equation Solver*, Middleton, WI: F-Chart Software, version 5.015.

[20] London, A. L., 1982, "Economics and The Second Law: An Engineering Methodology," *International Journal of Heat and Mass Transfer*, 25(6): 743-751.

[21] Madi, M. A., Johns, R. A., and Heikal, M. R., 1998, "Performance Characteristics Correlation for Round Tube and Plate Finned Heat Exchangers," *International Journal of Refrigeration*, 21(7): 507-517.

[22] Mirth, D. R., and Ramadhyani, S., 1994, "Correlations for Predicting the Air-Side Nusselt Numbers and Friction Factors in Chilled-Water Cooling Coils," *Experimental Heat Transfer*, 7: 143-162.

[23] Nakayama, W., and Xu, L. P., 1983, "Enhanced Fins for Air-Cooled Heat Exchangers – Heat Transfer and Friction Factor Correlations," *ASME-JSME Thermal Engineering Joint Conference Proceedings*, 495-502.

[24] Rich, D. G., 1975, "The Effect of Number of Tube Rows on Heat Transfer Performance of Smooth Plate Fin-and-Tube Heat Exchangers," *ASHRAE Transactions*, 81(1): 307-317.

[25] Rich, D. G., 1973, "The Effect of Fin Spacing on the Heat Transfer and Friction Performance of Multi-Row, Smooth Plate Fin-and-Tube Heat Exchangers," *ASHRAE Transactions*, 79(2): 137-145.

[26] Schmidt, T. E., 1949, "Heat Transfer Calculations for Extended Surfaces," *Refrigerating Engineering*, 57: 351-357.

[27] Sekulic, D. P., 1990, "The Second Law Quality of Energy Transformation in a Heat Exchanger," *Journal of Heat Transfer,* 112: 295-300.

[28] Stoecker, W. F., 1989, *Design of Thermal Systems*, 3rd edition, New York: McGraw-Hill Inc.

[29] Stoecker, W. F., 1986, *Refrigeration and Air Conditioning*, New York: McGraw-Hill Inc.

[30] Tagliafico, L., and Tanda, G., 1996, "A Thermodynamic Method for the Comparison of Plate-Fin Heat Exchanger Performance," *Journal of Heat Transfer,* 118: 805-809.

[31] Wang, C. C., personal communication, 2000.

[32] Wang, C.C., Lin, Y. T., and Lee, C. J., 2000, "Heat and Momentum Transfer for Compact Louvered Fin-and-tube Heat Exchangers in Wet Conditions," *International Journal of Heat and Mass Transfer*, 43: 3443-3452.

[33] Wang, C. C., Tao, W. H., and Chang, C. C., 1999b, "An Investigation of the Airside Performance of the Slit Fin-and-Tube Heat Exchangers," *International Journal of Refrigeration*, 22: 595-603.

[34] Wang, C. C., Lee, C. J., Chang, C. T., and Lin, S. P., 1999a, "Heat Transfer and Friction Correlation for Compact Louvered Fin-and-Tube Heat Exchangers," *International Journal of Heat and Mass Transfer*, 42(11): 1945-1956.

[35] Wang, C. C., and Chang, C. T., 1998, "Heat and Mass Transfer for Plate Fin-and-Tube Heat Exchangers, With and Without Hydrophilic Coating," *International Journal of Heat and Mass Transfer*, 41: 3109-3120.

[36] Wang, C. C., Chi, K. Y., Chang, Y. J., and Chang, Y. P., 1998, "An Experimental Study of Heat Transfer and Friction Characteristics of Typical Louver Fin-and-Tube Heat Exchangers," *International Journal of Heat and Mass Transfer*, 41(4-5): 817-822.

[37] Wang, C. C., and Chang, Y. J., 1997, "A Generalized Heat Transfer Correlation for Louver Fin Geometry," *International Journal of Heat and Mass Transfer*, 40(3): 533-544.

[38] Wang, C. C., Hsieh, Y.C., and Lin, Y. T., 1997, "Performance of Plate Finned Tube Heat Exchangers Under Dehumidifying Conditions," *Journal of Heat Transfer*, 119: 109-117.

[39] Wang, C. C., Chang, Y. J., Hsieh, Y. C., and Lin, Y. T., 1996, "Sensible Heat and Friction Characteristics of Plate Fin-and-Tube Heat Exchangers Having Plane Fins," *International Journal of Refrigeration*, 19(4): 223-230.

[40] Webb, R. L., 1981, "Performance Evaluation Criteria for Use of Enhanced Heat Transfer Surfaces in Heat Exchanger Design," *International Journal of Heat and Mass Transfer*. 24(4): 715-726.

[41] Wepfer, W. J., Gaggioli, R.A., and Obert, E.F., 1979, "Proper Evaluation of Available Energy for HVAC," *ASHRAE Transactions*, 85(1): 214-230.

[42] Witte, L.C., 1988, "The Influence of Availability Costs on Optimal Heat Exchanger Design," *Journal of Heat Transfer,* 110: 830-835.

[43] Xiao, Q., and Tao, W. Q., 1990, "Effect of Fin Spacing on Heat Transfer and Pressure Drop of Two-Row Corrugated-Fin and Tube Heat Exchangers," *International Communications of Heat and Mass Transfer*, 17: 577-586.

[44] Zubair, S. M., Kabada, P. V., and Evans, R.B., 1987, "Second-Law Based Thermoeconomic Optimization of Two-Phase Heat Exchangers," *Journal of Heat Transfer,* 109: 287-294.